VSB TECHNICAL UNIVERSITY OF OSTRAVA | FACULTY OF ELECTRICAL ENGINEERING AND COMPUTER SCIENCE

Software Defined Radio in SMART Technology

Využití softwarově definovaného rádia v oblasti SMART technologií

Ing. Lukáš Danys

PhD Thesis

Supervisor: prof. Ing. Radek Martinek, Ph.D.

Ostrava, 2023

Abstrakt a přínos práce

Moderní komunikační systémy jsou jednou z nejrychleji se rozvíjejících oblastí. Takového markantního posunu lze dosáhnout pouze skrze nový vývoj a aplikaci metodiky fast prototypingu. Tato disertace se zaměřuje na nasazení technologie softwarově definovaného rádia (SDR) v různých aplikačních oblastech. Samotné SDR je díky své adaptabilitě nástrojem, který stál na pozadí rozvoje mnoha moderních telekomunikačních systémů. Jedná se o ucelenou platformu pro fast prototyping, která se opírá o robustní softwarovou základnu. Právě telekomunikace jsou oblastí, kde je takové zařízení nedocenitelné, právě kvůli neustálému tlaku na inovace. Právě to je důvodem, proč je vhodné také testovat různé alternativní technologie pro přenos dat. Jednou z takových je komunikace viditelným spektrem světla (VLC), která je náplní této práce. Součástí praktické části je vývoj a popis několika verzí VLC systému založených na virtuální instrumentaci a SDR, které vznikly během autorova studia. Každá verze je samostatně popsána včetně výhod a nevýhod, které poskytují. Součástí je též první náčrt čtvrté verze, která bude součástí budoucího výzkumu. Prezentované výsledky z různých aplikačních oblastí jasně ukazují, že je celou platformu možné použít v různých aplikačních oblastech, včetně SMART technologií, automotive, úložišti jaderného odpadu anebo Průmyslu 4.0. Součástí jsou též výsledky z poslední verze, které dokazují, že je systém ve vnitřních prostorech komunikovat až na vzdálenost 50 metrů, zatímco ve venkovních podmínkách je to 35 metrů. Díky tomu je možné vytyčit nové oblasti výzkumu jako je například platooning (tandemová jízda) anebo podvodní komunikace.

Klíčová slova

Automotive, LED, Průmysl 4.0, OFDM, QAM, SDR, SMART technologie, VLC.

Abstract and Contributions

Modern telecommunication systems are rapidly evolving. This rapid development requires constant research and fast prototyping. This dissertation thesis focusses on deployment of software defined radio (SDR) in multiple application areas, including SMART technologies. SDR itself is a tool behind many breakthroughs in modern telecommunications, due to its major adaptability. It offers a comprehensive way of fast prototyping, which rely on suitable software platform. The field of telecommunications is ever-changing, due to the constant pressure on innovation. For this reason, it is desirable to test some of the alternative communication technologies. Visible light communication (VLC) system based on combination of virtual instrumentation and software defined radios was chosen for experimentation. This dissertation focusses on multiple versions of VLC system that were developed over the years. Each version is further discussed, and their advantages and disadvantages are presented. A draft of fourth and newest version is mentioned along with possible directions of the research. Results from multiple application areas are presented, which show the adaptability of the whole platform to different use cases including but not limited to: SMART technologies, automotive, nuclear waste disposal sites, or industry. It is demonstrated that the newest version of the system, which is based on OFDM modulation, can communicate up to 50 meters in closed environments and up to 35 meters in outdoor scenarios. This opens further research directions such as truck platooning or underwater communications.

Keywords

Automotive, Industry 4.0, LED, OFDM, QAM, SDR, SMART Technologies, VLC.

Acknowledgement

I would like to express my deepest appreciation to my supervisor, prof. Ing. Radek Martinek, Ph.D., for the ongoing leadership during my Ph.D. studies. I am also thankful to Ing. René Jaroš, Ph.D. for assistance with publications and general support.

Special thanks is reserved for my family - Kristyna and Martin, who supported me during these trying times. Their belief in me has kept my spirits and motivation high during the whole process.

Contents

List of symbols and abbreviations **7**

List of Figures **10**

List of Tables **13**

1 Introduction **15**

2 Software Defined Radio **17**

2.1 General Architecture of Software Defined Radio 18
2.2 Digital Part 18
2.3 Analog Part 19
2.4 Limitations of ADCs and DACs 19
2.5 SDR Hardware and Design 20
2.6 SDR Development Tools 24
2.7 SDR as Tool for SMART Technologies 25

3 Visible Light Communication **26**

3.1 Light-Emitting Diode 27
3.2 Advantages, Disadvantages and Challenges 28
3.3 VLC IEEE Standardization 30
3.4 Modulation Formats 32
3.5 Visible Light Positioning 38

4 Dissertation Thesis Objectives **41**

5 Experimental Platform for VLC Development **43**

5.1 First Version - QAM System 45
5.2 Second Version - Beta OFDM 46
5.3 Third Version - OFDM System 47

5.4 Fourth Version - Next-Gen OFDM System 49
5.5 Comparison of Individual Versions 51

6 Software and Hardware of the Current Version 53
6.1 NI USRP 2954R 54
6.2 Mini Circuits ZX85-12G-S+ 55
6.3 Mini Circuits ZX60-100VH+ 56
6.4 Mini Circuits ZFL-1000LN+ 56
6.5 Thorlabs PDA36A-EC and PDA100A2 57

7 Application Areas of VLC and Experimental Results 58
7.1 Vehicles 59
7.2 Smart Technologies and Buildings 76
7.3 Industry 84
7.4 Other Areas of Interest and Experiments 89

8 Conclusion 91

Bibliography 94
Publications and Outcomes Related to Thesis 106
Publications and Outcomes Not Related to Thesis 107

List of symbols and abbreviations

F_s	–	Sampling Frequency
T_s	–	Sampling Period
AD	–	Analog to Digital
A-QL	–	Asynchronous Quick Link
ARM	–	Advanced RISC Machine
ASIC	–	Application Specific Integrated Circuit
CM-FSK	–	Camera M-ary Frequency Shift Keying
CMOS	–	Complementary Metal–Oxide–Semiconductor
C-OOK	–	Camera On-Off Keying
CPU	–	Central Processing Unit
CSK	–	Color Shift Keying
DA	–	Digital to Analog
DFT	–	Discrete Fourier Transform
DRFS	–	Direct Radio Frequency Sampling
DSP	–	Digital Signal Processor
EMI	–	Electromagnetic Interference
FDM	–	Frequency Division Multiplexing
FFT	–	Fast Fourier Transform
FPGA	–	Field Programmable Gate Array
GOPS	–	Giga Operations Per Second
GPP	–	General Purpose Processor
GPU	–	Graphics Processing Unit
HA-QL	–	Hidden Asynchronous Quick Link
HLS	–	High Level Synthesis
HS-PSK	–	Hybrid Spatial Phase Shift Keying
ICI	–	Intercarrier Interference
IR	–	Infrared
ISI	–	Intersymbol Interference

LAN	–	Local Area Networks
LED	–	Light Emitting Diode
Li-Fi	–	Light Fidelity
LoS	–	Line of Sight
LNA	–	Low Noise Amplifiers
MAC	–	Medium Access Control
MIMD	–	Multiple Instruction Multiple Data
MIMO	–	Multiple-Input Multiple-Output
MPM	–	Mirror Pulse Modulation
NI	–	National Instruments
NLoS	–	Non Line of Sight
OFDM	–	Orthogonal Frequency Division Multiplexing
Offset-VPWM	–	Offset Variable Pulse Width Modulation
OLED	–	Organic Light Emitting Diode
OOK	–	On-Off Keying
OPWAN	–	Optical Personal Wireless Area Network
OWC	–	Optical Wireless Communication
pc-LED	–	Phosphor Converted Light Emitting Diode
PPM	–	Pulse Position Modulation
PWM	–	Pulse Width Modulation
QAM	–	Quadrature Amplitude Modulation
RF	–	Radio Frequency
RFSoC	–	Radio Frequency System on Chip
RS-FSK	–	Rolling Shutter Frequency Shift Keying
RTL	–	Registry-Transfer Level
S2-PSK	–	Spatial Two-Phase Shift Keying
SDR	–	Software Defined Radio
SFDR	–	Spurious-Free Dynamic Range
SIMD	–	Single Instruction Multiple Data
SNR	–	Signal-to-Noise Ratio
SoC	–	System-on-Chip
SRC	–	Sample Rate Conversion
SS2DC	–	Sequential Scalable Two-Dimensional Color
UFSOOK	–	Undersampled Frequency On-Off Keying
USRP	–	Universal Software Radio Peripheral
V2G	–	Vehicle-to-Grid
V2I	–	Vehicle-to-Infrastructure
V2P	–	Vehicle-to-Pedestrian

V2V	–	Vehicle-to-Vehicle
V2X	–	Vehicle-to-Everything
VLC	–	Visible Light Communication
VLP	–	Visible Light Positioning
VPPM	–	Variable Pulse Position Modulation
VTASC	–	Variable Transparent Amplitude-Shape-Color
Wi-Fi	–	Wireless Fidelity
WQI	–	Wavelength Quality Indicator

List of Figures

2.1 Common architecture of software defined radio. 18
2.2 General design of Ettus/NI based USRP [13]. 23
2.3 NI Ettus USRP X410. 24

3.1 Spectrum of electromagnetic waves. The visible light area is specified. 26
3.2 Device topologies according to the standard. 31
3.3 Diagram of the conventional OFDM system. 37

5.1 Cyclical process of VLC platform development both software and hardware wise. 44
5.2 First generation of developed system. 46
5.3 Second generation of developed system. 47
5.4 Third generation of developed system. 48
5.5 Experiments on the second version of OFDM system. 49
5.6 Early draft of the next generation of VLC OFDM system. 51
5.7 Comparison of individual versions. 52

6.1 NI USRP-2954R with LFTX and LFRX daughterboards. 54
6.2 ZX85-12G-S+ with SMA input ports. 55
6.3 ZX60-100VH+ construction and gain flatness over the whole frequency spectrum. 56
6.4 ZFL-1000LN+ construction gain flatness over the whole frequency spectrum. . 56
6.5 Thorlabs PDA36A-EC and PDA100A2 photodetectors. 57

7.1 Interoperability of VLC and RF in SMART city concept. 59
7.2 Vehicle-to-everything scenarios communication. 61
7.3 Octavia tail-light setup for early QAM tests. 62
7.4 Octavia taillight setup adjusted for testing scenario with empty box. 62
7.5 BER/distance relationship for Octavia tail-light with different M-QAM and bandwidths—empty box. 63
7.6 E_b/N_0 / distance relationship for Octavia tail-light with different M-QAM and bandwidths—empty box. 63

7.7 EVM/distance relationship for Octavia tail-light with different M-QAM and bandwidths—empty box. 64
7.8 Octavia tail-light setup adjusted for scenario 2-thermal turbulence. 64
7.9 BER/distance relationship for Octavia tail-light with different M-QAM and bandwidths—thermal turbulence. 65
7.10 E_b/N_0/distance relationship for Octavia tail-light with different M-QAM and bandwidths—thermal turbulence. 65
7.11 EVM/distance relationship for Octavia tail-light with different M-QAM and bandwidths—thermal turbulence. 66
7.12 Octavia tail-light setup adjusted for scenario 3 – Rain 42 l/min. 66
7.13 BER/distance relationship for Octavia tail-light with different M-QAM and bandwidths—Rain 42 l/min. 67
7.14 E_b/N_0 / distance relationship for Octavia tail-light with different M-QAM and bandwidths—Rain 42 l/min. 67
7.15 EVM/distance relationship for Octavia tail-light with different M-QAM and bandwidths—Rain 42 l/min. 68
7.16 Attenuation characteristics of Octavia tail-light for scenario with Rain 42 l/min – comparison of intended setup and adjusted setup without partition. 68
7.17 Octavia tail-light setup adjusted for scenario with Rain 22 l/min. 68
7.18 BER/distance relationship for Octavia tail-light with different M-QAM and bandwidths—Rain 22 l/min. 69
7.19 E_b/N_0 / distance relationship for Octavia tail-light with different M-QAM and bandwidths—Rain 22 l/min. 70
7.20 EVM/distance relationship for Octavia tail-light with different M-QAM and bandwidths—Rain 22 l/min. 70
7.21 BER comparison at distances around 28 m, 4-QAM modulation, carrier frequency 1 MHz. 72
7.22 BER comparison with variable headlight-photodetector distance. Carrier frequency 1 MHz, bandwidth 2 MHz. 72
7.23 Comparison of BER at various measured angles and distances, 4-QAM and 64-QAM modulation. Carrier frequency 1 MHz, bandwidth 400 kHz. 73
7.24 Comparison of BER at different measured angles and distances for all modulations formats. Carrier frequency 1 MHz, bandwidth 400 kHz. 73
7.25 Photo taken during the measurement. Default settings for the driving scenario measurement process. 75
7.26 BER with respect to time and distance in dynamic tests. Carrier frequency 1 MHz, bandwith 400 kHz. 76
7.27 Ceiling light setup. 77

7.28 BER/distance from center relationship for ceiling light with different M-QAM and bandwidths. 77
7.29 E_b/N_0 / distance from center relationship for ceiling light with different M-QAM and bandwidths. 78
7.30 EVM/distance from center relationship for ceiling light with different M-QAM and bandwidths. 78
7.31 Visualization of reached M-QAM modulation formats based on measured parameters— 3 MHz channel width and carrier frequency. 79
7.32 Dependence of E_b/N_0 on the distance and adaptive algorithm, bandwidth 1 MHz, 4-QAM. 80
7.33 Dependence of E_b/N_0 on the distance and adaptive algorithm used, bandwidth 4 MHz, 4-QAM. 80
7.34 Dependence of BER on the distance and used adaptive algorithm, bandwidth 1 MHz, 4–32-QAM. 82
7.35 Dependence of EVM on the distance and used adaptive algorithm, bandwidth 1 MHz, 4-QAM. 82
7.36 Integration of VLC Technologies into an Industry 4.0 Environment. 87
7.37 Integration of VLC into 3GPP Release 15 Standard (relevant part outsourced from [93]). 88

List of Tables

2.1 Comparison of SDR hardware platforms based on the controlling element. . . . 23

3.1 Device classifications according to the standard. 30

7.1 Comparison of BER from stationary tests at 0° and 15° with the median from dynamic tests. 75
7.2 Table of the measured parameters of the ceiling light, 4-QAM modulation format, bandwidth 1 MHz. 83
7.3 Table of measured parameters of the ceiling light, 256-QAM modulation format, bandwidth 1 MHz. 84

Chapter 1

Introduction

Wireless and alternative communication technologies are gaining on importance in multiple fields. In the past, it was usual, that the control nodes of individual institutions (i.e. servers or data centers) or personal devices of employees (i.e. mobile phones and computers) were connected to either local or wide networks. This trend is rapidly changing, as the whole industry or even mankind is pushing towards vast networks of intertwined devices and SMART technologies. Modern manufacturing plant is in general a huge well-oiled machine that heavily relies on sensors, wireless technologies and centralized or edge computing. Modern machines, or even workers, are constantly monitored and their condition is evaluated based on the gathered data. However even the most advanced sensor needs a way, how to transfer its gathered data to the local evaluation or control node. The choice of the ideal technology tends to be significantly different, based on the environment, requirements on transfer speeds/latency or even robustness. While the one approach might be ideal for warehouse deployment, it might be completely insufficient for manufacturing plant. Each technology is partially or completely different on the technological level - wired/wireless, operating frequency, modulation scheme, bandwidth, transfer speeds, latency etc. Thus, the hardware itself tends to be different as well. It is therefore hard to find an ideal platform for testing or development of new communication technologies. Apart from some software platforms, the researchers tend to default to Software Defined Radios (SDRs) from various manufacturers. These devices are designed for development and testing, as they offer wide operating frequency and robust platform, which can be considered as industry standard, high performance (Field Programmable Gate Array (FPGA) is often integrated) device. Most of the usually used analog components (filters, low-noise amplifiers, modulators, demodulators, detectors, mixers etc.) are implemented on a software level on a connected PC-based platform. This approach offers a unique utility for developers since they don't have to adjust their hardware during the prototyping and can debug their system quickly.

This dissertation thesis will focus on general overview of SDR platform, discussing individ-

ual SDR variants. The following part will focus on overview of Visible Light Communication (VLC) technology, along with standardization and most promising modulation formats. The third part specifies the dissertation thesis objectives. The fourth part summarizes current research of VLC platform and presents the design draft of the future fourth generation. The fifth part focus on the overview of the current version of the VLC platform while the sixth part describes individual application areas and discusses experimental results from individual fields of interest. The last part is the conclusion of the whole dissertation.

Chapter 2

Software Defined Radio

The term and first concept of SDR was presented by Joseph Mitola III in 1993 [1]. This new platform was meant to shift from the hardware-based design used in Radio Frequency (RF) prototyping towards systems, which mainly rely on software. The first publicly introduced SDR (SpeakEasy I and II) was a system designed for U.S. military [2]. These SDRs were very pricey and generally held back by their hardware. The rapid development of SDRs required a much more powerful components, which offered significant computational power and flexibility in a compact package. The main milestone was the year 2000, when Digital Signal Processors (DSPs) and FPGAs became much more powerful [3]. These new breakthroughs along with rapid development of Digital to Analog (DA) and Analog to Digital (AD) converters accelerated the SDR evolution. Nowadays, some SDR are even able to work in "standalone mode" with onboard Advanced RISC Machine (ARM) or x86-64 processors [4].

The vast flexibility of SDR was the driving force behind the shift from military sector towards the commercial sector. SDR as a platform offered a significant versatility, while having acceptable costs. That's why it was often chosen as a prototyping platform for wireless technologies and networks. The early adopters were developers of cellular networks, since the SDR was thought to be a center of future 3G networks [5]. However, at that time, this widespread deployment was not achieved and SDR stayed as a prototyping platform. In general, the SDR offers a way how to implement both old and new RF applications and test them in various environments. Widespread deployment of wireless devices into everyday life presented challenges for both development teams and manufacturers. A vast number of wireless standards, services or applications must be often supported across different devices, which operate in closed or limited environment. SDR, as a fully reconfigurable device, offer a one-in-all solution for testing and development - they reduce costs of infrastructure and provide the developer with much needed flexibility.

2.1 General Architecture of Software Defined Radio

Conventional radio is a device that relies on one-purpose specialized parts that are designed with a specific function in mind. Among them are for example coders and decoders or modulators and demodulators. The hardware therefore takes care of the signal processing. SDR elevates this concept and replace a part of hardware components with alternative software solutions.

Since only a part of hardware is replaced, every SDR has two separate parts in which it operates - digital and analog. Analog part takes care of narrowband frequency downconversion and analog-to-digital conversion (and reverse), while the digital part is focused on digital signal processing, such as modulation (and reverse), filtering or channel coding (and reverse). The typical block diagram of SDR can be seen in Figure 2.1.

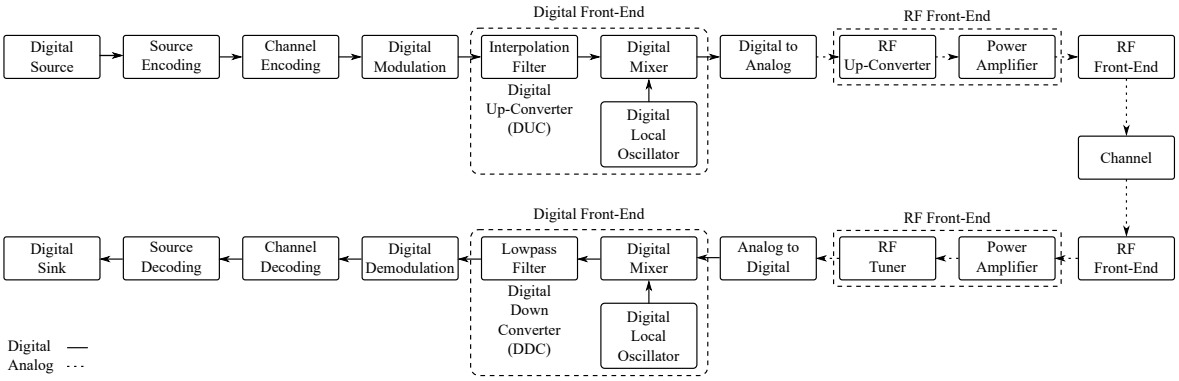

Figure 2.1: Common architecture of software defined radio.

Since the SDR is still evolving, the ADC part is slowly moving to the close vicinity of antennas. This provides flexible software reconfigurable RF front end.

2.2 Digital Part

The digital part of SDR platform covers digital front end and signal processing parts. Each block is specially designed to replace an analog part of conventional radio. Signal processing is focused on modulation and demodulation which map individual bits to electromagnetic waveforms. Coding or decoding blocks are designed to counter impairments of the wireless channel. Source encoders and decoders adjust the bit stream and remove unnecessary bits. Channel encoders and encoders in comparison add additional redundant bits to protect the transmitted data stream from potential errors. Each SDR also have a digital front end, which basically has two functions - Sample Rate Conversion (SRC) and channelization. SRC up/down convert sampling rate from one to another to synchronize both transmitting and receiving element. Channelization include up/down conversion of transceiver and receiver,

while also covering channel filtering, which extract individual channels divided by frequencies. Channelization is usually carried out by retuneable low-pass filters.

Signal processing blocks are usually implemented in a software and run on different central processing components, such as FPGAs, DSPs, Graphics Processing Units (GPUs), General Purpose Processors (GPPs) or their combinations. In general, GPPs offer the highest degree of flexibility, but have limited computational power and are not that power efficient. In comparison FPGAs and partially also GPUs provide the best performance, but they are either hard to program for or partially inflexible, so the prototyping phase is slowed down. While the GPPs were the main driving block of SDRs in the past, the industry is rapidly shifting towards FPGAs [6]. The computational power of conventional Central Processing Units (CPUs) is starting to struggle to meet the performance, that is needed to run 5G or military communications [7].

2.3 Analog Part

The analog part of SDR covers the RF front-end. DACs are used to convert individual digital samples into analog signal, which is then fed into RF front end (often called daughterboards). This converted signal has to be mixed with high frequency carrier signal and then modulated to a predetermined RF frequency (depending on the used technology) to be transmitted via a wireless channel. In comparison, the receiver has to successfully catch the received signal, downconvert it to baseband and then convert it via ADC. Many SDRs have inbuilt Low Noise Amplifiers (LNA), which are used to amplify signals without increasing noise components.

Each SDR usually use an array of antennas to operate at a wide range of frequency bands. These antennas are often described as SMART, since they are able to operate at a predetermined frequency band and adapt to environmental changes via mobile tracking or interference cancellation [8]. In case of experimental SDRs, the requirements for antennas tend to be high - they have to be self-adaptable (retunable), self-alignment based (offer beamforming) and interference resistant.

2.4 Limitations of ADCs and DACs

SDR heavily relies on the quality and speed of analog to digital and digital to analog conversion. It is necessary to convert continuous time signal to a discrete time signal using sampling or the other way around using reconstruction. During the sampling, instantaneous measurements are taken every T_s which gives us sampling frequency which equals to $f_s = \frac{1}{T_s}$. In addition, it is necessary to use a low pass filter to reconstruct the original signal from the sampled signal. The problem lies in the Nyquist theorem, which says that the f_s must be higher than two times the analog signal´s bandwidth (Nyquist frequency).

As mentioned before, ADCs and DACs are the core of every SDR. Their sampling frequency is the key factor of their versatility. Digitization of RF signal requires sampling at least at Nyquist frequency. In addition, higher data rates, along with more complex modulation schemes require higher resolution to reliably extract the information from the signal. For example, if the SDR process 802.11ax 80 MHz channel (which is not the limit of technology, since WiFi 6 offers even 160 MHz channels), it has to digitize signal bandwidth of 160 MHz, which gives us sample rate of at least 320 Msps. However, since the modern SDR usually use quadrature sampling, every sample is actually two, a real (in-phase) sample and an imaginary (quadrature) sample, thus the resulting sampling rate equals to the bandwidth [6]. If we consider the previous example, SDR would require sample rate of at least 160 Msps.

ADCs and DACs performance can be evaluated based on multiple parameters. Among them are Signal-to-Noise Ratio (SNR), bit resolution, Spurious-Free Dynamic Range (SFDR) or power dissipation. Recent advances in ADCs and DACs power consumption greatly affected their effect of lifetime of battery-powered devices and therefore skyrocketed deployment of SDR concept into mobile devices [9].

Recently a new concept known as Direct Radio Frequency Sampling (DRFS) surfaced [10]. DRFS replaces analog processing part, including mixer, local oscillator and filters and transform their functionality into digital domain. Receiver is therefore simplified. DRFS relies on a close relationship with ADC, which feed signal into a custom designed processing block, which extracts the data. The block leverages sub-sampling or bandpass sampling, which only requires alias of the signal in order to sample. This leads to lowering of the sampling rate. To avoid losing sensitivity, a bandpass filter is inserted in front of ADC. DRFS approach offers wide bandwidth potential together with high power efficiency.

2.5 SDR Hardware and Design

Over the 30 years, the SDR became the dominant industry standard. It can be stated, that SDRs are part of everyday life of humans. With the evolution of semiconductors and software, the radios are slowly shifting towards frequency-agile intelligent RF systems.

Due to their unquestionable advantages, the SDRs are very popular tools for prototyping and development of technologies in multiple fields. The latest major ripple happened with transfer of 4G LTE handsets to SDR-based architectures [7, 11]. Low-power/high-performance DSP were the main driving force behind this. This ripple accelerated the broadband deployment of SDRs and shifted this technology towards de facto industry standards for any radios.

Popularity goes hand-in-hand with commercial success and therefore, there are multiple platforms and manufacturers/developers of both SDR experimental hardware and software solutions. Powerful SDR hardware requires suitable software, that is capable of programming both CPUs and FPGAs.

The hardware side of SDR can be split into individual families based on the following criteria:

- *Flexibility of design and reconfigurability:* SDR can adapt to new modulation and air-interface algorithms simply by new software design.
- *Adaptability:* SDR adjust itself based on the network traffic and required parameters.
- *Computational power:* Processing rate of SDR in Giga Operations Per Second (GOPS).
- *Energy efficiency:* Power consumption of SDR. Very important for IoT, mobile and wearable devices.
- *Costs:* Price of the SDR platform, including training of staff, development time and hardware requirements.

The first set of SDRs rely on GPPs based on either x86-64 or ARM. Since GPPs can be used for several purposes, they are extremely versatile. Their design does not need a specialized circuits to execute specific tasks, which reduce the overall costs of running different apps. In general, GPP based SDRs are often the tool of choice for development and academia, since they are versatile, somewhat cheap and easy to program for. Their design is also familiar and their software is much more approachable in comparison to DSP and FPGA based solutions. The performance of these SDR is directly connected to the advances of conventional CPUs and GPUs. GPP based SDRs have some disadvantages as well. By design, GPPs are using sequential processing. This limits the SDRs operation in high-throughput/low-latency scenarios such as some broadband RF operations. These operations would overwork CPU and corrupt transmitted data, while discarding some frames as well. This disadvantage could be at least partially countered by deployment of GPU-based computing. GPUs are designed to process high amount of data in parallel, which is suitable approach for most of the SDR tasks. Their processing power comes at a cost - high power requirements. While the single precision and double precision of modern GPUs is growing rapidly (nVidia RTX 4090 has 73 073 GFlops) they require a significant power background (RTX 4090 requires whopping 450 W in peaks). In addition, they can't work in standalone modes and require CPUs as centralized nodes. However certain parallel operation, such as Fast Fourier Transform can be accelerated by GPU computing exponentially, which can offer real-time SDR operation. GPP-based SDR platforms include KUAR [12] and Universal Software Radio Peripheral (USRP) [13]. These platforms require desktop computers to successfully operate, which limits their portability. Desktop PCs are also power demanding in general, so their deployment into mobile SDR system is difficult and have limited capabilities of I/O. Data transfers are therefore limited by I/O bottlenecks, which leads into performance losses and difficult real-time operations.

Second variant of SDRs rely on DSPs. DSPs are basically specialized and somewhat simplified GPPs. They are designed to process digital signals in masse. In contrast to previously mentioned GPPs, they are designed with parallel processing in mind and execute some tasks faster. DSPs are usually split into two design groups - performance optimized, and energy con-

sumption optimized. Moreover, they can be further divided based on their instruction set into Single Instruction Multiple Data (SIMD) architecture and Multiple Instruction Multiple Data (MIMD) architecture. These specializations basically ensure, that each developer can choose specially what they need for the task in hand, which on the other side limit their versatility. However, DPSs have their limitations. In scenarios where massive amount of reconfigurability and/or parallelism is required, DSPs can meet their design limitations. To squeeze additional performance out of them, it is required to optimize code, which requires significant programming skills. In addition, they consume more power than FPGAs. DSP-based SDRs include the Atomix family [14].

The third variant include a FPGA of varying performance included on a motherboard. FPGAs, while having higher areas than single purpose Application Specific Integrated Circuits (ASICs), offer reconfigurability, while still maintaining high performance. In addition, any reconfigurations happen in fractions of milliseconds, so the SDR can swap from one RF technology to another. In comparison to GPPs and DSPs, they offer higher performance, lower power consumption and important portability aspect. While the FPGA based SDR offer significant advantages, they are also very hard to program for. The requirements on the programmer are enormous and it takes significant time to compile code for the platform. In addition, the programmer must have a detailed vision of the final hardware architecture in his mind to choose the ideal FPGA design pattern.

The last variant is considered by many as a future of SDR [15]. It is basically a hybrid design, where the SDR combines advantages of two or more other approaches. The newest core of hybrid SDRs is based on Radio Frequency System on Chip (RFSoC), where the RF customized FPGA is combined with multicore ARM processor. This monolithic integration eliminates need for external data converters, which enables flexible approach with up to 50 % reduced power, thanks to the elimination of FPGA-to-analog interfaces [16]. These SDRs offer the best of both worlds - flexibility of ARM based CPU and power of FPGA. There are many manufacturers that are slowly shifting towards this hybrid approach. The main disadvantage of this approach is the price of the final design.

The comparison of all designs can be seen in Table 2.1.

The USRP by Ettus/NI is one of the most commonly used SDR hardware solutions. USRP is a platform, that was developed by Ettus Research LLC, acquired by National Instruments (NI) in 2010, that provides an all-in-one high-performance SDR. The backbone of each USRP is set of four ADCs and DACs connected to daughterboards and a Xilinx FPGA. The FPGA then communicates with a PC via host connection (USB, Gigabit Ethernet, PCIe). In general, the USRP divides tasks of "digital part" of SDR between host high-performance CPU and built-in FPGA - waveform operations such as modulation and demodulation should be performed at CPU while high speed general processing is accelerated by FPGA. The general design of Ettus/NI USRP can be seen in Figure 2.2.

Table 2.1: Comparison of SDR hardware platforms based on the controlling element.

	GPP	**DSP**	**FPGA**	**Hybrid**
Computation	Fixed Arithmetic Engines	Fixed Configurable Engines	Arithmetic User Logic	Fixed Arithmetic Engine AND User Configurable Logic
Execution	Sequential	Partially Parallel	Highly Parallel	Highly Parallel with Sequential Parts
Throughput	Low	Medium	High	High
Data Rate	Low	Medium	High	High
Data Width	Limited by Bus Width	Limited by Bus Width	High	Limited by Shared Memory (CPU and FPGA)
Programmability	Easy	Easy	Moderate	High
Complex Algorithms	Easy	Easy	Moderate	High
I/O	Dedicated Ports	Dedicated Ports	User Configurable	User Configurable
Cost	Moderate	Low	Moderate	High
Power Efficiency	Low	Moderate	High	High
Form Factor	Large	Medium	Small	Medium

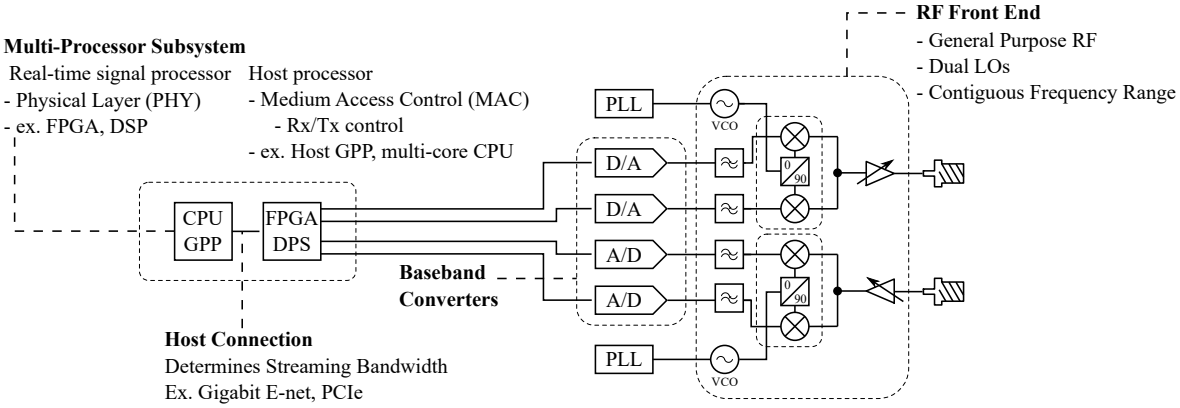

Figure 2.2: General design of Ettus/NI based USRP [13].

Since the acquisition of Ettus in 2010, the USRPs were sold under both brands. Ettus USRPs were intended for use with non-NI software, such as previously mentioned GNU radio, while the NI USRPs were developed for deployment with LabVIEW programming environment. This changed with the recent introduction of brand-new NI Ettus USRP X410 [17] which unified both platforms, see Figure 2.3). X410 is build on the new hybrid design mentioned before and offers Xilinx Zynq Ultrascale+ RFSoC which supports both Open-Source tools as well as LabVIEW FPGA programming environment.

Apart from this open-source software platform, there are others commercial solutions, that are supported by many SDRs, such as MATLAB, Redhawk or LabVIEW. Mainly the LabVIEW is an interesting platform, since its developer National Instruments (or NI nowadays) offers their own inhouse SDRs, that offers world-class hardware capabilities.

Figure 2.3: NI Ettus USRP X410.

2.6 SDR Development Tools

Development tools for SDRs can be basically split into two groups - HLS based and the rest [15]. Each have their own advantages and disadvantages, so it is up to the developers to choose the right solution for their problems.

Many software development tools rely on High Level Synthesis (HLS), which is an abstract method of designing hardware by using high level programming language. HLS are the main tool of FPGA and hybrid based SDR, since it requires no prior knowledge of hardware designs, while offering significant flexibility. Moreover HLS-based tools tend to offer similar design and features, making the platforms more accessible. HLS basically convert algorithms from high level programming language to Registry-Transfer Level (RTL) implementation [15]. HLS offers an optimized code that is comparable to hand-made code designed directly for the FPGA. These speeds up the development time, thus reduce the costs, and shift developers focus onto algorithms themselves instead of RTL implementation. HLS tools are usually offered by the major manufacturers of FPGA systems for their solutions, including Xilinx (Vivado HLS), Intel (HLS Compiler) or others which are independent on the vendor (Matlab HDL Coder) [15].

There is a plethora of other tools that can be used for SDR development. From the vast amount, only a selected few will be picked and briefly described:

- The first one is Matlab [18], which together with Simulink tends to be a building stones of many starting or even senior developers. It offers a vast range of built-in functions aimed at signal processing and communication protocols. To use the codes on other platforms, Matlab Coder and Simulink Coders have to be used to translate code from built-in language to C/C++. As mentioned before, it also offers a HDL coder. The platform supports FPGAs from Xilinx and Intel, with varying degree of optimization [19].
- The second one is GNU Radio [20], which is a well-known environment for SDR development. GNU Radio is a free and open-source software development toolkit that provides signal processing blocks to implement software radios. It can be used with low-cost

external RF hardware, as well as high-end SDRs or in in-built simulation environment. GNU radio represents the software side of SDR platform, therefore it carries out all the signal processing needed for implementation of RF technologies. It offers an array of preprepared blocks that can be extended with own custom solutions written in Python or C++ (performance-critical code) languages.

- The third one is LabVIEW [21] by NI, which is a widely used multifunctional tool. It offers a visual programming environment for testing and development of various applications for industry and academia, offering HLS like environment for FPGA programming. Its core is similar to Simulink or GNU Radio - the programmer connects multiple blocks to assemble a working application (or virtual instrument). Its main advantage is a complete integration of NI USRP platform into the programming environment, which offers a rapid prototyping platform for communication systems. If needed, the programmer can also use Matlab or C codes to substitute parts of the graphical code of an app. The employment of LabVIEW has a long history at the Department of Cybernetics and Biomedical Engineering at VSB-TUO, which is where author of this work currently resides and therefore will be used for a practical part of this dissertation.

2.7 SDR as Tool for SMART Technologies

With the rapid evolution of wireless technologies in SMART technologies, the array of currently used technologies significantly multiplied [22]. Modern manufacturing plants heavily rely on wired and wireless technologies to transfer data to centralized nodes. These technologies differ in multiple areas - transfer speeds, communication distance, latency etc [22]. The conventional technologies like LTE, 5G and WiFi are often explored by researchers all over the world [23, 24, 25, 26]. While these technologies have their massive advantages, they also tend to have their shortcomings. These small gaps can be filled in by smaller, currently rising technologies, that can be used together with the conventional solutions or completely in standalone mode.

Visible Light Communication (VLC), somewhat niche technology, is considered as a promising standalone solution, or 4G/5G/WiFi subsidiary, that has an untapped potential [23, 24, 25, 26, 27]. The dissertation will further focus on description of VLC technology and description of custom implementation in LabVIEW programming environment.

Chapter 3

Visible Light Communication

The optical wireless communications were envisioned in 1979 by Gfeller and Bapst when they carried out first experiments. At first, their pioneering work explored Infrared (IR) spectrum, but it was apparent that it could be used in other scenarios as well [28].

VLC is a type of communication, where a suitable luminaire is modulated to transmit data over light waves of visible spectrum (375–780 nm, see Figure 3.1.). VLC basically groups any technology of free-space light modulation, which is visible to human eye [27]. The main goal of this technology is to transmit data in a way that is seamlessly imperceptible to human perception. VLC seems to be capable technology for short-range or possibly in the future even long-range communications [29]. Future appliances vary greatly, spanning from vehicle-to-vehicle communications, infrastructure-to-vehicle communications or simply as an alternative to typical Local Area Networks (LAN) [LD1, 30].

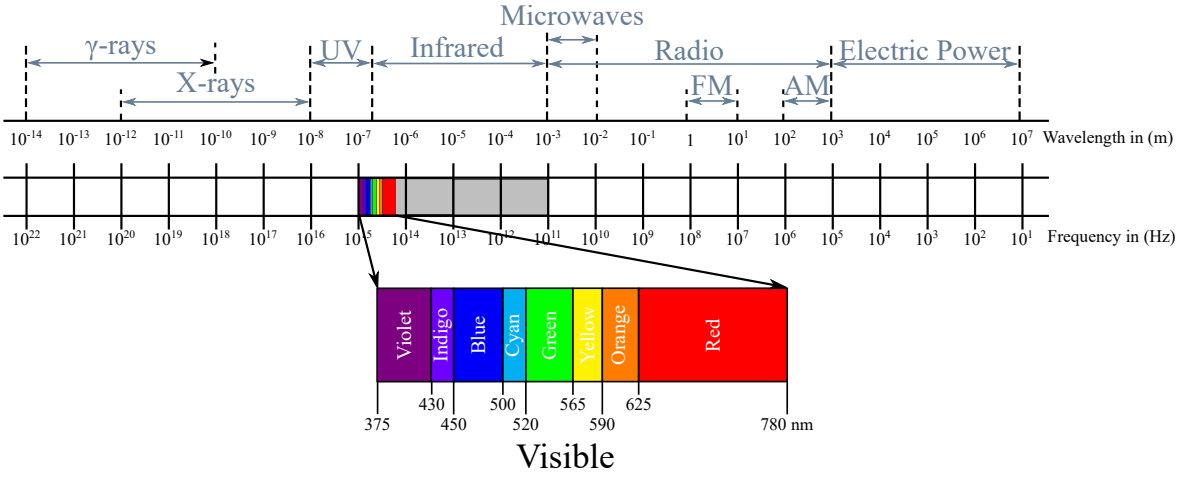

Figure 3.1: Spectrum of electromagnetic waves. The visible light area is specified.

VLC on SDR is evolving quickly. The ongoing research in this field is very volatile and trends are changing constantly. Versatility of SDR plays a significant role in research of new VLC approaches. In 2011, a 1 Mbps video stream was achievable over 3 m, when deployed on custom Light Emitting Diode (LED) matrixes [31]. In 2015, Hussain et al. tested the implementation of IEEE 802.15.7, they achieved results according to this standard, however transmission distance was limited to 1 m [32]. Nowadays, we are testing longer distances and mainly higher data rates, even on commercial light sources.

The focus of academia on VLC is rapidly increasing. With the widespread deployment of RF technologies to everyday life, the world is constantly searching for alternative or supplementary solutions to already existing infrastructure. Since the LEDs are rapidly expanding across the whole lighting industry, the technological limitations of luminaires are not pushing back VLC research any longer. LEDs are capable of precise and high-speed on-off control of illumination, which is required for successful implementation of VLC into practice. Moreover, traditional illumination devices are currently being replaced by LED light sources, and this trend is quickly accelerating. Energy savings and reduced maintenance costs are the major advantages and influence its urban deployment and car manufacturers integration [33].

3.1 Light-Emitting Diode

The widespread adaptation of LEDs was one of the main reasons, why VLC attracted attention. When the LED was invented, a new era of lighting begun [34]. Light-emitting diode has multiple significant gains such as long lifespan, low power consumption, high tolerance to humidity, high efficiency, and mainly fast switching capabilities, which is also a major difference to conventional incandescent and fluorescent lamps. This discovery and possibility of fast switching is the main reason why LED can be used for data communication [35].

LED itself is a semiconductor light source that is incoherent, which means that there is a phase difference between the individual emitted photons. The basis of the LED is the P-N junction, which is formed at the interface of two doped semiconductors. One is N-type (cathode, negative conductivity), the other is P-type (anode, positive conductivity). For the N-type semiconductor, elements from the fifth group of the periodic table of elements (arsenic, antimony, phosphorus) are used, for the P-type semiconductor elements from the third group of the periodic table of elements (aluminium, gallium, indium) are used. The area at the interface of the P-N transition is called the forbidden band or band gap. If we connect a diode in the pass direction with a applied field strength large enough to overcome the forbidden band, current will start to flow through the circuit. The width of the forbidden band is not constant in semiconductors. Radiative recombinations in LEDs are called spontaneous emission. Recombinations take place over a wide range of energy states, which is why LEDs have a wide spectrum.

Nowadays, the most common commercial LED is the white light LED. In comparison to other colors, which are created directly by introducing specific doped semiconductors, the white LEDs are created by two well-known methods. The first one is blue light LED covered in phosphor layer. The photons emitted by blue LED pass through the phosphor layer and part of them are converted into yellow light. By combining the remaining blue light with newly converted yellow light, a bright white light is generated. The second approach is to use RGB LEDs and combine all of the colors. Both approaches have their own advantages and disadvantages. In general, the first approach is much more common, due to the much lower price and higher efficiency. In contrast, RGB LED might be more suitable for VLC, since it offers direct modulation of individual colors [36].

In general, there are multiple types of LED, which based on their characteristics, are more or less suitable for VLC:

- *Phosphor Converted LEDs (pc-LEDs):* Low complexity and costs. Blue LED coated by a phosphor layer, which produce white light. Very limited band and slow response due to the construction.
- *Multichip LEDs:* Consists of three or more chips, which produce different colors (usually RGB). Ability to control individual colors and modulate them separately - Multiple-Input Multiple-Output (MIMO) communication. The main driving force behind color-shift keying modulation format.
- *Organic LEDs (OLEDs):* Consists of thin layer of organic films between semiconductors. Nowadays mainly used for displays. By construction very thin, light and even bendable. First generation of OLEDs suffered from various lifespan of individual colored LEDs.
- *μ-LEDs:* An array of very small LEDs. Usually used in the newest displays. Produce high density panels which can reach very high speeds. Very pricy.

3.2 Advantages, Disadvantages and Challenges

The main advantage of VLC lies in the employment of existing infrastructure. As mentioned before, LEDs are getting very popular - their deployment is rapidly accelerating. LED lights that are already used in majority of newly produced luminaires. These luminaires are all potential VLC transmitters, which could be modulated to transmit data - LED can perform communication functionality while maintaining the original function as illumination lighting, thus potentially saving energy [37].

VLC has major advantages over traditional radio-frequency systems. First and foremost, the VLC spectrum is unlicensed and currently unused and thus provide congestion free channels. Conventional Wireless Fidelity (Wi-Fi) standards are currently overused, as a number of free channels in highly urbanized areas are almost non-existent (Andjamba et al., 2016) [38].

While the WiFi can operate in a band from 2 kHz to 300 GHz, the visible light spectrum spans from 380 THz to 750 THz, which is more than 10 000 times larger [39].

VLC does not penetrate walls, so the whole spectrum can be theoretically reused for every factory, flat or even room. In addition, it provides a certain degree of security since the light would have to be directly reflected to eavesdrop on the data transmissions. The problematics of VLC security is currently explored by multiple teams [40, 41, 42].

VLC also has disadvantages. The main downside is that the achievable data rate decreases significantly with increasing link distance, which limits the range of high data rate VLC deployment possibilities. Since VLC is also non-coherent form of communication and the path loss is proportional to the distance raised to the fourth power, as opposed to RF. VLC link data rates are also degraded by shot noise when a photodiode receiver is exposed directly to the sunlight (saturation) [43, 44].

VLC also has a number of currently unsolved challenges. The first on is reliability on Line of Sight (LoS) communication. Most of the VLC systems assume, that the transmitting and receiving elements are in direct LoS situation . However there are situation, where even Non Line of Sight (NLoS) or diffused light can be used for communication. These variants are often plagued by limited data rates and problems with signal loss. The development of VLC NLoS communication and localization system is currently very actual topic and is explored by multiple teams [45].

Another challenge lies in the flickering of LEDs. By its definition, it is the fluctuation in the brightness of the light, which is perceptible by human eye. This challenge is usually avoided by deployment of sufficient modulation scheme in combination with suitable carrier frequency. In general, the threshold at which the human perceives flickering is around 3 kHz. The universal recommendation is, that when the LED is idle, the brightness should be maintained at a frequency, that is above this threshold [46].

VLC is also plagued by noise induced by different light sources, including the Sun itself. This is especially problematic in outdoor scenarios. In addition, the light have also problems with multipath propagation, which happens due to reflective surface, so the signal can be delayed in time. This problem can be countered by optical filters, which reduce or completely remove noise from natural sources or by sufficient amplification of the transmitted/received signal. Another possible solution is the usage of alternative receiver, such as cameras, Complementary Metal–Oxide–Semiconductor (CMOS) chips or diodes.

The possible biggest issue lies in uplink. While the downlink communication tends to be straightforward, getting data back to the node tends to be problematic. The main strength of VLC lies in its unidirectional design, where the indoor or outdoor light sources can be used as transmitters of information. The uplink is usually solved either via RF channel or infrared technology, which is not perceivable to human eyes. VLC itself can be also used for

uplink communication, but the transmitting devices tend to be limited in their designs (i.e., smartphones), so the integration of this technology might be difficult.

Dimming support of LEDs is also problematic, since most of them are controlled by Pulse Width Modulation (PWM), which interferes with any effective data transmissions. The dimming support has to be embedded into the modulation format itself, or there must be an alternative way how to influence the brightness of the LED bulbs. This issue is currently solved by usage of either color shift keying or variable pulse position modulation described further below.

3.3 VLC IEEE Standardization

Institute of Electrical and Electronics Engineers 802.15.2.7, known as Short-Range Wireless Optical Communication Using Visible Light and its amendment 802.15.2.7a called Short-Range Optical Wireless Communications Amendment: Higher Speed, Longer Range Optical Camera Communications are basic standards which define PHY and Medium Access Control (MAC) layers of visible light-based communications in transparent media [46, 47]. According to the scope, systems compliant with this standard should deliver data rates suitable enough for audio and video multimedia services, while considering mobility of the optical link.

The standard was created based on VLC research background and provides the following [47]:

- Access to several hundred terahertz of unlicensed spectrum.
- Immunity to electromagnetic interference and noninterference with RF systems.
- Additional security of visible light systems - user is allowed to see the communication channel.
- Communication augmenting and complementing existing services (e.g., illumination together with data transmission).

The standard itself considers three basic device classifications (Table 3.1) and three basic MAC topologies (Figure 3.2) [47].

Table 3.1: Device classifications according to the standard.

	Infrastructure	**Mobile**	**Vehicle**
Fixed coordinator	Yes	No	No
Power supply	Ample	Limited	Moderate
Form factor	Unconstrained	Constrained	Unconstrained
Light source	Intense	Weak	Intense
Physical mobility	No	Yes	Yes
Range	Short/long	Short	Long
Data rates	High/low	High	Low

Star topology consists of one centralized controller, which is called the coordinator. In case of peer-to-peer topology, one of two entities must take up the role of coordinator. In case of

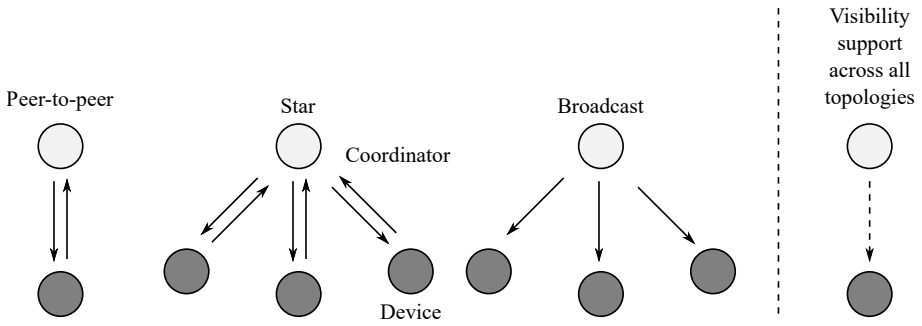

Figure 3.2: Device topologies according to the standard.

the broadcast topology, the centralized node transmits one-way messages to every participant. In general, the coordinator is usually grid connected, while the individual devices are battery powered. Each coordinator has a unique 64-bit address, while the individual devices have shortened 16-bit address that identifies them [47].

Optical Personal Wireless Area Network (OPWAN) node requires a PHY layer, which contains the light transceiver along with low-level control mechanism and a MAC sublayer, which provides access to the physical channel for all types of transfers.

MAC sublayer specifications have multiple important roles in the concept of VLC:

- Generating beacon for coordinators.
- Synchronize the network across individual beacons.
- Provide color functions, if available.
- Provide visibility if the link.
- Provide dimming capabilities of luminaires.
- Introduce flicker-mitigating scheme.
- Provide channel quality information along with visual indication of device status.
- Provide a link between individual MAC entities to further expand functionality.
- Provide a system for mobility of nodes.

Each MAC frame consists of three parts - header, payload and footer [47]. These change according to the PHY layer class (described further below) and network topology.

The standard specifies six PHY tasks, that are a necessary part of every OPWAN node [47]:

- Activation or deactivation of Overview of Optical Wireless Communication (OWC) transmitter and receiver.
- Wavelength Quality Indicator (WQI) for received frames.
- Channel selection.
- Data transmission and reception.
- Error correction techniques.
- Synchronization techniques.

Based on the deployment scenarios and requirements of individual technologies, six PHY service classes are defined, limited mainly by reachable transmit speed and environmental limitations. They are defined by different modulation schemes, forward error correction techniques and data rates. First three were part of the original standardization and therefore use LED light sources and suitable photodetectors [46]. The last three were added during the amendments and are mainly focused on camera-based communications [47]. These classes are:

1. *PHY I:* PHY I is designed for applications that rely on low data rates. PHY I services either use On-Off Keying (OOK) or Variable Pulse Position Modulation (VPPM) and data rates in hundreds of kbps.
2. *PHY II:* PHY II is in comparison designed for applications requiring high data rates. These services use either the OOK or VPPM and data rates in tens of Mbps.
3. *PHY III:* PHY III is mainly designed around Color Shift Keying (CSK) modulation scheme. It operates at comparable speeds to PHY II, but is used in scenarios, with multiple individual channels, each at different wavelength (color).
4. *PHY IV:* PHY IV class was added in the mentioned amendment. This class combines modulation techniques that employ cameras as receivers: Undersampled Frequency On-Off Keying (UFSOOK), Twinkle VPPM, Spatial Two-Phase Shift Keying (S2-PSK), Hybrid Spatial Phase Shift Keying (HS-PSK), Offset Variable Pulse Width Modulation (Offset-VPWM). It is designed to be used with discrete light sources.
5. *PHY V:* PHY V class is another extension of the original standard. It is designed to operate with diffused surface light sources. Suitable modulation schemes include: Rolling Shutter Frequency Shift Keying (RS-FSK), Camera On-Off Keying (C-OOK), Camera M-ary Frequency Shift Keying (CM-FSK) and Mirror Pulse Modulation (MPM).
6. *PHY VI:* PHY VI is designed to operate with video displays. Suitable modulation schemes are: Asynchronous Quick Link (A-QL), Hidden Asynchronous Quick Link (HA-QL), Variable Transparent Amplitude-Shape-Color (VTASC) or Sequential Scalable Two-Dimensional Color (SS2DC).

While the standard and its amendment introduced important concepts and helped to accelerate VLC research, it is still constrained by the choice of modulation formats and therefore the maximal reachable transfer rates. The following subchapter will focus on modulation formats, that are widespread in the VLC development.

3.4 Modulation Formats

There are multiple modulation formats, that can be considered as suitable for VLC. Their employment heavily relies on correct receiver design and choice. While some can employ conventional photodetector to capture the transmitted signal, others rely on CMOS chips

or highspeed cameras. This chapter will summarize the current trends in VLC modulation formats.

3.4.1 On-Off Keying

OOK is a simple type of amplitude modulation. The datastream is represented by presence or absence of the source signal, which means, that zeroes and ones are directly connected to the level of amplitude of the transmitted/received signal. OOK is freely transferable to VLC, since the luminaire standardly operates in on and off conditions. Therefore, this modulation scheme is basically the easiest to implement. The main drawback is the effective transmit speed - higher speeds can be only reached by employment of massive MIMO operation.

3.4.2 Variable Pulse Position Modulation

VPPM is the second most popular modulation format for VLC. It is a combination of two modulation formats - Pulse Position Modulation (PPM) and PWM. PPM use a constant value of width and amplitude of individual pulses. These pulses are distributed in variable positions in time, which corresponds to their digital value. The main drawback of PPM modulation is limited data rate, since only one pulse per symbol is transmitted at specific time. In comparison, PWM recognize the pulse length at a specific time period to determine its value. Their combination, VPPM, is used in scenarios with dimmable light source. While the position of pulse determine its value, the length corresponds to the brightness of the luminaire. The main drawback is the high reliance on robust dimming solution.

3.4.3 Color Shift Keying

CSK modulation is based on the modulation of individual color elements. The intensity of individual colors is used to determine the value of signal. This modulation heavily relies on multi-chip LED design. In contrast to OOK and VPPM, CSK offers significantly higher transmit speeds. CSK is closely connected to CIE 1931 diagram, which defines seven available wavelengths, which can be used as basis for RGB source. The resulting constellation points are influenced by intensity modulation of individual color chips.

3.4.4 Quadrature Amplitude Modulation

Quadrature amplitude modulation is a type of digital modulation in which both amplitude and phase components to provide a form of modulation that can provide high levels of spectrum usage efficiency. It uses two carrier signals that are offset from each other by $\frac{\pi}{2}$. The two carrier signals are modulated separately, then summed, this sum gives the Quadrature Amplitude Modulation (QAM) modulated signal. At the destination, the carriers separate, and the

data is extracted from each. Then, the data is incorporated into the original modulating information. The system itself use both phase and amplitude variations to boost the efficiency of VLC system. However, the whole system can be susceptible to noise, since in case of higher order QAM formats, the individual transmission states are close to each other, and the receiver might have trouble distinguishing between them.

3.4.5 Orthogonal Frequency Division Multiplexing

Orthogonal frequency division multiplexing (OFDM) is a digital multi-carrier modulation scheme that employs a series of partially overlapping and closely spaced orthogonal subcarriers to transmit data stream through a frequency limited channel. Each individual subcarrier is modulated using a conventional and simpler modulation scheme like (usually M-QAM or QPSK) at much lower symbol rates. This approach allows the system to transfer data with transmit speeds similar to single carrier modulations while offering much more robust communication channel [48].

OFDM can be freely compared to conventional Frequency Division Multiplexing (FDM). FDM also use sperate parallel frequency channels, but they are individually separated by a configurable frequency band. In comparison OFDM employs a set of orthogonal subcarriers and a guard interval is added to each symbol, which functions like a guard band against inter-symbol interference (ISI) [49]., channel delay spread, thus also again multipath propagation. The core of OFDM lies in the close relationship between frequency and time domains. When operating in frequency domain, each subcarrier is modulated with complex data and then fed into an inverse Fast Fourier Transform to produce OFDM symbol in time domain. Symbol is then further processed in time domain – guard interval is inserted between symbols. A set of OFDM symbol is then used to produce the final OFDM signal. The receiver then has to carry out an inverse process to the receiver – deletion of guard interval and Fast Fourier Transform to convert signal from time domain back to frequency domain, which contains the original data.

OFDM signal can be in frequency domain described as a set of subcarriers, that take a form of *sinc* function with side lobes that are overlapping with neighboring subcarriers. Since these lobes could be considered as a noise in closely spaced FDM system, orthogonality must be maintained to avoid it. At these orthogonal frequencies, maximum of each subcarrier lines with minimum of the surrounding subcarriers. The system is therefore not compromised and is able to extract the original signal. The orthogonality must be therefore maintained at all costs. When the signal is received, it is processed and multiplied by a set of sinusoids, so the original bit stream can be extracted. Since the spacing of subcarriers is so close, the OFDM offers a spectrally efficient way of transmitting data. In addition, the system is much more resistant to ISI, in comparison to conventional FDM [49].

A single OFDM symbol consists of N output samples from the IFFT. During the IFFT frequency-domain input data is processed and converted into the time-domain output data. Individual input bits are specifically grouped and consequently mapped to data symbols, that are a complex number that represents the modulation constellation point of the specific modulation format, such as N-QAM. These mapped symbols are processed by the transmitter as the frequency-domain signals and are the inputs to an IFFT block which therefore converts the signal into the time-domain. The IFFT use N source symbols, where N corresponds to the number of subcarriers which will be used by the system. Each input symbol has a symbol period of T seconds. After IFFT, a set of N orthogonal sinusoids, is converted. Individual sinusoids each correspond to a different carrier frequency. The individual symbols can be considered as complex values which represent the mapped constellation point, so they specify the amplitude and phase parameters of the subcarrier sinusoid. The signal is then transmitted via a suitable medium. At the receiving side, an FFT block is used to process the signal and convert it back into the frequency domain.

As mentioned before, OFDM is highly reliant on the orthogonality. To maintain it, individual carriers must be mathematically orthogonal. Since the receiver can be considered as a wide bank of demodulators that translate signal back to DC, each of the subcarriers has to be integrated over a symbol period to recover the original data. Subcarriers can be considered linearly independent or orthogonal, if the spacing of subcarriers is a multiple of $\frac{1}{t}$ [49].

If represented mathematically, lets suppose that a set of signals Ψ is present, where Ψ_p is the p-th element in the set. The signals can be considered orthogonal if:

$$\int_a^b \Psi_p(t)\Psi_q^*(t)dt = \begin{cases} K \text{ for } p = q; \\ 0 \text{ for } p \neq q, \end{cases} \tag{3.1}$$

where * indicates the complex conjugate and interval $[a, b]$ is a symbol period of the individual signal.

Since its necessary to avoid a large number of modulators/demodulators and filters at both transmitting and receiving side, it is better to be employ modern digital signal processing techniques (such as FFT).

Each subcarrier can be described as a complex wave:

$$S_c(t) = A_c(t)e^{j|\omega_c t+\phi_c(t)|}. \tag{3.2}$$

The real signal corresponds to the real part of $S_c(t)$. Both $A_c(t)$ (amplitude) and $f_c(t)$ (frequency) are variable on a symbol by symbol basis. However values of these parameters are constant during the symbol duration period t.

Since OFDM consists of multiple subcarriers, the complex signals $S_s(t)$ are therefore rep-

resented by:

$$S_s(t) = \frac{1}{N} \sum_{n=0}^{N-1} A_n(t) e^{j|\omega_n t + \phi_n(t)|}. \tag{3.3}$$

where

$$\omega_n = \omega_0 + n\Delta\omega. \tag{3.4}$$

This signal is continuous. If the waveforms of each component of the signal over one symbol period are considered, then the variables $A_c(t)$ and $f_c(t)$ have specific fixed values, which rely on the current frequency of that particular subcarrier. The equation can be rewritten as:

$$\begin{aligned} \phi_n t &\Rightarrow \phi_n, \\ A_n t &\Rightarrow A_n. \end{aligned} \tag{3.5}$$

When the signal is sampled with $\frac{1}{T}$ sampling frequency, the resulting signal can be represented by:

$$S_s(kT) = \frac{1}{N} \sum_{n=0}^{N-1} A_n e^{j|(\omega_0 + n\Delta\omega)kT + \phi_n|}. \tag{3.6}$$

At this point, the time over which the signal is analyzed is restricted to a set of N samples. Since the system samples over the period of one data symbol, this relationship can be considered:

$$t = NT. \tag{3.7}$$

By simplifying the previously mentioned Eq. (3.6), by setting $\omega_0 = 0$, the signal is transformed to:

$$S_s(kT) = \frac{1}{N} \sum_{n=0}^{N-1} A_n e^{j\phi_n} e^{j(n\Delta\omega)kT}. \tag{3.8}$$

This equation can be further compared to the general form of the inverse Fourier transform:

$$g(kT) = \frac{1}{N} \sum_{n=0}^{N-1} G\left(\frac{n}{NT}\right) e^{\frac{j2\pi nk}{N}}. \tag{3.9}$$

By examining the Eq. (3.8) closer, it is noticeable that the function $A_n e^{j\phi_n}$ is basically a definition of the processed signal in the sampled frequency domain, and $S_s(kT)$ corresponds to the time domain representation. Both equations can be considered equal when:

$$\Delta f = \frac{\Delta\omega}{2\pi} = \frac{1}{NT} = \frac{1}{t}. \tag{3.10}$$

This specific condition was set earlier as a strict requirement for orthogonality of subcarriers.

During the operation of usual OFDM system (Figure 3.3), the incoming serial data is converted from serial to parallel and grouped into series of x bits, that form a set of complex numbers [49]. The number x determines the signal constellation of the modulation format used for the corresponding subcarrier (i.e. N-QAM). These complex numbers are modulated in a baseband style by IFFT and then summarized back into to serial data stream that is prepared for transmission. A guard interval of specific length is inserted between symbols to avoid ISI caused by multipath propagation – length is chosen as tradeoff between robustness of the link and transmit speed. The individual discrete symbols are processed to analog and filtered to be prepared for RF up conversion by heterodyne or superheterodyne transmitter. The receiver performs the inverse process.

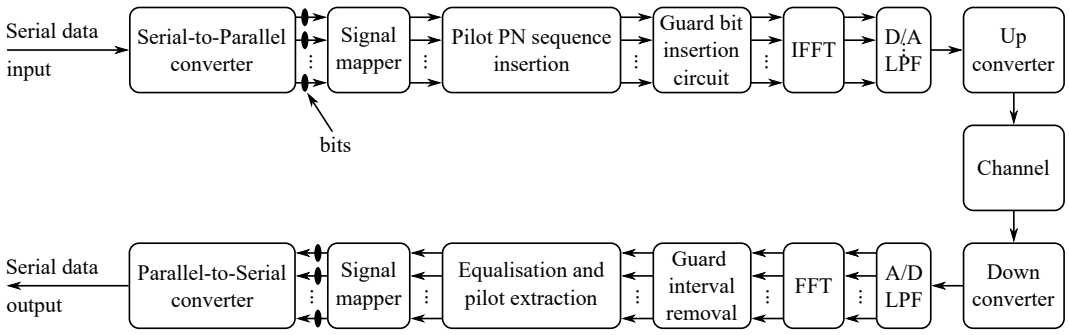

Figure 3.3: Diagram of the conventional OFDM system.

Since the OFDM brings along significant number of advantages, it is nowadays a go-to technology for many high speed telecommunication systems. The most important advantages of OFDM are:

- **Immunity to selective fading** — OFDM is much more resistant to frequency selective fading than single carrier systems since the the channel is divided into multiple narrowband signals that are affected individually as flat fading sub-channels.
- **Resilience to interference** – Channel interference can be bandwidth limited so not every subchannel is affected. This means that not all the data is lost.
- **Spectrum efficiency** – Using close-spaced overlapping sub-carriers means that the spectrum is utilized much more efficiently.
- **Resilient to ISI** – OFDM is very resilient to inter-symbol and inter-frame interference.
- **Resilient to narrow band effects** – When adequate channel coding and interleaving is used it is possible to recover some symbols that were lost due to the frequency selectivity of the channel and narrow band interference.
- **Simpler channel equalisation** – As the OFDM is using multiple sub-channels, the channel equalization becomes much simpler.

However there are also some disadvantages that must be mentioned:

- **High peak to average power ratio (PAPR)** – An OFDM signal has a noise like amplitude variation and has a relatively high PAPR. This impacts the RF amplifier efficiency as the amplifiers need to be linear and accommodate the large amplitude variations.
- **Sensitive to carrier offset and drift** – OFDM is also sensitive to carrier frequency offset and drift. Single carrier systems are in comparison much less sensitive.

3.5 Visible Light Positioning

Visible Light Positioning (VLP) holds the potential to overcome the instability of radio frequency multi-path propagation in cramped or EMI impaired environments. It offers a centimeter-level positioning accuracy, low-cost, and high security. While this technology is not standardized yet, there is currently a steadfast push for international standardization. VLP systems basically employ LED-based illumination light sources for positioning and/or communication. VLP can work in standalone mode with all the mentioned advantages and disadvantages of VLC (mainly occasional LoS blockage or the sparce density of lighting in some industrial complexes) or it can be combined with other energy efficient approach to create a hybrid platform for centimeter grade localization of workers, pedestrians or industrial machines [50, 51, 52].

Basic VLP can be basically distinguished into separate groups, based on their internal functionality. According to a VLC-based positioning survey by Do et al. [53], many solutions well known from radio frequency technologies can be used for positioning. Among them is Cell-ID identification, which was also proposed by Krommenacker et al. [54]. Since the LED lighting sources are deployed as a part of newly constructed building or industrial complexes, the localization system would not require any additional infrastructure and meets the availability, coverage and scalability requirements for this type of application. Furthermore, Cell-ID is a straightforward positioning method based on cell information. It is usually implemented in cellular networks to locate mobile phones according to a unique identifier of each transmitting element forwarded by Base Transceiver Stations (BTS). The accuracy of such a system varies according to the cell size (from 150 m micro-cells in urban areas up to 30 km for rural areas) but is reliable enough for weather and traffic reports. While this approach is not common for indoor positioning, VLC could fill in the missing gap. Industrial LEDs can be engineered to operate even in extremely harsh environments and produce a pure flicker-free white light, thus improving safety. Ceiling-mounted LED lights can therefore be used as VLC transmitters. By assigning a unique Cell-ID to transmit light sources a reliable positioning system can be built. Cell-ID is a code that corresponds to a cell identification number stored in a position database. Each LED light source would be therefore assigned with a specific geographic location. The Cell-ID technique can be therefore somewhat reliably

used for positioning reaching even higher reliability when used for True Range Multilateration or in addition to scene analysis techniques.

Apart from the Cell-ID variant, also known as proximity identification, fingerprinting, or scene analysis is another candidate for localization. This technique is based on the estimation of relative position by matching online measured data with pre-measured location-related data. Given the irregularities in the distributions of base stations, the indeterminism in the presence of barriers in the environment, and even the inherent variance of each base station, the features (or fingerprints) of measured data vary at different locations. For example, due to the uneven distribution of LEDs, the reflections and the scatter of light caused by walls and passing vehicles, and the received power varies at different positions in the tunnels.

Triangulation is another type of positioning method used for VLP. It determines the absolute position by using the geometric properties of triangles. There are actually two derivations of triangulation: (i) lateration, and (ii) angulation. *Lateration techniques,* which involve the Time of Arrival (ToA), the Time Difference of Arrival (TDoA), and the Received Signal Strength (RSS), estimate the position based on the measured data distances from the vehicle to multiple LEDs light sources. *Angulation,* map or Angle of Arrival (AoA) relies on the measured angles relative to multiple base stations to find the position of the vehicle. However, apart from RSS-based schemes, which could be significantly influenced by impurities on transmitting/receiving elements, the other techniques require precise synchronization, since they are dependent on received/transmitted timestamps. The precise synchronization is nowadays often carried out via GNSS (Global Navigation Satellite Service) – the system would instead require a centralized synchronization server. A disadvantage of GNSS is the applications' option because this synchronization can be used only outdoor for navigation satellites. Indoor synchronization can be provided by fixed tags or by connecting to an external GNSS station.

Another technique is based on (computer) vision analysis. It involves the geometric relations between the 3D positions of objects in the real world and their 2D positions in their projections on the image sensor. All of the geometric relations in vision analysis are derived from the pinhole camera model. Vision techniques have the biggest accuracy among all localization variants. However, the computational requirements are significant and might be therefore unsuitable for the dynamic localization of multiple elements (such as in the case of a manufacturing plants or shopping malls).

VLP techniques can be also divided into active and passive solutions, which are categories well-known from common localization techniques. *Active localization techniques* require a tag or active component, such as a photodetector, a mobile phone, a CMOS camera or any other embedded solution, which must be directly equipped by the monitored user/device. In addition, most of these techniques require a direct LoS, which is both an advantage (security) and a disadvantage (coverage). In comparison, *passive VLP techniques* omit the previous requirements and do not require an explicit intervention of the user or monitored device.

These algorithms not only use the direct LoS but also the scattered or diffused components of the light [55]. The localization itself is typically based around existing infrastructure, which is analysed beforehand, instead of using a piece of dedicated wearable equipment. These methods often estimate the location of the monitored object by studying the effects of received power due to the shadows formed by the object itself. These methods are therefore often using some kind of fingerprinting together with AI algorithms or machine learning.

The researched solutions usually build upon one of these technologies or combine specific aspects from multiple design schemes. There are also somewhat unique solutions, which were not introduced before. Among them is a study by Sato et al. [56], where the team used a phone ambient light sensor to measure received signal level, the deployment of a similar technique might be difficult in an industrial environment. While the mentioned work introduced a very interesting and functional concept, that is also reaching satisfactory localization precision, its deployment might be difficult in industrial plants, which have very strict rules and often dangerous environments. However, the presented approach offers an affordable solution for indoor localization.

Another system was presented by Li et al. in 2021 [57]. Their system used a dual-model LED solution, which worked in a multi-path propagation scenario. The solution relied on a Cramér-Rao lower bound derivation of radiation angle approach. They state, that in a highly reflective indoor environment, the contribution to the total light power from multi-path propagation may be even greater than that from LoS transmission. This information is even more important in the case of industrial complexes, which are often heavily using glass and metal surfaces, which tend to be reflective. The presented experimental results confirmed earlier simulations and reliably verified that the VLP system can be used in reflective environments, as the team managed to mitigate NLoS multi-path reflections.

Platooning and collision avoidance is another important topic, especially for manufacturing plants and truck transportation. Forklifts and other vehicles are usually driven at the highest possible speed (in regards to safety protocols). In many highly congested situations, the vehicles are in close vicinity and even slight deviations can lead to disasters. Soner et al. in 2021 [58] designed a system, that is based on VLC and VLP principles. The designed system reached a higher frequency rate than LIDAR, while also offering cm-level accuracy under harsh road-like conditions. Their receiver is implemented as an AoA-sensing high-accuracy and high-rate solution with low costs called QRX. Further tests, including the real driving scenarios, are currently planned, as the research was currently backed up only by simulations.

The classification and comparison of VLP based techniques are difficult, as the environment is currently highly volatile due to extensive research. The early research shows, that the VLP-based system can be fully compared to the radio frequency-based one, but real-world tests are still needed.

Chapter 4

Dissertation Thesis Objectives

From the results of the research activities published by the author and based on the general overview of the VLC problematics, several directions have emerged which, in the author's opinion, have not been sufficiently addressed yet. In particular, there is insufficient application research on VLC OFDM implementation in some specific fields of interests.

The objectives of the PhD thesis are supported by three impacted publications [LD1, LD2, LD3, LD4], in which the author summarizes the basic research and the results of the initial experiments. Depending on the above-mentioned facts, the objectives of the doctoral dissertation have been determined as follows:

1. *State of the art research of SDR platforms, VLC systems, modulations or technologies and SDR-based VLC solutions* – VLC area is even more volatile than RF – new modulation formats are introduced periodically, including optical OFDM variants. The state of the art overview has to be repeated constantly to maintain at least a general overview of the whole problematics. Based on this research a suitable modulation which can be implemented on SDR must be chosen.
2. *Creation of the function description of the next generation of modular VLC platform, pinpointing important design choices and hardware/software limitations* – Requirements for the final platform tend to vary greatly, mainly according to the current research in other areas of interest. The platform must adapt to these changes and be steered into the right direction (i.e., medicinal deployment has different requirements than smart water meters).
3. *Development of new iteration of VLC system, that offers high degree of modularity while maintaining its key multidisciplinary concept* – The hardware available at the university is constantly changing. New SDR might be acquired as part of research project and the hardware implementation should reflect that.
4. *Experimental verification of the developed VLC system, along with optimization of the whole platform and evaluation of the obtained results* – The platform should be tested

in multiple scenarios to discover its limits. These tests should be performed both in the laboratory and in the field in order to create a sufficient sample.

The primary benefit of robust modular OFDM SDR-based VLC system is its adaptability to different environments. The developed platform could be tested in multiple scenarios, spanning from conventional indoor lighting to smart water metering, V2X communication, medical devices deployment, home occupancy detection and others. Alternative communication technology is especially interesting for explosive or highly volatile environments, in which the deployment of RF-based technologies is limited or completely forbidden. The ongoing advances in the SDR area might accelerate the whole research even further.

Chapter 5

Experimental Platform for VLC Development

Research of standalone SDR based VLC platform at Technical University of Ostrava started in years 2017–2018, when the search for the most suitable system begun. High level of modularity was the main criteria for final solution, as the system was planned for testing of both indoor (ceiling lights) and outdoor (public lighting and vehicular lights) light sources on one platform without unnecessary modifications to backbone software/hardware. Extensive experience with NI hardware and LabVIEW environment led to a system based on virtual instrumentation. NI software defined radios (USRPs) provides robust platform, which can be quickly modified by software edits. However, there were some limiting factors, such as operating frequency of original RX/TX cards and lower throughput of gigabit LAN interface, which had to be solved. So far, three consecutive versions of VLC system were designed, with fourth one currently in development by the author.

As mentioned before, main goal was to develop a platform for testing of multiple scenarios. The first one is indoor VLC, where ceiling light are used as transmitters. By covering a room with intersecting light sources, it is possible to switch to Light Fidelity (Li-Fi) completely, instead of Wi-Fi. Li-Fi also offers somewhat higher security, as the receiver must be in direct line of sight of transmitting light source. However, it is possible to reflect light by a mirror and eavesdrop that way. That's why multiple teams explore VLC security in their studies. Li-Fi also doesn't interfere with devices in hospital and can be therefore used for internet connection instead of Ethernet cables.

Another possible VLC deployment includes scenarios with pedestrians or vehicles. Public lighting or car tail/front lights can be used as transmitters. Recently, VLC resurfaced as possible candidate for Vehicle-to-Everything (V2X) communication. V2X concept include many other solutions, such as Vehicle-to-Vehicle (V2V), Vehicle-to-Infrastructure (V2I), Vehicle-to-Pedestrian (V2P) or also Vehicle-to-Grid (V2G). Comprehensive system, where conventional

vehicles or even autonomous vehicles communicate with infrastructure could be crucial for their further technological advances. That's why a cooperation with industry leading manufacturers of car lights was established. Currently, lights from Skoda vehicles, provided by mentioned partners, are used for experiments.

Apart from research on commercially available lights, influence of LED quality on VLC system was also tested. Two testing stands with interchangeable LED matrixes of varying quality were developed. Search for the best price/performance ratio is crucial, since even slight increase of manufacturing costs might be influential for manufacturers of commercial lights.

The development of the platform is practically a cyclical process with some optional steps, as can be seen in Figure 5.1. The whole system relies on periodically updated knowledge base about VLC system design, modulation formats, hardware platforms etc. These insights are then used to adjust two foundation stones - software and hardware. Software is designed as a virtual instrument in LabVIEW, since this brings in additional advantages. The most important is the software portability - the whole system can be freely transferred to a new, NI compatible, hardware platform, thus significantly shortening the development time. The code can be also swiftly adjusted and tested on the fly, thanks to the concept of virtual instrumentation. Hardware design is built around the SDR itself - any optional parts are used as standalone modules. The individual parts can be therefore exchanged at will, i.e. new amplifiers can be introduced, new improved receiving elements can be tested etc. This also brings a huge disadvantage – dimensions of the system. Even when they are small, the individual modules and connecting cables, together with additional power sources occupy a significant amount of space.

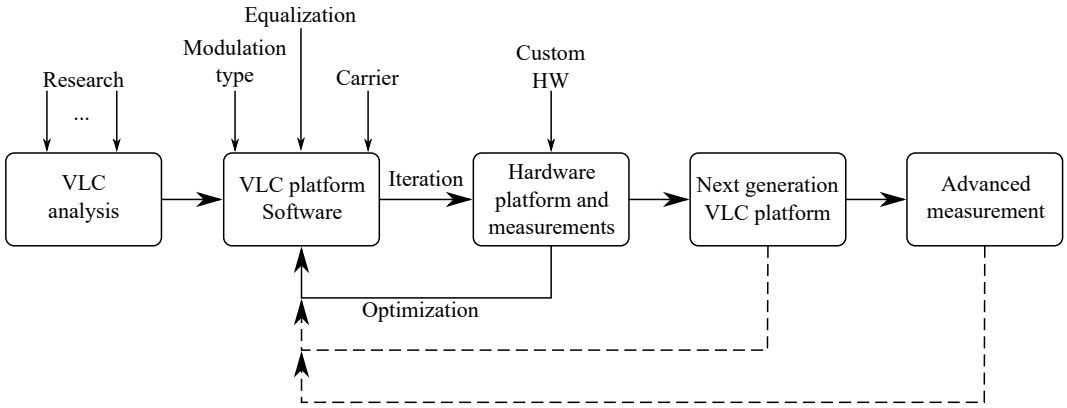

Figure 5.1: Cyclical process of VLC platform development both software and hardware wise.

Individual optimization steps are carried out based on measurements in different scenarios. First optimizations are noticeable right in the beginning, when static tests are carried out. These early problems are distinguishable in the overall performance of the platform or on

constellation or eye diagrams. If the system passes through these early tests, it is used for more advanced scenarios, like those with movable parts or in harsher conditions. These other tests are designed to test the effective limits of the whole platform, so they provide additional info, which might be incorporated into the controlling software or hardware.

5.1 First Version - QAM System

First version of VLC system based on virtual instrumentation was using QAM modulation. The control software was based on heavily modified Modulation Toolkit code, that is available as part of the official NI distribution. Two older NI USRP-2921 were used as transmitting/receiving elements. However, since the original TX and RX cards operate in GHz bands, they had to be replaced with older Ettus LFRX/LFTX Daughterboards, that operate in 0–30 MHz. This is crucial, as VLC systems are often designed to operate in sub 10 MHz band. Thorlabs PDA36A-EC PIN photodetector with switchable gain and 13 mm^2 of active area was chosen as receiver, since at the time, it was the most suitable candidate from the available university portfolio. Commercial ZX85-12G+ bias tee, which operates from 0.2 MHz to 12 GHz was chosen for modulation of light sources. Outgoing signal was also amplified by 1.6 W amplifier, effectively working from 1–200 Mhz. Whole experimental part was split into two branches - indoor and outdoor application. Skoda Octavia III taillight with modified connector was used for outdoor scenario, while Phillips Fortimo DLM 300 44 W/840 Gen3 ceiling light was used for indoor scenario. Apart from conventional testing in direct visibility, Octavia taillight was also tested in a special box which simulates variable nature conditions. USRPs were connected to the PC hosting LabVIEW application via ethernet. For detailed description of the whole system and results of experiments refer to this article [LD1].

Figure 5.2 shows the whole diagram of first version. This system was also used for testing of adaptive equalization algorithms. Needless to say, equalization systems significantly improve maximal reachable data rates. Whole system is highly modular, so it's possible to quickly adapt to any changes needed.

This first version was developed by master´s students at Technical University of Ostrava and author was only partially part of this first team.

While the first version worked reliably during the experimental part, it had its limitations. The maximal reachable distance was low, so it was unsuitable for any dynamic tests. Some parts were not designed for the operating frequency that was used and had highly non-linear characteristics (mainly the amplifier). Other parts, such as receiver had limited effectively useful bandwidth or active area of the chip. It was obvious, that both the software and hardware will have to be adjusted over time. These insights were a basis for the second version.

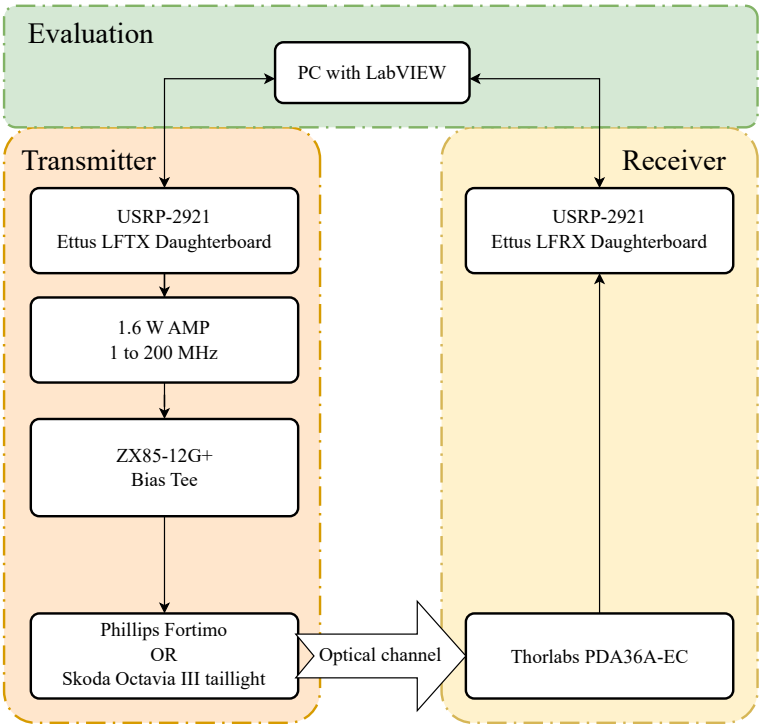

Figure 5.2: First generation of developed system.

5.2 Second Version - Beta OFDM

Second version of VLC platform was a first attempt of fully OFDM modulation based system. During the measurement phase of the first version, the development of next system was already on its way. However, multiple problems were encountered during development, so in the end, it never went out of "beta" version. As mentioned before, the system was designed to be highly modular, so this version is basically very similar to the first one, since most of the changes were carried out in the code. OFDM is more complicated modulation, and it came with multiple problems which had to be solved. First one was synchronization. OFDM needs very strict synchronization since it consists of hundreds of subcarriers. USRPs of the developed system had problems with hardware synchronization through special proprietary cable, so a third NI USRP-2921 had to be used to synchronize both transmitting and receiving elements. Other than that, limits of gigabit ethernet interface were reached and problems with buffering were encountered. This led to constant crashes, so long-term measurements were not possible - either there were memory problems, or the buffer was overwhelmed. One major addition was the webcam, which was used as data source for transmissions. However, the older USRPs severely limited processable quality, so in the end only low resolution of 100×60 pixels was usable. This was also mainly caused by gigabit ethernet interface. Whole system was planned with 256 subcarriers in mind, but in the end, only center 200 were used for data.

The whole system was working but since it was not reliable enough, development of third and significantly improved version started. However, this system still reached at least 20 % longer communication distance and at least 30 % higher transmit speeds in comparison to the previously used QAM system.

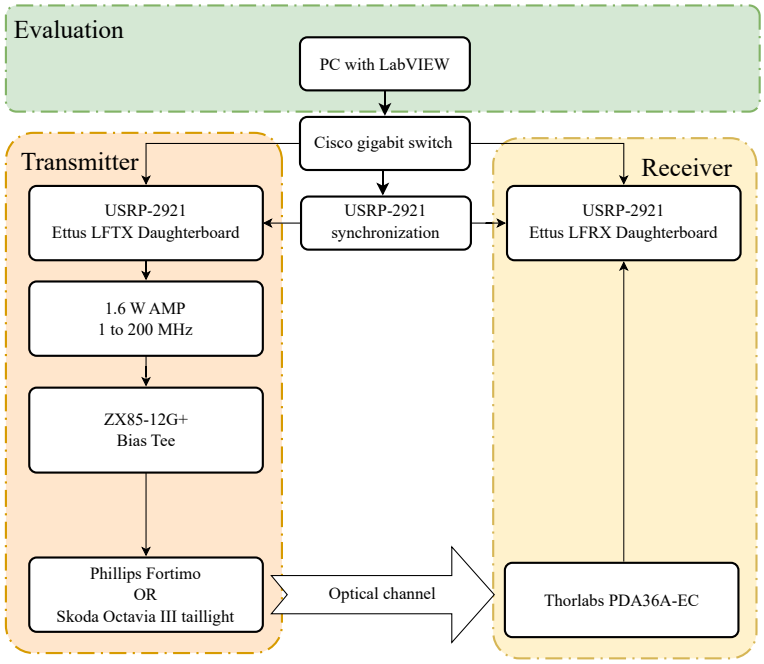

Figure 5.3: Second generation of developed system.

Figure 5.3 shows the whole diagram of second version. This system is basically improved version 1.0, so most of the parameters stay the same. The only exception is number of states for QAM modulation, which is in this case used for individual OFDM subcarriers. Apart from camera streaming, it is possible to transmit pseudo random bit stream, which can be also evaluated. Brief measurements were carried out on this version, but its instability was the main reason, why the development of full-fledged OFDM system was sped up. The author was the main developer of this version.

5.3 Third Version - OFDM System

Third version and its slight modifications is currently used for measurements and experiments. It is programmed in branch of LabVIEW NXG 64-bit, called LabVIEW Communications, which is a significant upgrade over conventional LabVIEW 2018 32-bit, as its not limited by 32-bit software environment and thus also by memory. Problems, which were encountered in previous version were identified and partially fixed. Since gigabit ethernet was a major limiting factor for OFDM system, NI USRP-2954R which is connected to PC running LabVIEW via

a modified PCI-Express (called MXI) was used instead, providing enough bandwidth for continuous operation without major problems. LFRX/LFTX daughterboards from Ettus still must be used, since the original 2954R board works in 10 MHz to 6 GHz band. System is using a new generation of LabVIEW code, which also has basic equalization technique implemented. That's why it managed to get up to 50 m of successful communication distance, which is more than 6 times more than in version 1.0 and 1.5. Cyclic prefix used in LTE is also employed. New Skoda lights were used for early testing, namely Skoda Karoq taillight and Skoda Kodiaq front lamp.

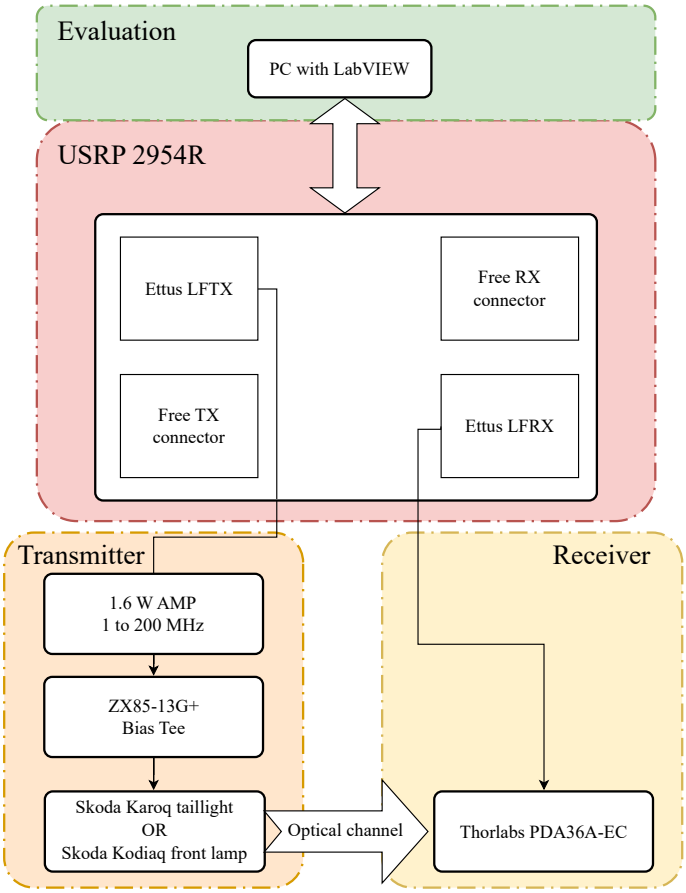

Figure 5.4: Third generation of developed system.

Figure 5.4 shows the whole diagram of third version. One USRP design was used, as it's much easier to synchronize transmitter and receiver via in-built bus. Experiments can be seen in Figure 5.5 and will be described further in this work.

The third version of the experimental platform is plagued by three major problems. The first one lies in Ettus LFTX/LFRX boards. These boards are officially nowadays not supported on newer USRPs. Therefore by combining them with newer USRP 2954R platform, an unsupported combination was created. Any encountered problems are therefore not properly

discussed with NI, since the official statement of the NI support is, that this combination should not be used at all. An alternative radio, which operates in a suitable band was released only recently (X410) and will be probably incorporated into the fourth version of the platform.

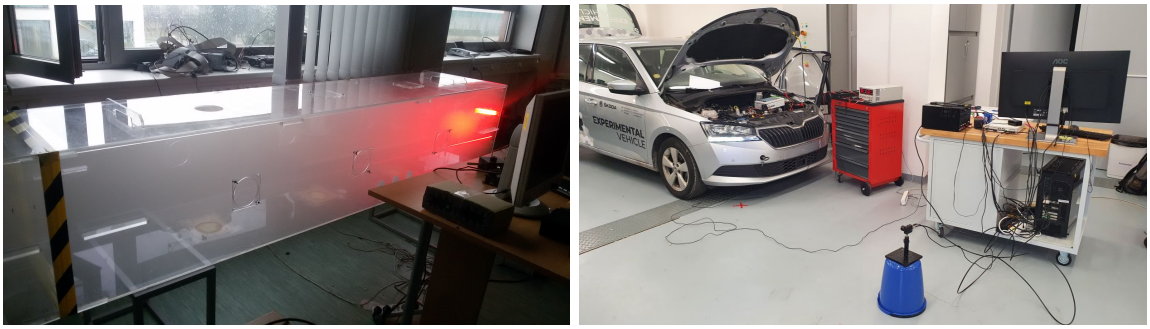

Figure 5.5: Experiments on the second version of OFDM system.

Second problem is the forced synchronization through bus, which complicates measurements, where the receiver and transmitter must be separated. A direct link to the centralized node must be maintained, ideally via a coaxial cable. The system will have to be separated again into individual transmitter/receiver parts. This is directly connected to the previous problem. There are only two newer USRP 295XR SDRs in the portfolio of our research group, both are currently utilized to the fullest and both are using the officially unsupported Ettus boards.

The third problem is the ongoing issue of unsuitable parts. While passive parts, such as bias-t are more than suitable, amplifiers and receivers should still be exchanged for more suitable parts. The platform needs amplifiers that are highly linear at sub 10 MHz frequencies or receivers with the biggest active area possible.

5.4 Fourth Version - Next-Gen OFDM System

The fourth version is currently in early development. Many modifications were considered, and many other challenges are still unresolved. Third version is still plagued by many bottlenecks that will have to be resolved, so that the whole platform can be successfully deployed in many other scenarios.

Currently the biggest issue lies in the performance of the control PC and in the synchronization of the OFDM system. The whole platform is designed around CPU-bound calculation - CPU is processing most of the work, including IFFT/FFT, frame creation, parsing and evaluation of transmitted data. This pushes the whole computer to its limits and introduces a significant lag, so the platform can't reliably work in a real-time. This problem is clearly connected to the design of the whole system, as similar issues were mentioned in the hard-

ware characteristics of individual SDRs. Moreover, the new generation of NI USRPs were designed to leverage FPGA as much as possible. It can accelerate on-board DAC/ADC and thus increase the sample rate of the developed system and increase the maximal effective bandwidth.

The other major issue is synchronization. Since moving to the OFDM from QAM, the system had to be run on a single USRP. This is due to the bus-driven synchronization of transmitter and receiver. OFDM itself is very sensitive to precise synchronization since the receiver must distinguish individual subcarriers and extract data from them. Simplifying the design of the whole platform ensured somewhat reliable operation, but the next logical step is to separate transmitter and receiver into two individual USRPs again.

There are other smaller issues, that were already partially solved. Most of the previously used components were not fully suitable for VLC. Both amplifiers were exchanged and the whole system was retested. In addition, a new variant of photodetector (avalanche photodetector) was introduced, and the previously used PIN photodetectors were exchanged in favor of new model with bigger active area.

The design of the whole system will have to reflect current trends and needs of the research team. According to authors publications in high-impact journals, there are many fields of research, which could leverage VLC technology for transmission of data. Ranging from vehicular VLC to detecting occupancy in house, Industry 4.0 (together with Operator 4.0 concept), indoor VLC and smart water metering, the VLC has a potential to offer a low-energy alternative for specific use-cases or scenarios. These areas will be discussed further in following chapters.

Due to the time constraints and lack of hardware, it will not be possible to finish the next gen version in time for the conclusion of this dissertation thesis. A modified third version was mostly used for all of the experiments, since there are additional problems that were introduced only lately. However, the fourth version is still planned and the early draft is still clear.

The new generation will be implemented on any pair of sufficiently powerful USRPs or on a much more powerful single USRP. The limiting factor is possibly mainly the price of the device. The current choice is between older USRP 2921 series, newer 2954R or newest Ettus USRP X410. Most of the ongoing problems could be solved by the previously described Ettus USRP X410, which even offers a brand-new RF optimized System-on-Chip (SoC). In addition, the code should be at least partially transferred to FPGA. Mainly the massive FFTs are stressing out the CPU and slowing the whole application down. Development for FPGA is a time-consuming activity and requires a significant knowledge, which slows it down. Exploration of all these topics is very difficult in a single person team and is therefore progressing slowly.

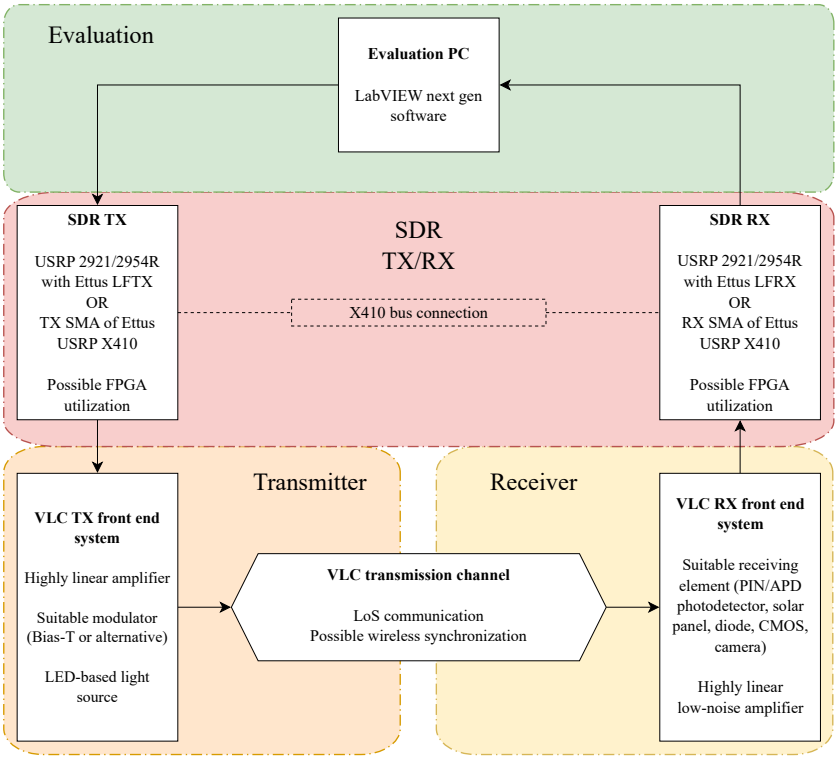

Figure 5.6: Early draft of the next generation of VLC OFDM system.

In addition, LabVIEW Communications based on NXG branch of LabVIEW application was deprecated due to unsatisfactory sales, so the code will have to be ported back to the original LabVIEW branch. Many of the library functions from NXG are still not available in the classical LabVIEW, which complicates the development further.

In addition, a performance of GNU Radio and LabVIEW for VLC could be compared, since the X410 supports both environments. The community behind open-source GNU Radio is significantly bigger, so many of the encountered problems might be solved by other developers and the development can therefore progress much faster.

The acquisition of the Ettus USRP X410 is planned for the second part of 2023 or the first part of 2024, which is beyond the submission term of this dissertation thesis. However, the author would like to work on the system further and push the limits of the whole platform.

Possible variant of the fourth generation of OFDM system can be seen in Figure 5.6.

5.5 Comparison of Individual Versions

Figure 5.7 shows the evolution of the VLC platform over multiple versions and years. As was mentioned before, since the fourth versions is not ready yet, the modified third version is currently used. Apart from very small changes to the controlling software, non-linear

hardware components were exchanged in favour of newer, much more suitable, parts. Since the original amplifier was damaged during one of the experiments ZX60-100VH+ from Mini-Circuits was used instead. Additional amplifier was also introduced at the receiving part. While the previously used photodetector offered a built in amplifier, it severely influenced the effective bandwidth of the system. Therefore it was necessary to use ZFL-1000LN+ LNA at receiving side to further amplify received signal. In addition, the PDA36A PIN photodetector from Thorlabs was exchanged in favor of PDA100A2 with much bigger active area. Further information about these new elements will be a part of following chapters.

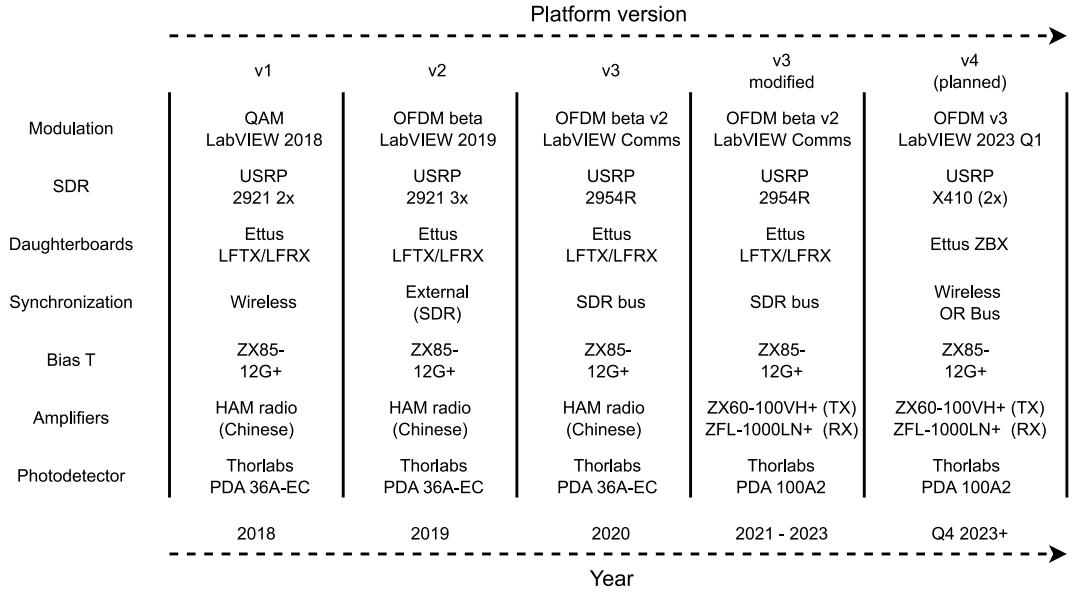

Figure 5.7: Comparison of individual versions.

It is expected that the fourth version of the system will provide the biggest leap in functionality. The introduction of Ettus USRP X410 with superheterodyne Ettus ZBX daughterboard will solve the incompatibility issues of older Ettus LFTX/LFRX daughterboards.

Chapter 6

Software and Hardware of the Current Version

The current version of the OFDM VLC system is implemented as a virtual instrument in LabVIEW Communications. The application serves as both transmitter and receiver, due to the limitantions mentioned in previous chapter. A pseudorandom sequence of 125 bits is generated as a source of data. These bits are afterwards mapped to symbols, according to the order of M-QAM modulation which is used for individual subcarriers. A pilot carrier is inserted after each sixth symbol to achieve slight frequency and time corrections, which effectively creates 150 symbols. These symbols are afterwards padded with zeroes to create a total number of 256 symbols, which are prepared for IFFT. A short part of the signal (64 samples) is inserted at the beginning to create a cyclical prefix. The complete sequence is then transmitted via the USRP at designed frequency and consequently received and evaluated. Due to the limitations of the PC and computational complexity of the designed code, the platform transmit six sequences and then pause for a short while to empty the USRP buffer. The receiving side, as expected, carries out a reverse process.

The user can set multiple parameters:

- Carrier frequency: max 30 MHz – limited by Ettus LFTX/LFRX daughterboards.
- Bandwidth.
- Sample width.
- Number of M-QAM states for individual subcarriers: max 4096-QAM.
- TX/RX gain.
- TX/RX device IP address OR automatic fetch of USRP information (if connected via MXIe).

Since, during the experiments, conventional LED based light sources were used, certain limitations apply. These light sources are mostly designed as a combination of blue light LED coated with fluorescent layer – these LEDs have suitable illumination properties, while also

having low costs. However, they are not as suitable for VLC, which is based on fast on/off LED switching. When a certain frequency threshold is exceeded, the fluorescent layer is not able to dim enough, so the off state is not recognized properly by the receiving element. Therefore, in general, the lower the carrier frequency was, the better the system performed. While Ettus daughterboards operate from DC up to 30 MHz, other elements, especially amplifiers, operate in certain frequency range, so the platform must still comply with these requirements. Specifications of individual parts will be explored further below.

6.1 NI USRP 2954R

NI USRP 2954R (Figure 6.1 is heterodyne SDR that use a pair of Ettus UBX daughterboards. Each UBX daughterboard is a full-duplex wideband transceiver that covers frequencies from 10 MHz to 6 GHz. Coherent and phase-aligned operation across multiple UBX daughterboards on USRP X Series motherboards enables users to explore MIMO and direction finding applications. The UBX daughterboard is supported by the USRP Hardware Driver (UHD) software API for seamless integration into existing applications.

Figure 6.1: NI USRP-2954R with LFTX and LFRX daughterboards.

USRP 2954R can be connected to the computer either via SPF+ or via PCIe x4 (MXIe) interface. Xilinx Kintex-7 410T is embedded inside and a JTAG interface for debugging is included as well. NI USRP 2954R is vendor locked to LabVIEW only and therefore relies on compatibility of individual parts.

Due to the specifications, both original UBX daughterboards were exchanged with Ettus LFTX/LFTX daughterboards. LFTX/LFRX utilize two high-speed operational amplifiers to allow transmission from 0–30 MHz. The LFTX is ideal for applications in the HF band, or for applications using an external front end to up-convert and amplify the intermediate signal. The outputs of the LFTX can be processed independently, or as a single I/Q pair. Example applications include HF communications, radios with external front ends and direct signal generation below 30 MHz (i.e. for VLC). The LFTX/LFRX daughterboards are also supported by the UHD driver, but were deprecated by the introduction of the new ZBX daughterboards in NI USRP X410.

USRP-2954R is connected to a high performance PC with Intel Core i9 9980XE, 64GB of DDR4 3600 MHz, GTX 1050 Ti and connected via NI PCIe-8371, which provides four lane MXIe interface. MXIe is proprietary modification of PCIe bus used in modern computers. It adds additional functionality, such as daisy chaining or remote control of PXIe chassis.

6.2 Mini Circuits ZX85-12G-S+

Mini Circuits ZX85-12G-S+ (Figure 6.2) is a wideband bias tee, a three port component that is used for setting DC bias point of specific component, while thanks to its shielding, not influencing other active elements of the communication chain. Every bias tee has three connectors – one input port allows AC through but blocks the DC bias, while the other blocks AC but allows DC. The output port combines bias and radio frequency elements. Bias tee is in general used for biasing of various components, such as lasers, antennas or amplifiers. It is usually limited by the input voltage and mainly the current, while also operating at designated frequencies. ZX85-12G-S+ can work with DC current of up to 400 mA, while having 25 V at DC voltage input and offering wideband operation from 0.2 MHz up to 12 GHz, which is more than suitable for VLC purposes.

Figure 6.2: ZX85-12G-S+ with SMA input ports.

6.3 Mini Circuits ZX60-100VH+

Mini Circuits ZX60-100VH+ power amplifier was used on the transmitting side. It has high gain flatness in the whole 0.3–100 MHz operating spectrum (+- 0.3 dB – see Figure 6.3), low noise, excellent directivity and rugged unibody construction with heatsink that integrates SMA connectors into the case body. ZX60 family is designed for microwave point-to-point radios, military EW, radar satellite systems and sub 100 MHz applications.

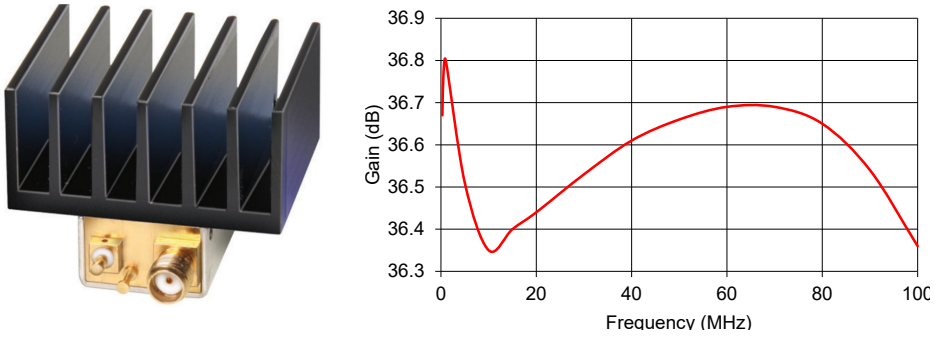

Figure 6.3: ZX60-100VH+ construction and gain flatness over the whole frequency spectrum.

6.4 Mini Circuits ZFL-1000LN+

Mini Circuits ZFL-1000LN+ LNA amplifier was used at receiving side. It provides a 2.9dB low noise figure and a 0.1 MHz to 1200 MHz wideband frequency range, while amplifying the signal by 20 dB (while operating at 12V – see Figure 6.4). It is usually used for cellular applications or small signal amplifiers offering a rugged case with two SMA connectors.

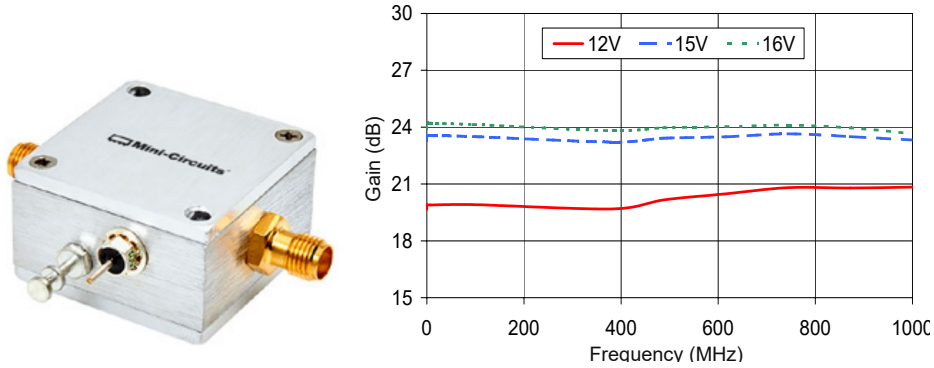

Figure 6.4: ZFL-1000LN+ construction gain flatness over the whole frequency spectrum.

6.5 Thorlabs PDA36A-EC and PDA100A2

Thorlabs PDA36A-EC and PDA100A2 are both Si PIN photodetectors with switchable gain, that were used during experiments (Figure 6.5). Their operating wavelength is from approximately 320 nm to 1100 nm, while their effective bandwidth ranges from DC levels up to 11 MHz. The main difference between those two models lies in the active area of individual photodetectors and their noise-equivalent power (NEP). PDA36A-EC has active area of 13 mm^2, while PDA100A2 has 75.4 mm^2. Regarding the NEP, PDA36A-EC has 29.1 pW/Hz while PDA100A2 has 71.7 pW/Hz, so the PDA36A-EC is much more sensitive. The deciding factor is therefore tradeoff between the active area and sensitivity of the receiver. Thanks to the integration of transimpedance amplifier, both photodetectors offer switchable gain ranging from 0 dB up to 70 dB with 10 dB step – however each step up in configuration significantly narrows the effective bandwidth of the photodetector. Thats why additional LNA, that was described earlier, was introduced as a replacement. BNC connector is used for direct signal output – since the whole platform use SMA connectors, a reduction from BNC to SMA is used. The peak responsitivity of both photodetectors is around 960 nm, which corresponds to the red light.

There are other candidates for receiving elements, that can be used in VLC. CMOS cameras or APD photodetectors can also be used instead. However, it was decided that basic PIN photodetectors are more than suitable for early tests, since their price tends to be much lower, while the performance is still satisfactory.

Figure 6.5: Thorlabs PDA36A-EC and PDA100A2 photodetectors.

Chapter 7

Application Areas of VLC and Experimental Results

Visible Light Communications, similarly to conventional RF systems, offers a high degree of adaptability and multidisciplinarity. Over the course of the research, many different areas of interest were discovered and the deployment of VLC in these scenarios was tested. Each area has specific needs. The individual receiving/transmitting elements might be stationary (smart water meters), semi-stationary (manufacturing lines and robots) or completely movable (vehicles or workers). There is often a combination of these elements, such as moving vehicle and stationary road sign or roadside units. Many of those are already outlined in the aforementioned standardization, but since the developed system avoided standardized classes (mainly due to the custom modulation and SDR deployment), it had to be adjusted to different use cases.

Most of the tested scenarios did not rely on high-speed transmissions, since the required data was often only a small bit/byte sequence (smart water meters) or the transmitted sensory data required a continuous stream instead of higher speed bursts.

Environments were the main driving factor behind the variability in experimental part. Laboratory conditions, underground parking lot, smart water meter shaft, industrial manufacturing plant or in the future even hospitals, each have specific environmental conditions, with variable reflectivity of surfaces and noise sources. An example of such smart city with VLC/RF interoperability can be seen in Figure 7.1.

Different areas were therefore investigated during the development of VLC system, to ensure that the multidisciplinary factor and performance of the whole platform is suitable for future deployment.

The following sections will focus on individual application areas. Each application area is further explored in experiments, which were published by the author – results are therefore a compressed compilation of author's articles.

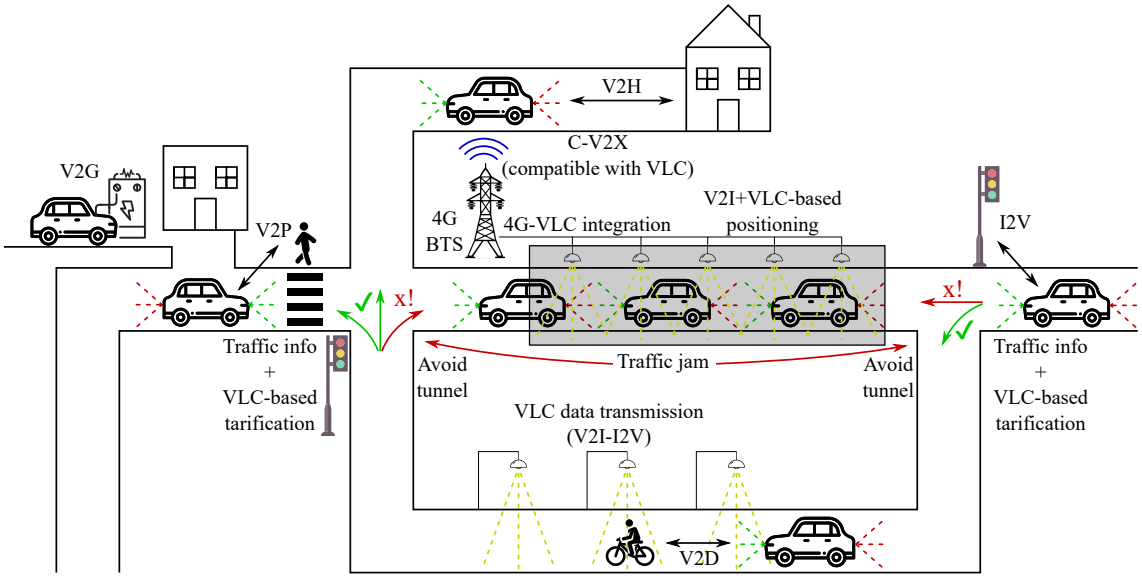

Figure 7.1: Interoperability of VLC and RF in SMART city concept.

7.1 Vehicles

Vehicular deployment of VLC was tested regularly during the whole development process. It is one of the most popular areas for VLC deployment in general. During the experimental verification of individual platform versions, the system progressed from early stationary experiments to more dynamic experiments, in which a driving scenario was semi-simulated.

Early experiments used a fixed light source, most of the time it was a slightly modified sample of real vehicular lamp (either a tail light or front lamp). These samples were supplied directly from manufacturing plants to ensure, that the final platform can be ported to commercial vehicles. Multiple variants of different lights from Skoda vehicles were tested, including samples from Fabia, Octavia, Kodiaq and Karoq.

These tests were mainly used to determine limits of the platform, since those lamps provide a directional light with a specific angle. It was necessary to investigate, if the communication can be maintained at a safe distance (two second rule for vehicles) or would work only at limiting distance (for truck platooning). This distance was considered as a reachable goal of the whole platform and was attained in the third version of the platform which used OFDM.

In addition, during the development of OFDM platform, another series of tests were carried out with a special box that simulated different environmental conditions. It was necessary to test, if VLC would work in certain conditions, such as thermal turbulence or rain. This box clearly defined limiting factors for both low-speed and high-speed communication.

This overall static approach was changed in 2022, when the first dynamic tests were carried out. A scenario, where a transmitting testing car (Skoda Fabia) was towed by receiving testing

car (Skoda Octavia) at a fixed distance was tested. These test, together with others mentioned in this work, therefore confirmed both integrability and multidisciplinarity of the developed platform.

Evolution of the platform together with individual tests will be described in following sub section, which will discuss results achieved in individual publications.

7.1.1 Early Laboratory Tests with QAM Modulation and Vehicular Lights

Early tests are described in an article called "Visible Light Communication System Based on Software Defined Radio: Performance Study of Intelligent Transportation and Indoor Applications" [LD1], which combined both vehicular and indoor use cases. The vehicular side mainly focused on implementation of a vehicle-to-everything (V2X) system with highly modular design [59, 60, 61]. Each individual component can be swiftly exchanged, without any necessary adjustments to original code. Concept of V2X is based on the passing of information from a vehicle to any appropriate entity and vice versa. It is also often divided into different subsections, such as vehicle-to-infrastructure (V2I) [62, 63], vehicle-to-network (V2N) [64, 65], vehicle-to-vehicle (V2V) [66, 67], vehicle-to-pedestrian (V2P) [68, 65], vehicle-to-device (V2D) [69, 70], vehicle-to-grid (V2G) [71, 72] and vehicle-to-home (V2H) [73, 74]. As Skoda cars are the most widespread vehicles in the Czech Republic, we have picked Skoda Octavia III tail-light as the transmitter in V2X scenarios. So far, the partnership with manufacturers of these lights have yielded results, as multiple samples of planned or already available products were received for testing.

Figure 7.2 describes different ways of V2X communication [60, 75, 76], mentioned earlier. V2V is a system, which enables car to communicate with each other. Its main goal is to reduce vehicle collisions and crashes. It will be a backbone of multiple levels of autonomy, delivering assisted driver services like collision warnings [62, 77, 78]. One key issue with V2V is that to be most effective, it should reside in all cars on the road. V2D is a system, that links cars to many external receiving devices and will be particularly useful to bikers. Vehicles can communicate with V2D device on cycle to alert rider to potential danger or to avoid accidents [69, 70, 79]. V2P is a system which should be particularly useful to elderly persons, school kids and physically challenged persons. V2P maintains a link between pedestrian's smart devices and vehicles to act as an advisory to avoid collisions [80]. V2H communications involve a link between a vehicle and the owner's home, sharing the task of providing energy [81, 82]. During power outages, a vehicles battery can be used as a critical power source. V2G is a system which can communicate with the power grid to adjust the vehicle's charging rate [83, 84]. It will be an element in some electric vehicles and is used as a power grid modulator to dynamically adjust to the energy demand [85].

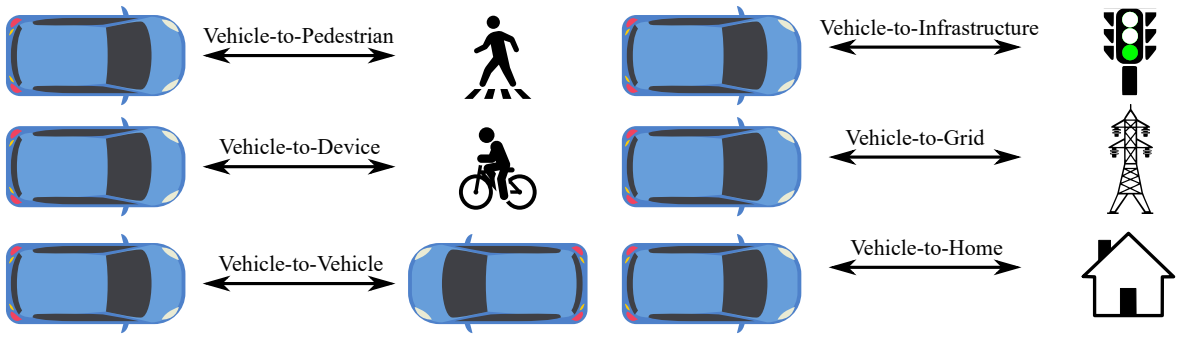

Figure 7.2: Vehicle-to-everything scenarios communication.

When approaching the problems of V2V communication, the natural conditions are major concerning factor, as they significantly vary throughout the year. Carrying out a number of experiments in this area is a logical first step in implementation of channel equalization, as it was estimated that it will significantly improve transmit speeds or reachable distance. The modular platform was also tested in previously mentioned conditions, as it will become a basic platform, which will be modified and improved in the future.

These early tests were carried out on the first version of the VLC platform, which used QAM modulation in its core – the previous decription of the first generation apply. Together with the next series of experiments, its goal was to reach limits of QAM modulation in VLC communications.

Tests were carried out using static modulation formats. Long term measurements were essential to specify threshold for successful modulation switching in adaptive modulation. We were aiming for a similar system, which is used in case of microwave point-to-point links, where both units are capable of quickly changing modulation scheme according to natural conditions and measured parameters. Sacrificing part of the transmission speed in favor of link robustness is the main concept of this system.

Measurements using car taillight were carried out in multiple meteorological conditions. This problem was approached differently, as in real-life scenarios, meteorological conditions tend to vary often. These conditions were simulated in a plastic box made of plexiglass with dimensions of 50 $\times$ 50 $\times$ 500 cm. Maximal measured distance in this scenario was 550 cm, which was effective threshold for functional communication. The first step was to measure the empty box as reference values for future comparisons. After that, three scenarios were simulated: thermal turbulence and two intensities of rain. These scenarios were discussed further.

Figure 7.3 describes the tested setup, used for testing of Octavia taillight. To carry out different scenarios the simulation box was inserted between transmitting light and receiving photodetector. Also using plano-convex lens was suitable for reaching higher RSL values and thus better transmit speed.

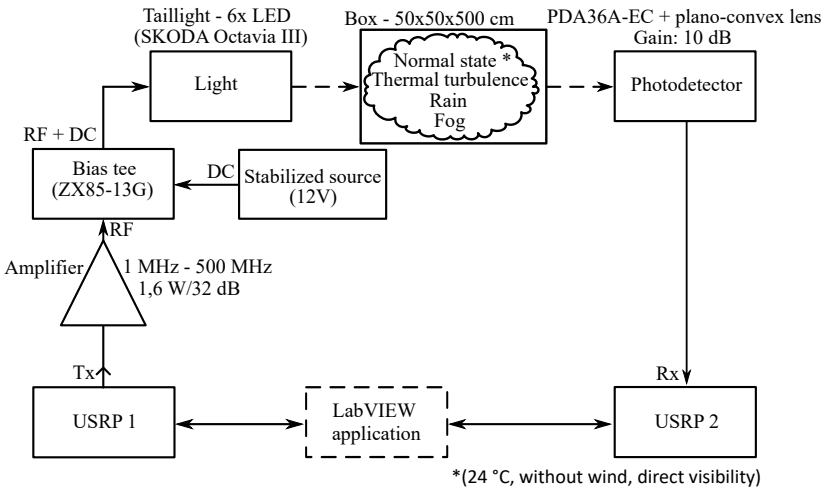

Figure 7.3: Octavia tail-light setup for early QAM tests.

The following configuration was used during measurements:

- Carrier frequency: 3 MHz
- Bandwidth: 1–4 MHz
- Modulation type: M-QAM
- TX/RX gain: 0 dB
- Message symbols: 10,000
- Tx filter: root raised cosine
- Sample width: 16-bit
- Measured parameters: E_b/N_0, BER, EVM, MER

The first scenario focused on empty box and reference values for further comparisons. To ensure conformity of measured data, these conditions were set as referential: 24 °C, direct visibility, windless. Setup can be seen in Figure 7.4.

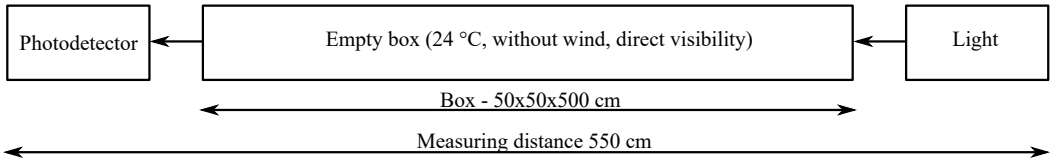

Figure 7.4: Octavia taillight setup adjusted for testing scenario with empty box.

Comparison of BER values with different bandwidths can be seen in Figure 7.5. It is noticeable that up to 64-QAM, BER values tended to stay below 10^{-5} threshold set earlier. On the contrary, 128-QAM and higher modulations suffered from much higher BER values. Bit error ratio of 256-QAM was even below 10^{-2} in every bandwidth combination. These values were too high for FEC and communication is impossible in these conditions. Figure 7.6 and

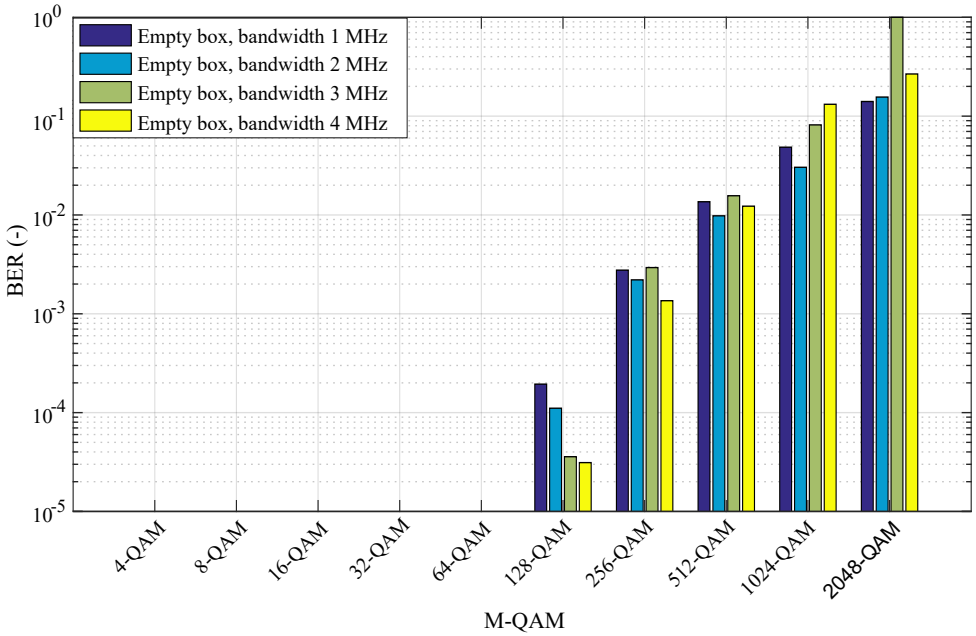

Figure 7.5: BER/distance relationship for Octavia tail-light with different M-QAM and bandwidths—empty box.

Figure 7.7 describe E_b/N_0 and EVM values for every M-QAM and bandwidth combination. It is noticeable that starting from 256-QAM modulation, the difference between each bandwidth tended to increase rapidly.

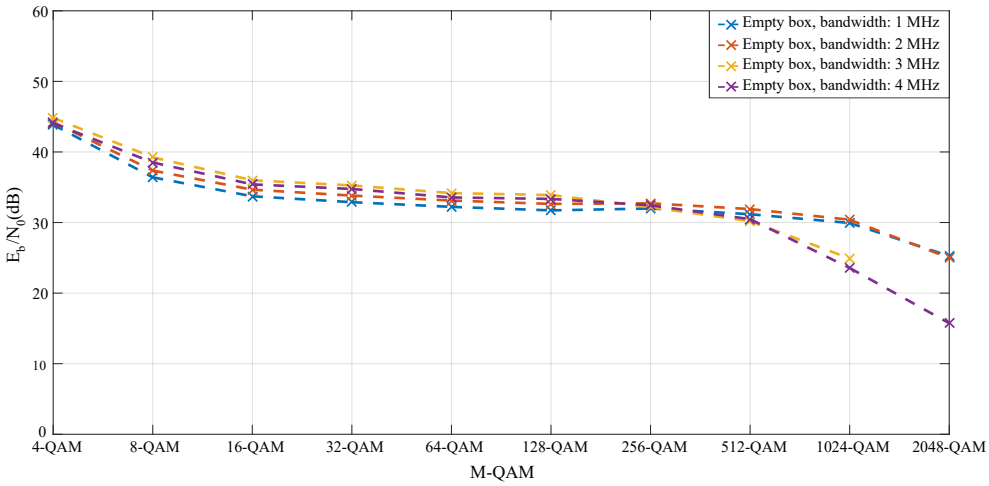

Figure 7.6: E_b/N_0 / distance relationship for Octavia tail-light with different M-QAM and bandwidths—empty box.

Measurements with thermal turbulence were carried out with modified box. The bottom part was removed, and multiple hot-air blowers were mounted instead. The top part of box

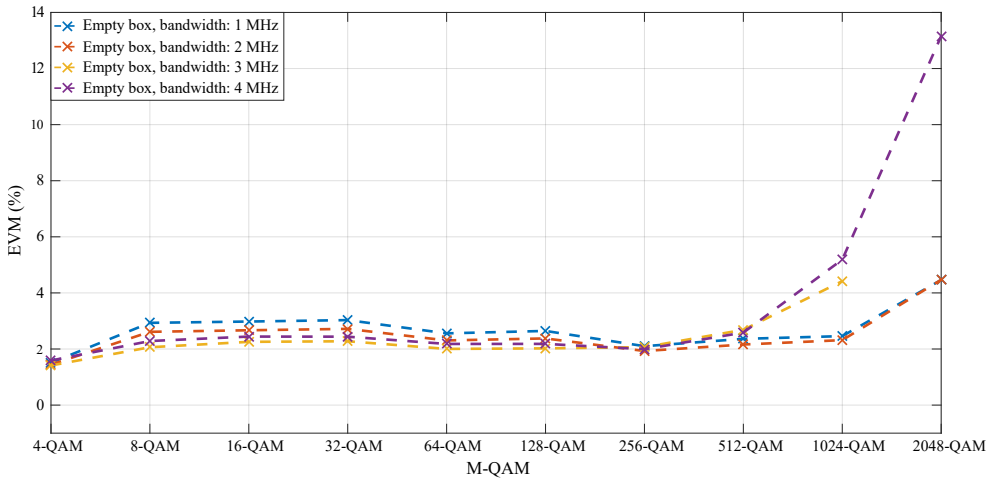

Figure 7.7: EVM/distance relationship for Octavia tail-light with different M-QAM and bandwidths—empty box.

was perforated to ensure sufficient air flow. Each blower heated the air to 50 °C. Heated air then steadily flowed through box and slowly cooled to 44 °C, which were measured directly at perforations. The horizontal airflow was 0.3 m/s and vertical was 2.5 m/s. Whole measurement was carried out multiple times until temperature inside box stabilized. Setup can be seen in Figure 7.8.

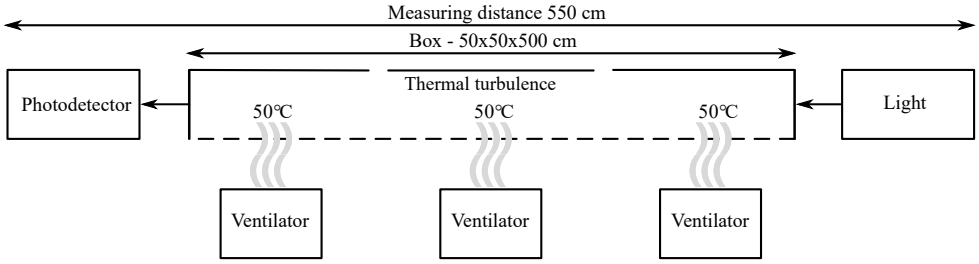

Figure 7.8: Octavia tail-light setup adjusted for scenario 2-thermal turbulence.

Comparison of BER values with different bandwidths can be seen in Figure 7.9. It is noticeable that up to 32-QAM, BER values tended to stay below 10^{-5}. On the contrary, 64-QAM and higher modulations suffered from much higher BER. Figure 7.10 and Figure 7.11 describe E_b/N_0 and EVM values for every M-QAM and bandwidth combination. By comparing these values to the reference, a slight decrease of E_b/N_0 and increase of EVM values can be noticed. The most significant changes began at 128-QAM and progressed further. Communication ceased to work, so 2048-QAM was not measurable.

The first part of measurements with rain were carried out in modified box as well. In this scenario, the top part of the box was removed and exchanged with three water nozzles. The box was equipped with compressor which pumped water from the bottom of the box back

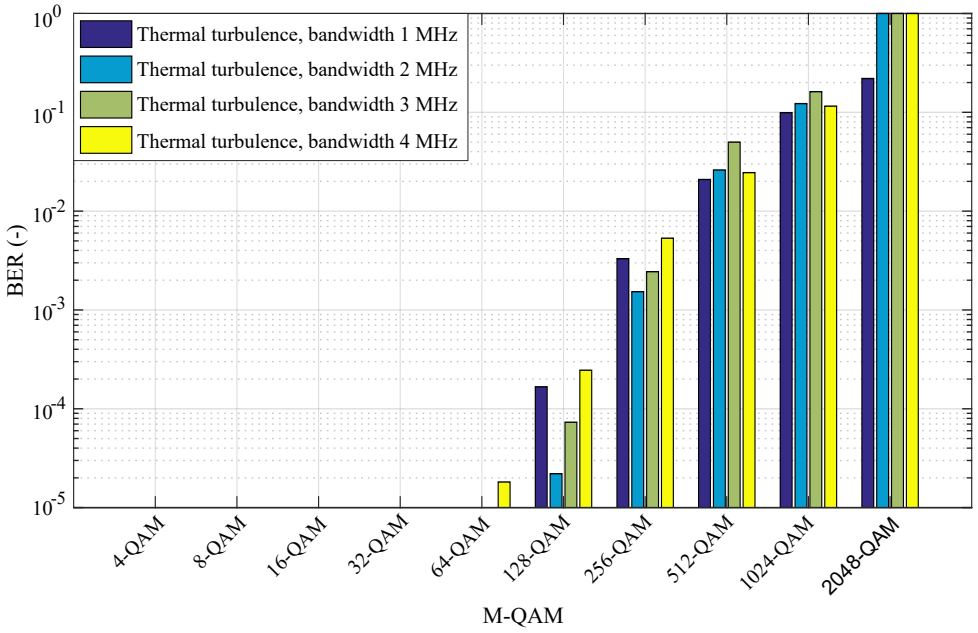

Figure 7.9: BER/distance relationship for Octavia tail-light with different M-QAM and bandwidths—thermal turbulence.

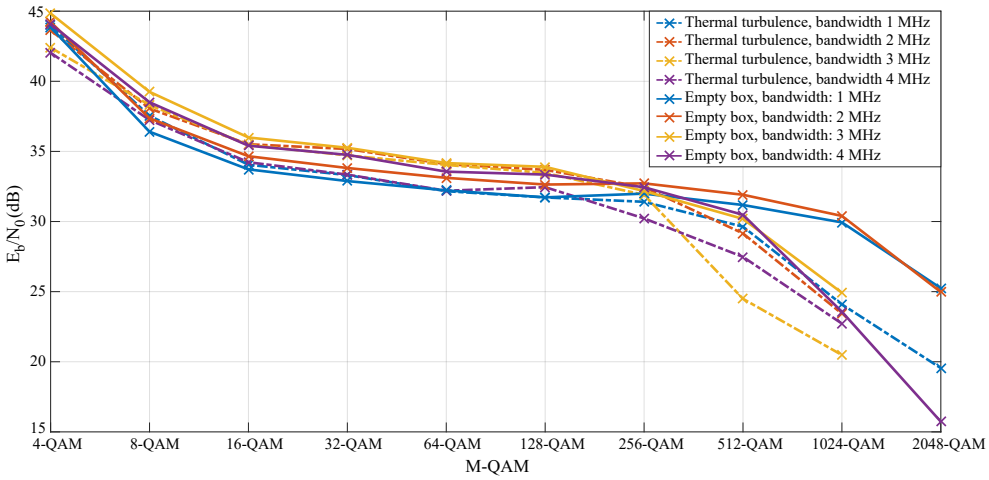

Figure 7.10: E_b/N_0/distance relationship for Octavia tail-light with different M-QAM and bandwidths—thermal turbulence.

into nozzles. The transmitter and receiver were located outside the box, which was opened from both sides. In this scenario, the water flow was set to 42 l/min. Setup can be seen in Figure 7.12.

Measurements were carried out in a room at 22–25 °C. Water temperature was stabilized at 22–25 °C before each measurement. Both transmitter and receiver were located 25 cm from open side of the box. This way, it was impossible for them to get fogged up. To investigate the

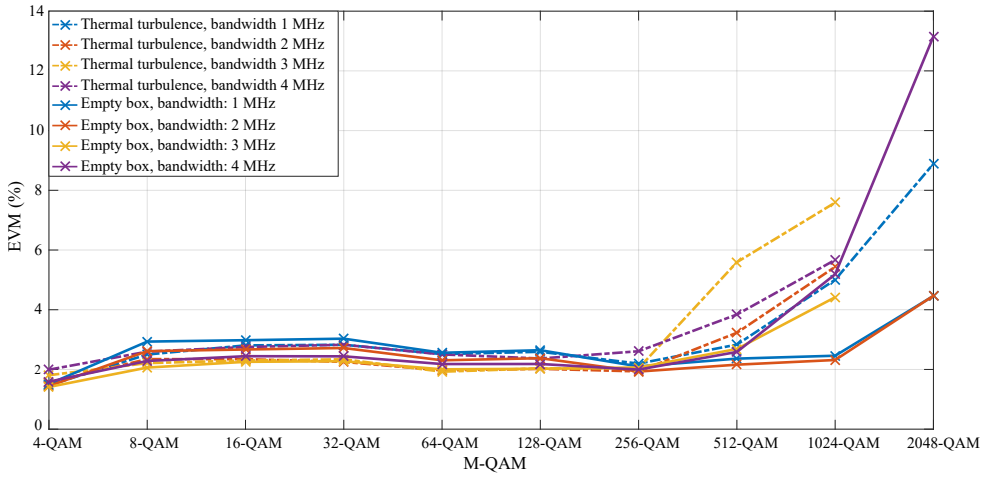

Figure 7.11: EVM/distance relationship for Octavia tail-light with different M-QAM and bandwidths—thermal turbulence.

influence of walls or partitions a series of tests without a box and in a completely dark room were carried out before. The box had minimal influence, as its construction was adjusted to prevent it. Transmitting light was precisely focused into the box to avoid interference, which could be caused by possible reflections. Incoming light was also focused into photodetector by planoconvex lens, as mentioned earlier. Box construction was spacious enough to avoid unnecessary reflections on running water.

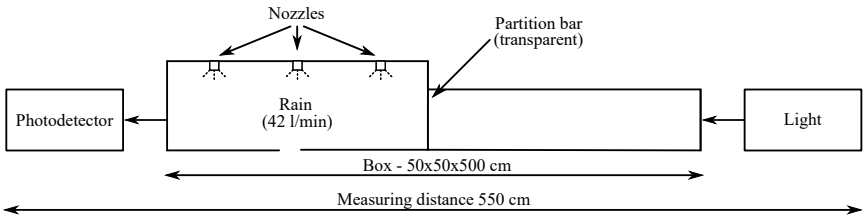

Figure 7.12: Octavia tail-light setup adjusted for scenario 3 – Rain 42 l/min.

Comparison of BER values with different bandwidths can be seen in Figure 7.13. This time, up to 8-QAM, BER stayed below 10^{-5}. On the contrary, 16-QAM and higher modulations suffer from much higher BER.

E_b/N_0 and EVM values are displayed in Figure 7.14 and Figure 7.15. By comparing these values to reference setup, there was a significant drop in signal quality. For example, in case of 4-QAM modulation and 1 MHz bandwidth, SNR was nearly 10 dB lower than the reference. Significant decrease in signal quality was observed, which also led to lower maximal reachable modulation/bandwidth combination, which was 128-QAM/1 MHz.

This setup was also influenced by the drops of water on the sides of the box. Mainly the "separation wall" between box sections caused concerns. To analyze this concerning

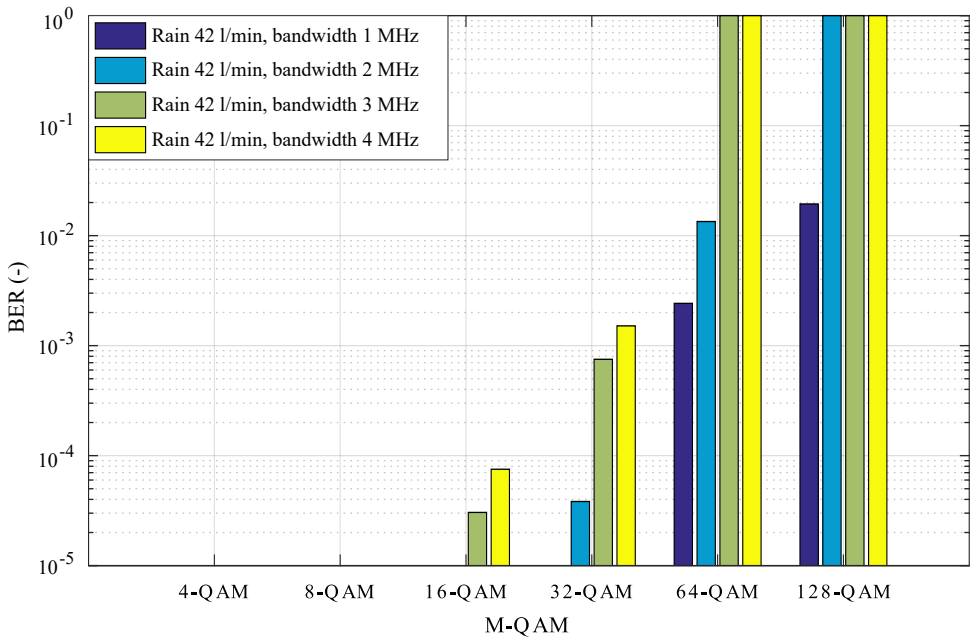

Figure 7.13: BER/distance relationship for Octavia tail-light with different M-QAM and bandwidths—Rain 42 l/min.

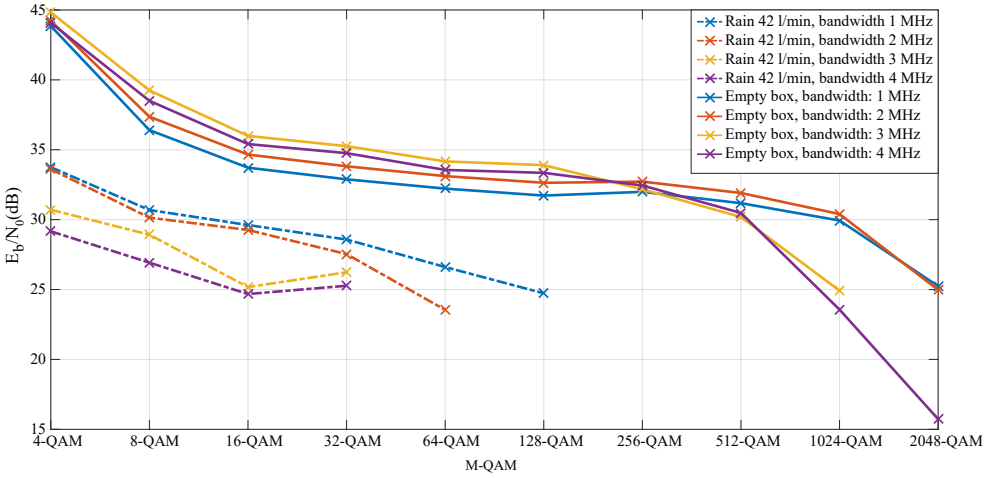

Figure 7.14: E_b/N_0 / distance relationship for Octavia tail-light with different M-QAM and bandwidths—Rain 42 l/min.

issue, several measurements with different box setups were carried out, results can be seen in Figure 7.16. The first curve corresponds to the empty box, second one to the box with rain but without partition and the last one was the original measured setup. By comparing these values, there is a noticeable 3 dB increase in attenuation between second and third curve.

The second part of measurements with rain were carried out in the modified setup from previous scenario. The main difference was a different water flow of 22 l/min. Setup can be

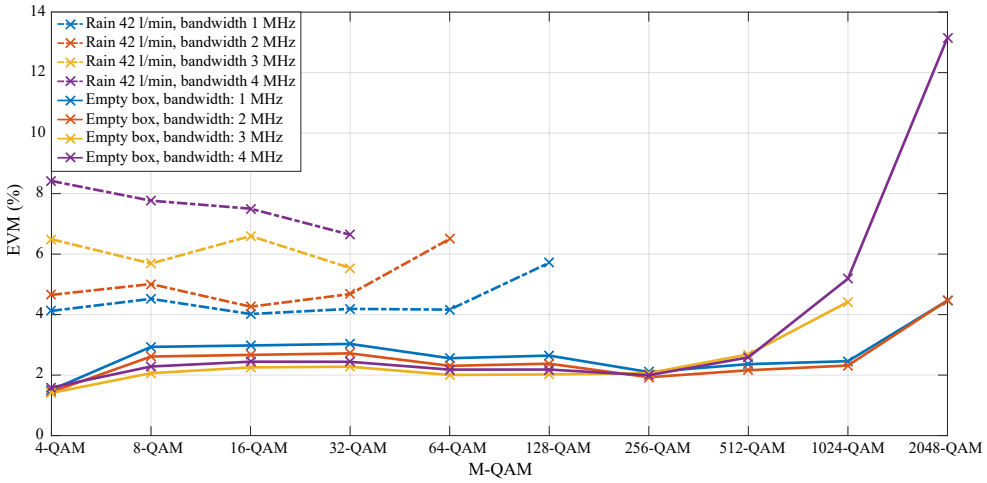

Figure 7.15: EVM/distance relationship for Octavia tail-light with different M-QAM and bandwidths—Rain 42 l/min.

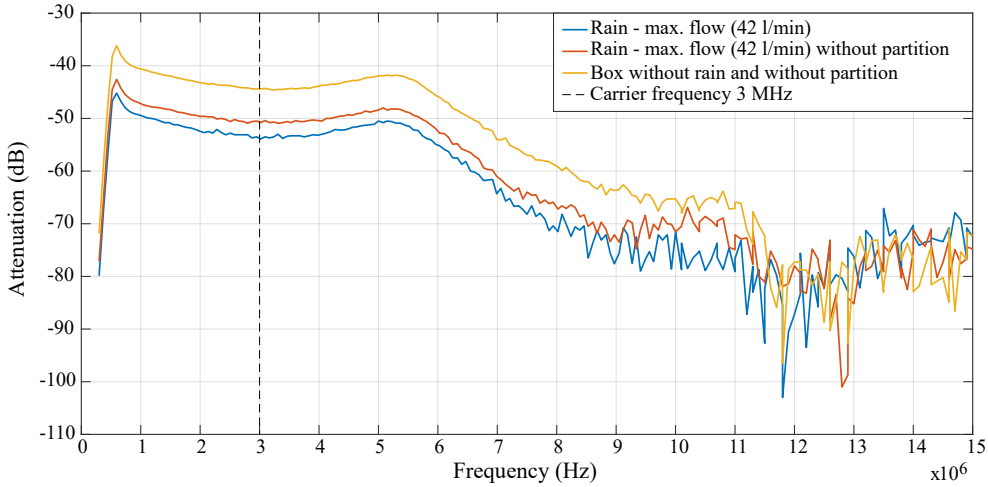

Figure 7.16: Attenuation characteristics of Octavia tail-light for scenario with Rain 42 l/min – comparison of intended setup and adjusted setup without partition.

seen in Figure 7.17.

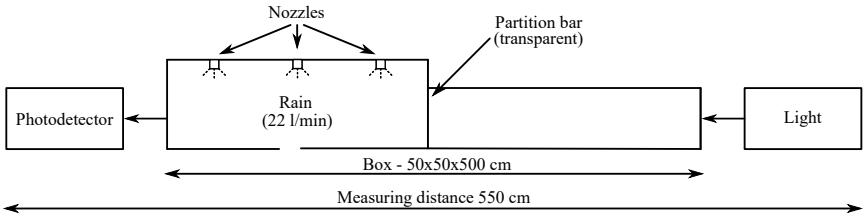

Figure 7.17: Octavia tail-light setup adjusted for scenario with Rain 22 l/min.

Comparison of BER values with different bandwidths can be seen in Figure 7.18. This

time, up to 16-QAM, BER stayed below 10^{-5}. On the contrary, 32-QAM and higher modulations suffer from much higher BER.

E_b/N_0 and EVM values (Figure 7.19 and Figure 7.20) tended to follow the trend from previous scenario. This time, in case of 4-QAM modulation and 1 MHz bandwidth, SNR is nearly 7 dB lower than the reference scenario. Significant decrease in signal quality was observed, which also led to lower maximal reachable modulation/bandwidth combination, which was 256-QAM/1 MHz.

The main advantage of this experiment was deployment of commercially available lights as transmitters. Excessive modifications of original designs were avoided. However, it is estimated, that modification of an Octavia taillight LED cluster might increase effective maximal communication distance by at leat 20%, as original LED matrixes tend to be of variable quality.

In summary the maximal measuring distance was constant 550 cm. A special box was inserted between transmitter (tail light) and receiver (photodetector), which simulated different conditions such as: thermal turbulence or rain with variable intensity. The highest reachable transmit speed was 28 Mbps for combination of 256-QAM and 4 MHz, which was reachable only in the empty box. These experiments proved that VLC can even work in scenarios with variable optical conditions (moving water – rain) and in addition revealed a new possible VLC use-case: underwater communications.

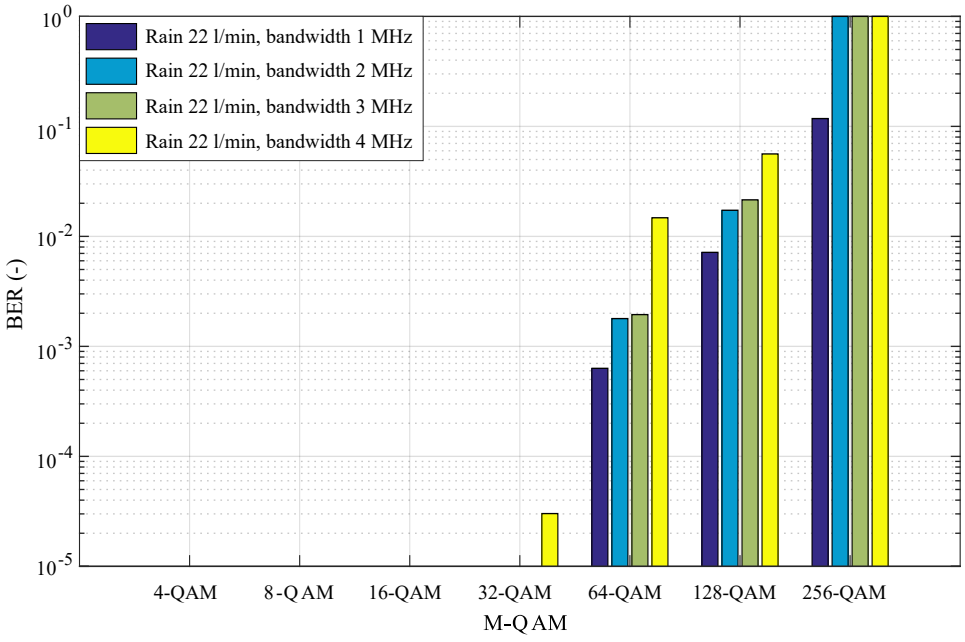

Figure 7.18: BER/distance relationship for Octavia tail-light with different M-QAM and bandwidths—Rain 22 l/min.

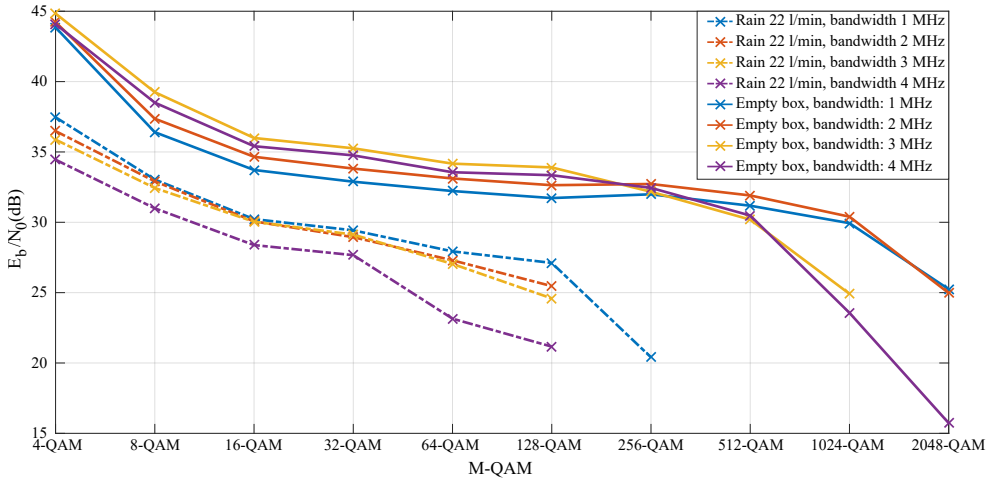

Figure 7.19: E_b/N_0 / distance relationship for Octavia tail-light with different M-QAM and bandwidths—Rain 22 l/min.

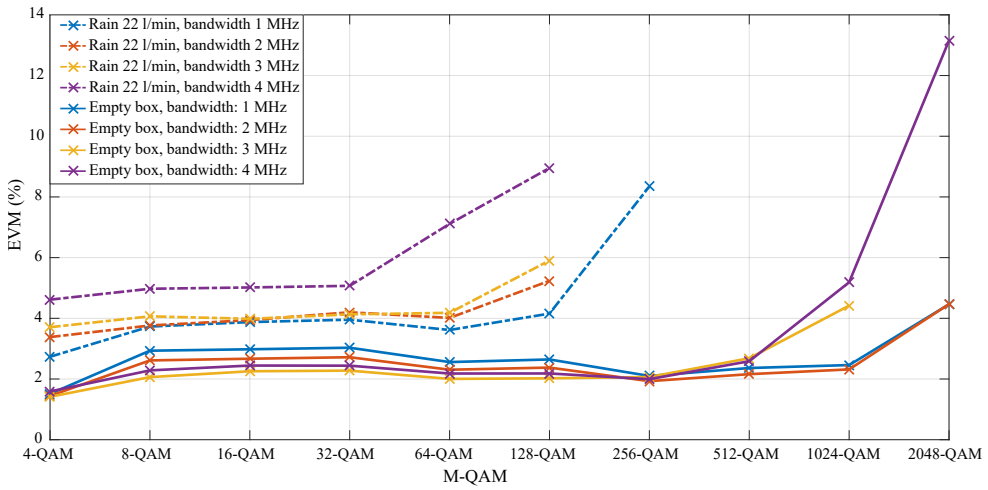

Figure 7.20: EVM/distance relationship for Octavia tail-light with different M-QAM and bandwidths—Rain 22 l/min.

7.1.2 Integration of Second Generation OFDM into Vehicles

Results from the latest experiments are the subject of the newest work-in-progress publication, which focus on integration of the modified third version of VLC system into Skoda Fabia commercial vehicle. This article focus on the measurement of the bit error rate and the achievable bit rate and try to outline realistic scenarios that may occur in real driving scenarios. The original light of a Skoda Fabia III car was used as a light source. Only DRL (daylight running light), a matrix of 4 LEDs was used, since its mandatory to have it turned on in majority of european countries.

Three measurement scenarios were chosen for the experiments. In the first scanario, the

effective distance limits of the used communication system were tested. The second scenario focused on stationary tests to measure the beam angles from the LED headlamp. The third scenario was mainly about dynamic testing of the entire communication system in two vehicles in an outdoor environment.

During the first set of experiments, the following configuration was used: base carrier frequency 1 MHz, with variable step 0.4 MHz up to 3.8 MHz and different orders of M-QAM modulation (4-QAM, 8-QAM, 16-QAM, 32-QAM and 64-QAM). Measurements were taken up to a distance of 32 m for technical reasons (maximal diagonal length of the underground parking garage) and carried out at the Faculty of Electrical Engineering and Computer Science of the Technical University of Ostrava. During the second and third sets of experiments the following configurations were used: base carrier frequency 1 MHz, bandwidth 400 kHz. M-QAM modulation orders were the same. Measurements were taken at beam angles of 15°, 30°, 45°, 60° and 75°, up to the maximum possible distance from the headlight relative to the BER. During dynamic tests, a straight distance with a possible deviation of up to 15° was maintained.

The first series of experiments were focused on the limits of the tested system. They were designed with respect to the safe distance between vehicles and the associated maximum speed limit in European cities. The speed limit in urban areas is limited to 50 km/h [86] in basically all EU countries. In general, a 2 second delay between vehicles is recommended to maintain the safe distance. At 50 km/h (13.88 m/s), that distance is approximately 28 m. [87] states that drivers should maintain a distance equal to at least one-half of the reading on the tachometer under all circumstances.

Figure 7.21 shows the bit error rate of 4-QAM modulation at a carrier frequency of 1 MHz. When individual BER values are compared, a certain trend can be observed as the bandwidth used increases. It should be noted that measuring at the recommended safe distance of 28 m, the 4-QAM modulation remains below the BER of 10^{-3} throughout the measurement. The results at this distance below a bandwidth of 1 MHz were more than adequate since the BER was so small that it was not measurable by our system. Our system also achieved a bit rate of 1.52 Mbit/s using 4-QAM modulation and a bandwidth of 2 MHz.

Figure 7.22 shows the overall comparison of the used modulation formats, at variable distance from the transmitting vehicle. The comparison was carried out at a bandwidth of 400 kHz and a carrier frequency of 1 MHz. It can be clearly seen that 4-QAM modulation achieves the best results at all distances since its BER is not measurable. For the 8-QAM and 16-QAM modulations, it can be seen that the BER is around 10^{-5} and 10^{-3}, respectively, at 28 m. For the 32-QAM modulation, we observe that the appropriate BER limit is 25 m from the vehicle, which is the minimum safe distance between vehicles according to [87]. Meanwhile, 64-QAM can be used at shorter distances, where a large volume of data needs to be transmitted.

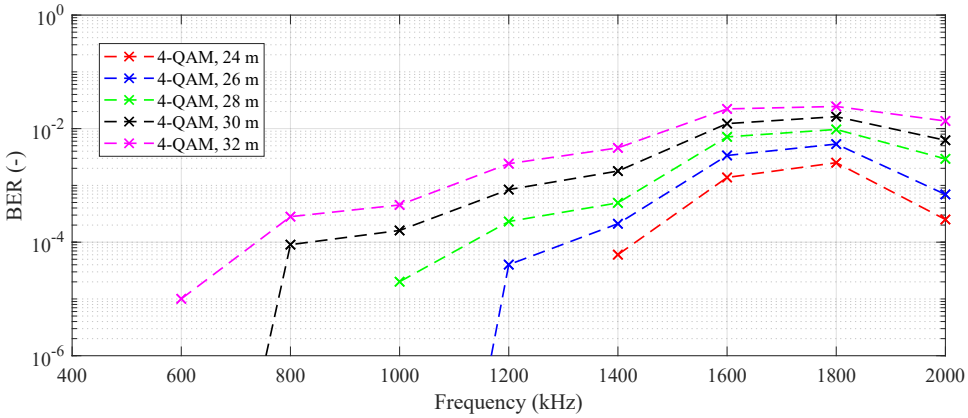

Figure 7.21: BER comparison at distances around 28 m, 4-QAM modulation, carrier frequency 1 MHz.

Because the measurements were taken in an enclosed space, it can be stated that they were carried out under very favorable conditions. Our first measurements were not influenced by the Sun, which would introduce additional noise. The subject of future publications will be the testing of communication in harsher outdoor conditions.

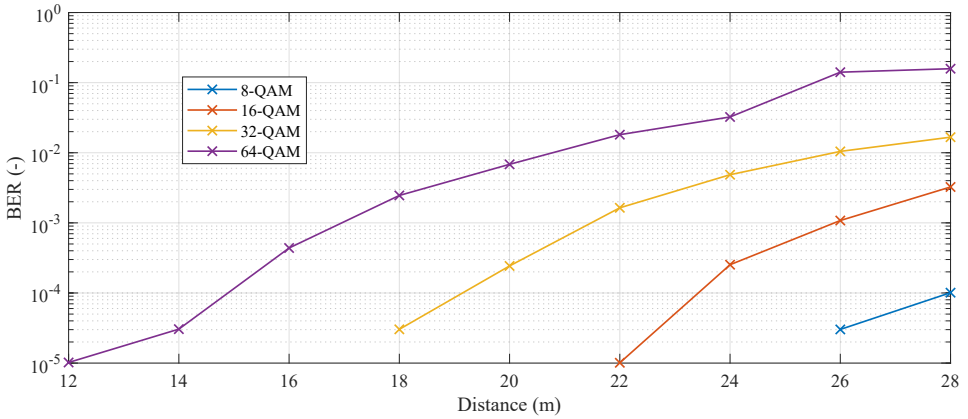

Figure 7.22: BER comparison with variable headlight-photodetector distance. Carrier frequency 1 MHz, bandwidth 2 MHz.

The second batch of experiments focused on stationary tests with variable angles between transmitter and receiver. The main reason was to test, if the VLC can maintain functionality while both vehicles are at other than favorable positions.

Figure 7.23 shows a comparison of 4-QAM and 64-QAM modulation at different measured angles. Lines with crosses indicate 4-QAM modulation, while lines with squares indicate 64-QAM modulation. The individual modulations are marked in the same color on the graph to easily distinguish between them. When measuring the 4-QAM modulation, it can be observed

that at 15° the BER is just at the 10^{-3} error limit, while 64-QAM at the same angle reaches this limiting value at 13 m. At 75° from the headlamp, the 64-QAM modulation is unusable, while 4-QAM can still be used up to 5 m. Thus, it can be seen that the 64-QAM modulation is almost unusable at larger angles and distances. Therefore, according to the presented results, it is better to use 64-QAM at shorter distances, where a larger amount of data can be transmitted faster simply due to the nature of higher modulation formats. When measured at 30°, it can be seen that 4-QAM modulation starts to be measurable at 15 m, where the BER is on the order of 10^{-4} and the signal gradually degrades at 19 m due to the high error rate. With 64-QAM, BER starts to become apparent at 6 m from the headlamp and is usable up to 8 m.

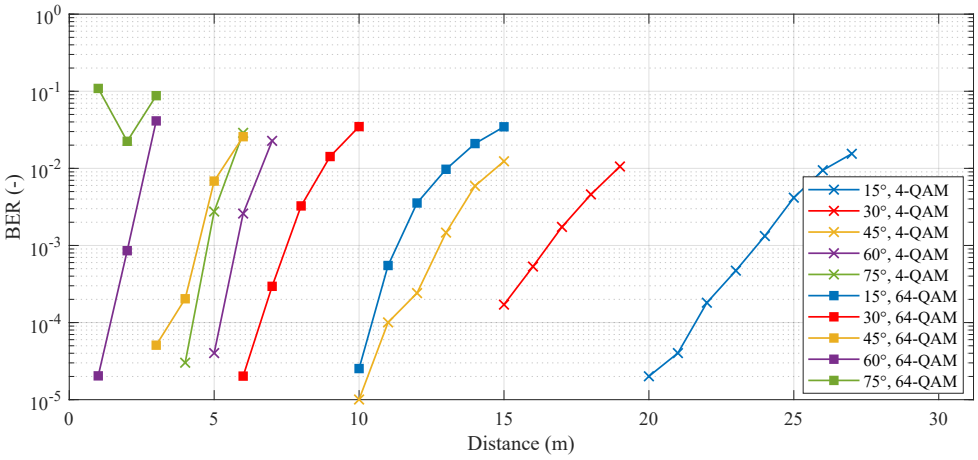

Figure 7.23: Comparison of BER at various measured angles and distances, 4-QAM and 64-QAM modulation. Carrier frequency 1 MHz, bandwidth 400 kHz.

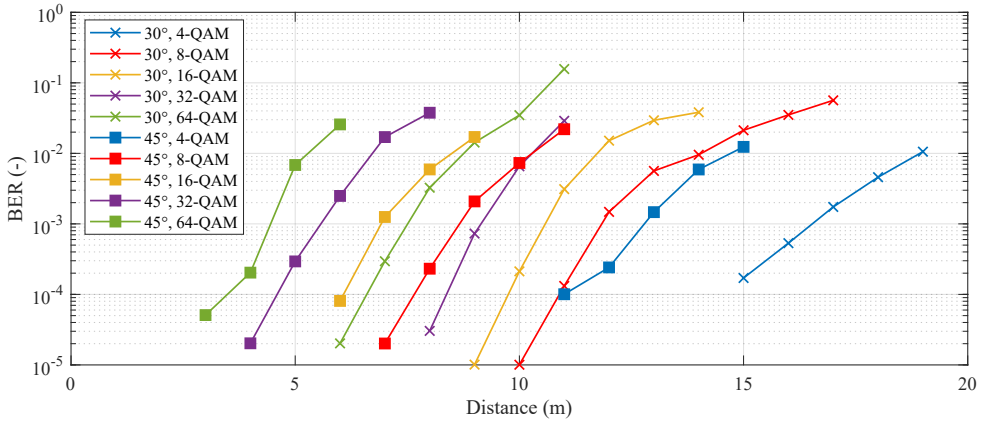

Figure 7.24: Comparison of BER at different measured angles and distances for all modulations formats. Carrier frequency 1 MHz, bandwidth 400 kHz.

Figure 7.24 shows a comparison of the individual modulations measured at 30° and 45°. It can be observed that at 45 degrees, the 4-QAM modulation can be used relatively well up to 14 m, where the BER is equal to 10^{-3}. However, it might be better to use the 16-QAM modulation to simulate real-world scenarios (i.e. parking), as its almost error-free at 6 m from the headlight. 64-QAM modulation can also be used, but only at distances up to 4 m, where the BER is on the order of 10^{-5}–10^{-4}. If a 30-degree measurement is considered that corresponds to scenarios such as overtaking or lane changes, the 4-QAM modulation can be used up to 18 m, where the BER is in order of 10^{-3}. During the experiments,the transmission rates of the communication system were also explored. The 4-QAM modulation achieves a transmission rate of 305.34 kbit/s with a carrier frequency setting of 1 MHz and a bandwidth of 400 kHz. At 8 m, 32-QAM modulation can be used effectively, which means the system can achieve a maximum bit error rate of about the order of 10^{-5} and a bit rate of 1145.98 kbit/s. These results are preliminary, since the platform is still in development and tested regularly.

The final series of tests was focused on dynamic driving scenarios. The photodetector was placed on the right side of the rear bumper of the Skoda Octavia II (receiving vehicle) at the same height as in the previous experiment (46 cm). The wiring of the measurement system was identical to that in the first measurement scenario. A PC with LabVIEW Communications evaluation software, a USRP 2945R, and both amplifiers were placed in the trunk. The Skoda Fabia III (transmitting vehicle) had a power supply and Bias-Tee connected to the vehicle's headlight. During the experiment, vehicles were connected with an SMA shielded coaxial cable that transferred the generated and amplified signal from the USRP to the headlight. As all components require 230 V (AC) to operate, the extension cable had to be used to bring a constant supply of power to both vehicles and also to ensure other factors during driving tests, such as keeping all cables tightly stretched so that they were not in danger of being run over while driving. The two vehicles were always connected by rope to ensure a constant distance between the vehicles. During the tests, the BER was measured with a refresh time of one second. A recording device was placed behind the windshield of the transmitting vehicle to record the entire measurement process using 4K video. The recording then showed the actual BER value, but also the position of the vehicles, and since the distances were marked on the measured route, it was easy to associate individual values with a specific distance and position. The actual measurement process can be seen in the Figure 7.25.

Before the actual measurement, a 15 m distance was driven to start and stabilize a constant speed of 10 km/h. A 15 second measurement was then performed, covering approximately 42 m. At the end of the measurement there was another 15 m window for a slow catch-up to avoid damage to coaxial cables. Measurements were taken for every modulation format tested. If an error rate of 10^{-3} was measured three times, throughout the measurement period, the higher-order modulation was no longer worth measuring, as the signal quality requirements would be even higher. Before each measurement, the vehicles were parked as parallel as

Table 7.1: Comparison of BER from stationary tests at 0° and 15° with the median from dynamic tests.

	4-QAM			8-QAM			16-QAM			32-QAM			64-QAM		
dist (m)	0°	15°	dynamic	0°	15°	dynamic	0°	15°	dynamic	0°	15°	dynamic	0°	15°	dynamic
5	0	0	0	0	0	0	0	0	0	0	0	0	0	0	0
10	0	0	0	0	0	0	0	0	0	0	$1.96{\cdot}10^{-2}$	$1.68{\cdot}10^{-5}$	0	$5.50{\cdot}10^{-4}$	$6.10{\cdot}10^{-5}$
15	0	0	0	0	$4.03{\cdot}10^{-5}$	0	0	$7.27{\cdot}10^{-4}$	$4.04{\cdot}10^{-5}$	$2.03{\cdot}10^{-5}$	$1.28{\cdot}10^{-2}$	$7.03{\cdot}10^{-5}$	$3.05{\cdot}10^{-5}$	-	-
20	0	$2.01{\cdot}10^{-5}$	0	0	$7.79{\cdot}10^{-3}$	$6.81{\cdot}10^{-5}$	0	-	$9.81{\cdot}10^{-4}$	$2.43{\cdot}10^{-4}$	-	-	$6.84{\cdot}10^{-3}$	-	-
25	0	$7.17{\cdot}10^{-3}$	$6.74{\cdot}10^{-3}$	0	-	-	$3.84{\cdot}10^{-4}$	-	-	$7.96{\cdot}10^{-3}$	-	-	-	-	-

possible. During the run, the measurements were then carried out in a straight line and at a 15° angle due to the very limited space that influenced maneuverability of both vehicles. For all measurements, a carrier frequency of 1 MHz and a bandwidth of 400 kHz was maintained.

Figure 7.25: Photo taken during the measurement. Default settings for the driving scenario measurement process.

Figure 7.26 compares the BER values with the measurement time for each distance. For each distance, the highest usable modulation order was selected. It can be seen that the value of the bit error rate is always around its mean value throughout the run. This means that the BER value was almost the same during the measurement time, i.e. the BER values for each modulation were similar throughout the measurement time, and a deviation from its trend, for example, a jump of several orders, is rather an exception. We can see that during the experiment at both 5 m and 10 m, the error rate of the 64-QAM modulation was in the order of 10^{-5} throughout the measurement phase. On the other hand, at 25 m, even with the most robust 4-QAM modulation, the BER was within 10^{-3}.

Comparing the results of static and dynamic tests, it is noticeable that at the same measured distance, the BER differs by about one order of magnitude. This allows us to observe a certain trend and predict the behavior of the communication in future driving scenarios. An example is the comparison of the 16-QAM modulation, which in the static tests achieved a BER of 10^{-5} at 20 meters, while in the driving scenario the BER was around 10^{-4} at the same distance. Stable communication using 64-QAM modulation was also achievable up to a distance of 10 meters between vehicles while driving with a bit error rate of 10^{-5}.

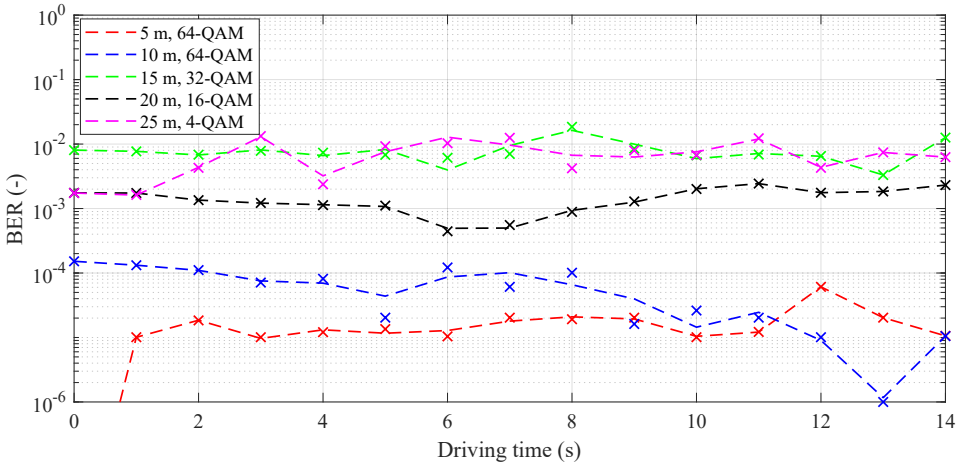

Figure 7.26: BER with respect to time and distance in dynamic tests. Carrier frequency 1 MHz, bandwith 400 kHz.

7.2 Smart Technologies and Buildings

Smart Technologies scenarios varied greatly, based on different use cases. First set of tests simulated indoor VLC communication, so the tests were mainly static. A fixed light source (indoor Philips ceiling light) was used to simulate a transmitting element in indoor scenarios at a fixed height, which corresponds to usual height of laboratory ceilings. These tests simulated the basic indoor scenarios, in which VLC could be used instead of conventional RF technologies, such as WiFi. This scenario was basically explored with every version of the platform, as it is the most basic use-case apart from the vehicular deployment.

7.2.1 Early Laboratory Tests with QAM Modulation and Indoor Lights

Early tests with indoor light sources were also described in "Visible Light Communication System Based on Software Defined Radio: Performance Study of Intelligent Transportation and Indoor Applications" [LD1]. The testing platform was practically the same as in the previously mentioned V2X scenarios, but since the light was mounted on an ceiling rail system, the nature condition simulating box was not used. The configuration of the QAM control application was also the same, but since the transmitting element was mounted at a fixed position, a different scenario was devised.

Measurements using ceiling light were carried out under laboratory conditions (calm wind, 24 °C). Figure 7.27 describes the tested setup. The tested light source was capable of covering a conical area with radius of approximately 350 cm. The measurements were firstly carried out at a right center of this covered area, directly under light source. Then, the measurements were periodically repeated but the receiving element was slowly moved to the edge of covered

area with a step of 25 cm. The distance between receiver and transmitter (height) was 202 cm – this simulated communication channel between ceiling mounted transmitter and receiver, that is sitting on a table.

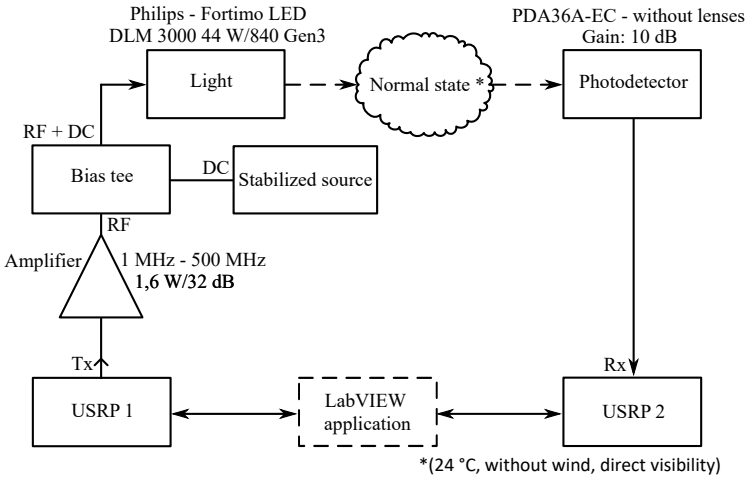

Figure 7.27: Ceiling light setup.

Figure 7.28 describes BER values of multiple channel widths and M-QAM modulation combinations. The graph itself also shows highest possible communication distance for measured modulation in which a certain level of communication can still be maintained. Values located next to the arrows correspond to BER.

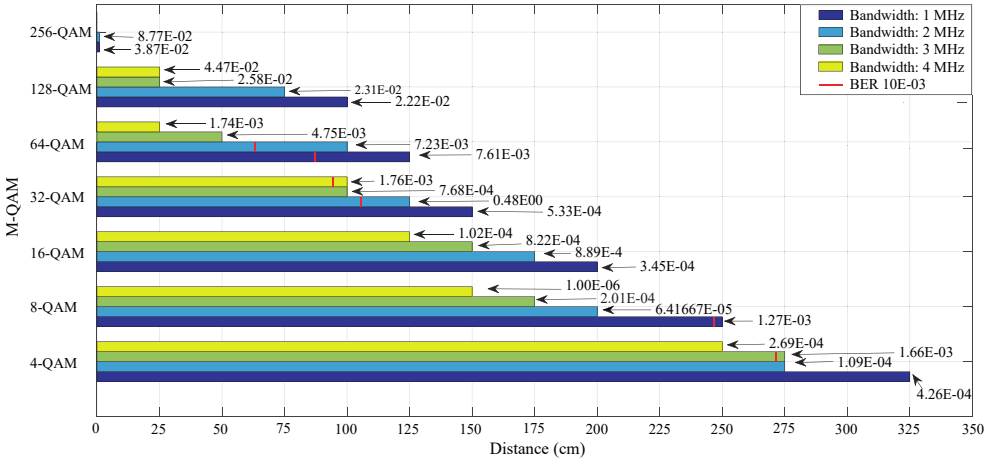

Figure 7.28: BER/distance from center relationship for ceiling light with different M-QAM and bandwidths.

Figure 7.29 and Figure 7.30 represent a comparison of 1 MHz and 4 MHz channel widths, the highest and lowest measured variants. It is visible that E_b/N_0 values slowly decreased with increasing measured distance. In comparison, EVM values shows opposite trend. Wider

channels were also much more limited in maximal reachable operation distance. Simpler modulation schemes in combination with narrow channel are much more robust, which is visible in Figure 7.28.

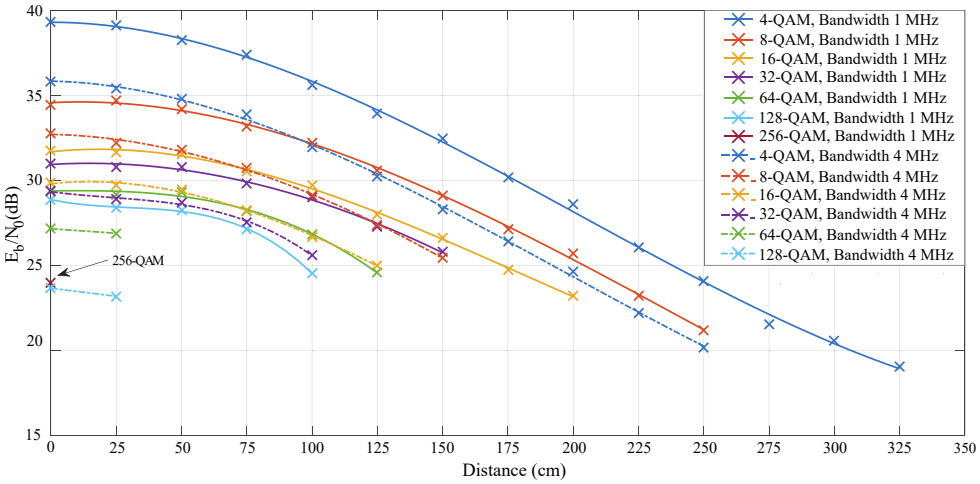

Figure 7.29: E_b/N_0 / distance from center relationship for ceiling light with different M-QAM and bandwidths.

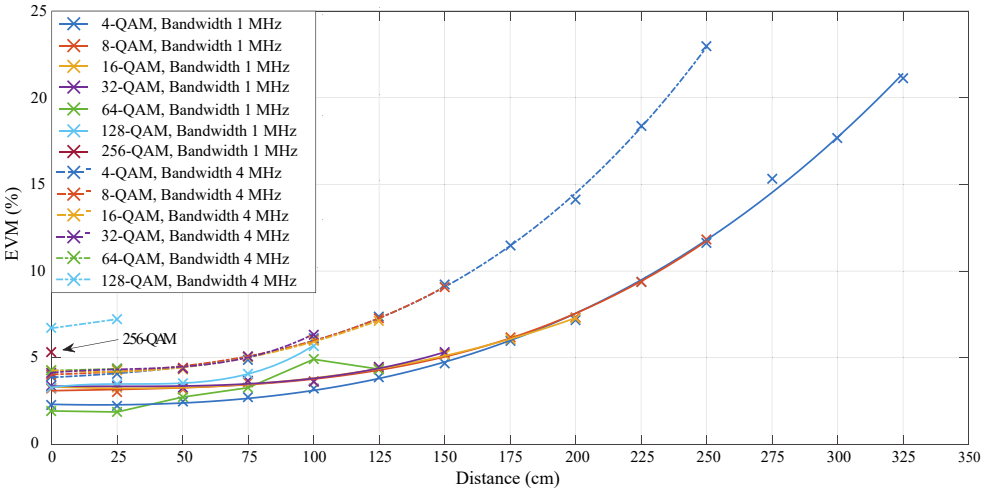

Figure 7.30: EVM/distance from center relationship for ceiling light with different M-QAM and bandwidths.

7.2.2 Early Tests of Equalization Techniques with QAM Modulation and Indoor Lights

The second oldest article called "Adaptive Software Defined Equalization Techniques for Indoor Visible Light Communication" [LD4] focused on testing of equalization techniques on

the first version of the VLC platform. A setup very similar to the previous experiment was used – The Philips Fortimo ceiling light was mounted on a moveable holder, which could be freely adjusted on a custom ceiling rail system. The receiving photodetector was mounted on a movable laboratory cart. Therefore, it was possible to change the position of the detector, but always keeping the same height. This scenario can be seen in Figure 7.31. The Philips light source illuminated conical area with diameter of 700 cm.

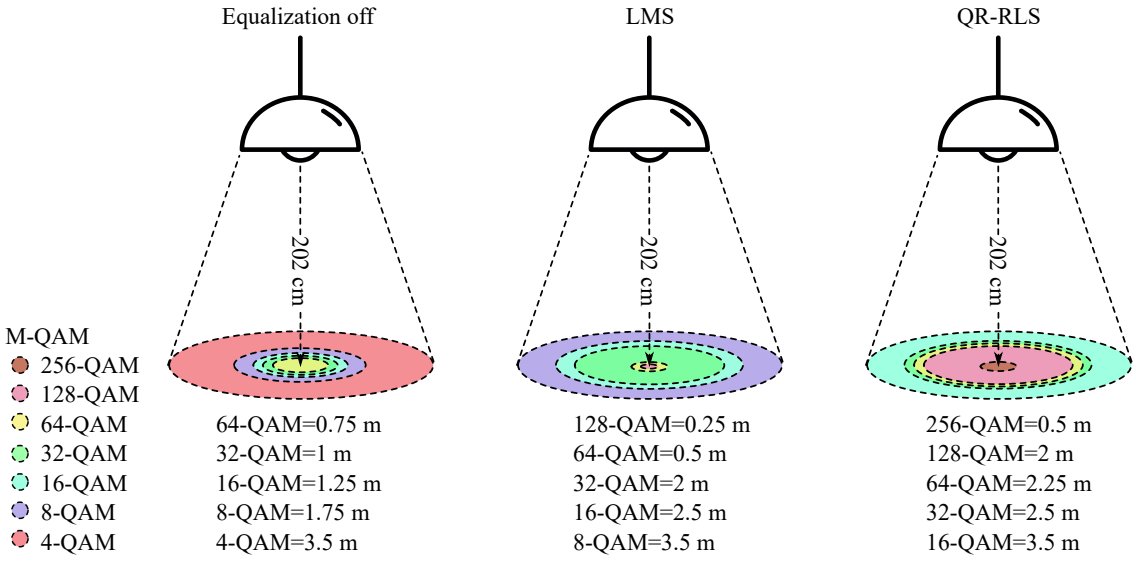

Figure 7.31: Visualization of reached M-QAM modulation formats based on measured parameters—3 MHz channel width and carrier frequency.

The measurement itself was carried out only in the X-axis up to a maximum distance of 350 cm, which corresponded to the radius of the illuminated area (Figure 7.31). As the illuminated area was a symmetrical cone, the measurement was carried out only in one direction: from the center to the "right" side. Therefore, the measured values for one direction corresponded to the measurements in every other direction (this statement was tested and verified by random short measurements).

The dependence of E_b/N_0 on the measured distance and configured adaptive algorithm can be seen in Figure 7.32 and Figure 7.33. These figures correspond to measurements with 4-QAM modulation and the 1 MHz or 4 MHz bandwidth. It is noticeable that the QR-RLS adaptive algorithm provided the best results of E_b/N_0 across the board (in comparison to the non-equalized data). The parameter was improved by 9 dB at the center of the illuminated area and by 11 dB at a threshold value of almost 300 cm. The other algorithms improved the measured signal as well, but the difference was lower. LMS managed to improve the E_b/N_0 by 2 dB at the center and 7 dB at the threshold. NLMS improved the values by 3 dB at the center and 8 dB at the threshold. As is visible, each algorithm noticeably improved the received signal.

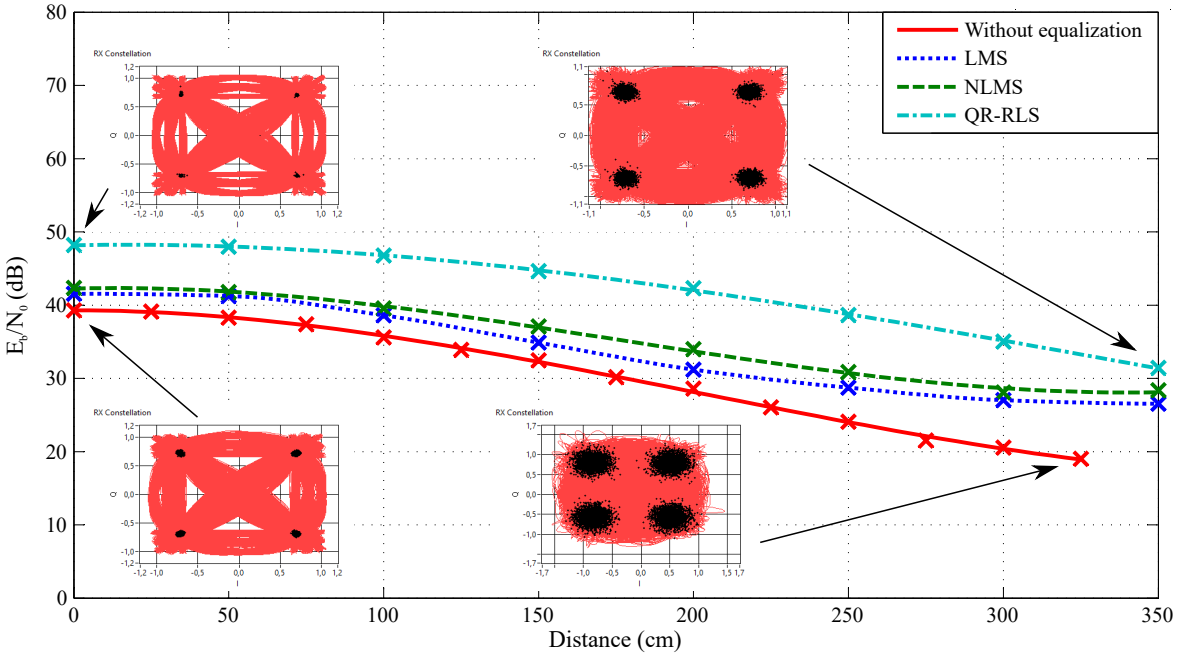

Figure 7.32: Dependence of E_b/N_0 on the distance and adaptive algorithm, bandwidth 1 MHz, 4-QAM.

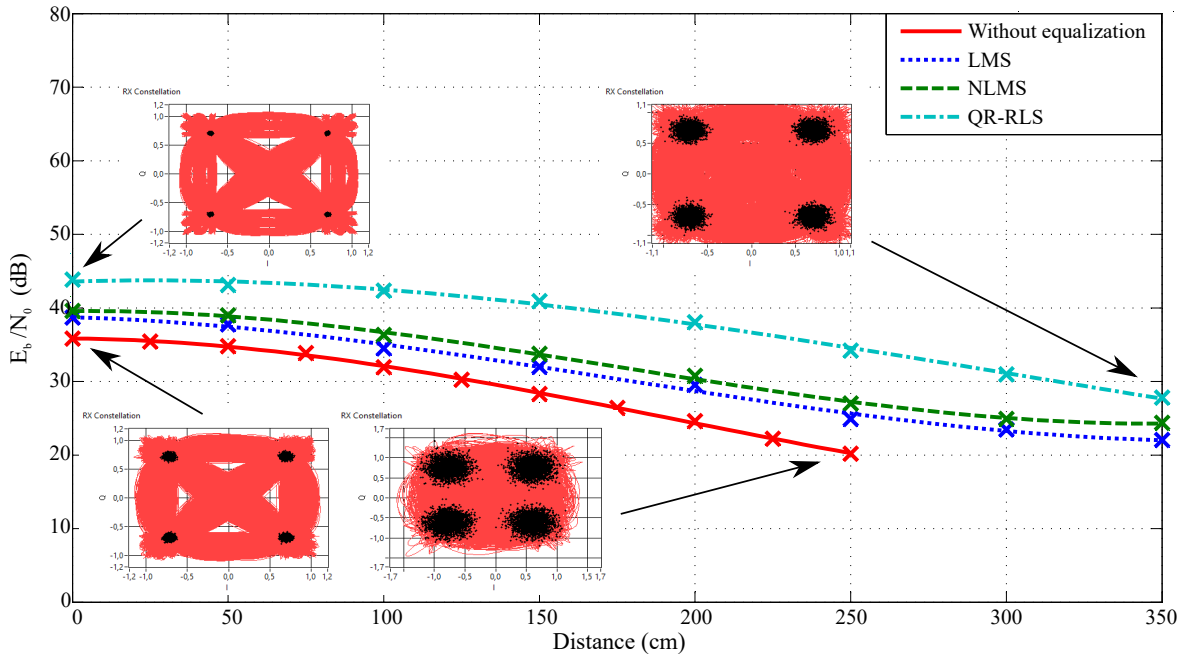

Figure 7.33: Dependence of E_b/N_0 on the distance and adaptive algorithm used, bandwidth 4 MHz, 4-QAM.

These figures also include two sets of constellation diagrams, one for the scenario without equalization and one with the QR-RLS adaptive algorithm. Each set had two constellation

diagrams corresponding to the values in the center of the illuminated area and at the measurable threshold (350 cm for QR-RLS and 325 cm for the scenario without equalization). By comparing both figures, it can be seen that wider bandwidths had a significant impact on E_b/N_0. Figure 7.32 shows the better results of E_b/N_0 by approximately 4 dB in comparison to Figure 7.33. However, wider channels also offered higher transmit speeds.

Figure 7.34 and Figure 7.35 show the comparison of the BER and EVM parameters. Both figures displayed a bit error rate for the 1 MHz bandwidth and 4–32 QAM modulation formats. Some waveforms are not present in the figures, as they tended to copy the horizontal axis (their BER was out of the platform measuring range). This fact mainly affected the 4-QAM modulation scheme in combination with various adaptive algorithms and was caused by the limited number of transmitted symbols, effectively influencing the range of the measurable bit error rate. Modulated signals without equalization had significantly higher error rates. The 32-QAM modulation scheme at 300 cm never exceeded the order of 10^{-5}, when the QR-RLS algorithm was used. In comparison, the whole platform easily exceeded the order of 10^{-4} at 150 cm without any equalization algorithms. The 4-QAM modulation would need to be used to reach a distance of 300 cm without equalization algorithms; therefore, the effective transmit speed would be lowered significantly. The system with this configuration might be able to transmit even on 325 cm, but the BER decreased rapidly (10^{-4} at 325 cm).

The EVM comparison in Figure 7.32 shows that the QR-RLS exhibited the best results. QR-RLS managed to improve EVM by 1.4% at the center of the illuminated area and by up to 10% at 300 cm. LMS and NLMS had very similar results: LMS improved EVM by 0.02% at the center and 5% at 300 cm, while NLMS improved EVM by 0.25% at the center and 7% at 300 cm.

All the above figures show that QR-RLS appeared to be the best adaptive algorithm, improving the measured parameters significantly. It was followed by NLMS and LMS, which had very similar results. Part of the results can be seen in Table 7.2 and Table 7.3.

While the presented equalization algorithms definitely improved the measured parameters, there was still room for improvement. The system vastly improved the first generation of our VLC system, mentioned previously. In addition, the non-linearity of hardware components significantly influenced the results, and it was estimated that the values might be even improved by at least 30% if more suitable parts were used.

7.2.3 Interoperability of KNX with VLC

The integration of VLC technology into smart housing was introduced as well. In 2022, an interoperability between LabVIEW (VLC), BACnet, IoT system and KNX smart housing system was described by the author and his colleagues [LD5]. VLC was in this case study introduced as a tool for Cell ID based occupancy determination of individual rooms. This

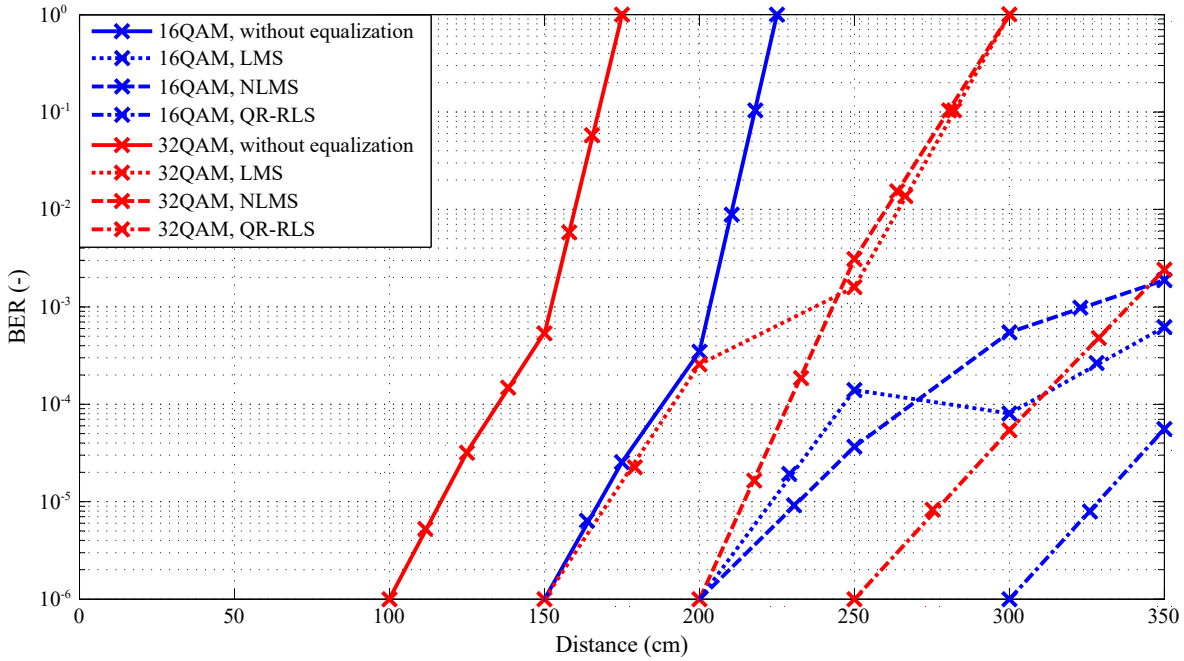

Figure 7.34: Dependence of BER on the distance and used adaptive algorithm, bandwidth 1 MHz, 4–32-QAM.

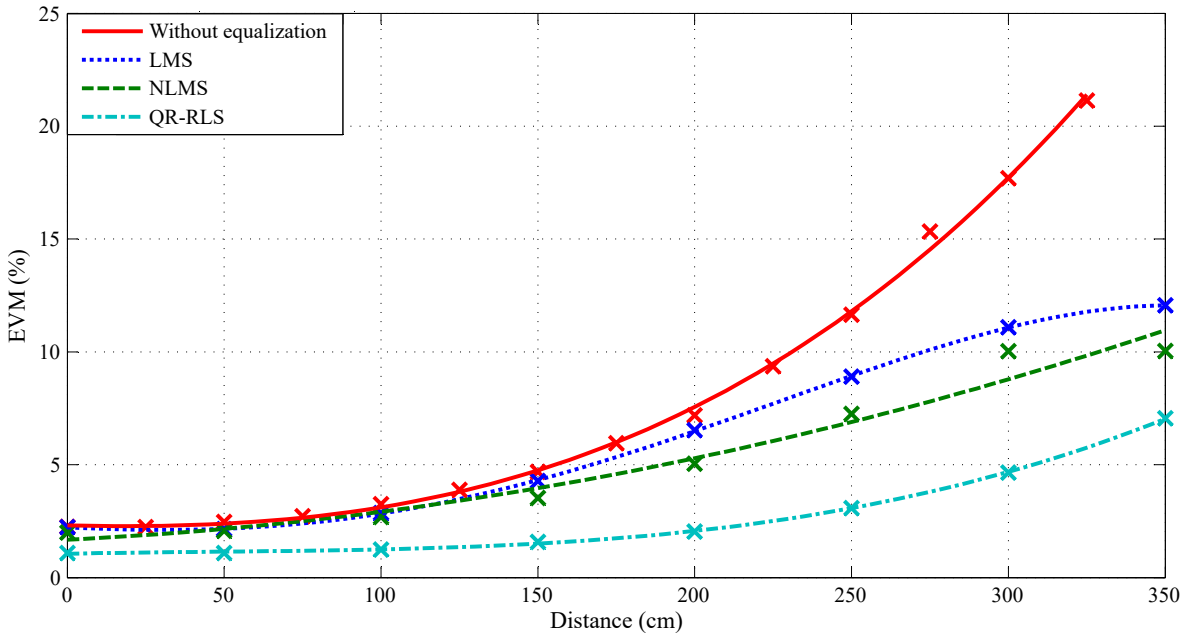

Figure 7.35: Dependence of EVM on the distance and used adaptive algorithm, bandwidth 1 MHz, 4-QAM.

concept could be further expanded, since there are other approaches for localization, including those that are used as NLoS solutions [88].

Table 7.2: Table of the measured parameters of the ceiling light, 4-QAM modulation format, bandwidth 1 MHz.

4-QAM									
Without EQ					LMS				
Distance (cm)	**E_b/N_0 (dB)**	**EVM (%)**	**BER (-)**	**MER (dB)**	**Distance (cm)**	**E_b/N_0 (dB)**	**EVM (%)**	**BER (-)**	**MER (dB)**
0	39.29	2.25	—	32.97	0	41.56	2.23	—	33.35
50	38.27	2.47	—	32.13	50	41.25	2.15	—	33.05
100	35.58	3.25	—	29.75	100	38.61	2.86	—	30.89
150	32.46	4.68	—	26.59	150	34.88	4.28	—	27.37
200	28.61	7.19	—	22.86	200	31.20	6.53	—	23.70
250	24.08	11.65	—	18.68	250	28.73	8.90	—	21.01
300	20.56	17.69	—	15.05	300	27.03	11.09	—	19.10
350	19.02	21.14	4.26^{-4}	13.50	350	26.54	12.06	—	18.37
4-QAM									
NLMS					QR-RLS				
Distance (cm)	**E_b/N_0 (dB)**	**EVM (%)**	**BER (-)**	**MER (dB)**	**Distance (cm)**	**E_b/N_0 (dB)**	**EVM (%)**	**BER (-)**	**MER (dB)**
0	42.35	2.00	—	33.98	0	48.21	1.09	—	39.46
50	41.79	2.07	—	33.68	50	47.96	1.09	—	39.25
100	39.54	2.68	—	31.45	100	46.78	1.24	—	38.13
150	37.10	3.52	—	29.08	150	44.65	1.58	—	36.03
200	33.99	5.05	—	25.93	200	42.32	2.04	—	33.80
250	30.87	7.25	—	22.79	250	38.65	3.08	—	30.23
300	28.07	10.03	—	19.98	300	35.03	4.66	—	26.64
350	28.37	10.04	—	19.97	350	31.42	7.05	—	23.03

— represents immeasurable BER (values below 10^{-5} threshold).

That article described proposed hardware and software solutions to enable communications and interoperability in smart home technology used to detect human occupants. The solution employs the KNX open data protocol, which provides interoperability and interworking with other technologies. Novel methods of enabling interoperability between KNX technology (smart home automation) and a VLC testing platform, IoT platform, or BACnet technology are also described.

The proposed system is split into three parts, where one is focused solely on VLC. A proposed architecture (for the interoperable solution) is applied to existing decentralized KNX technology in a smart home for the purpose of monitoring occupancy in individual rooms. A future interoperable implementation of KNX technology LabVIEW and VLC technology is described, and a basic experiment was conducted with an interoperable LabVIEW/KNX communication solution for a VLC testing platform to measure the VLC communication parameters for future occupancy detection in a specified room.

Basic experiments were based on a third version of the VLC platform. During measurement, the order of N-QAM modulation of the subcarrier OFDM symbols was changed from 4- to 64-QAM. The bandwidth was gradually changed from 500 kHz up to the system's limit.

Table 7.3: Table of measured parameters of the ceiling light, 256-QAM modulation format, bandwidth 1 MHz.

256-QAM									
Without EQ					LMS				
Distance	**E_b/N_0**	**EVM**	**BER**	**MER**	**Distance**	**E_b/N_0**	**EVM**	**BER**	**MER**
(cm)	**(dB)**	**(%)**	**(-)**	**(dB)**	**(cm)**	**(dB)**	**(%)**	**(-)**	**(dB)**
0	23.98	5.32	3.87^{-2}	21.21	0	32.69	1.90	1.00^{-3}	30.18
50	—	—	—	—	50	30.09	3.00	3.03^{-2}	27.50
100	—	—	—	—	100	29.49	2.78	6.38^{-3}	26.90
150	—	—	—	—	150	23.25	6.16	9.16^{-2}	20.39
200	—	—	—	—	200	—	—	—	—
250	—	—	—	—	250	—	—	—	—
256-QAM									
NLMS					QR-RLS				
Distance	**E_b/N_0**	**EVM**	**BER**	**MER**	**Distance**	**E_b/N_0**	**EVM**	**BER**	**MER**
(cm)	**(dB)**	**(%)**	**(-)**	**(dB)**	**(cm)**	**(dB)**	**(%)**	**(-)**	**(dB)**
0	32.10	1.99	1.48^{-3}	29.78	0	40.62	0.79	0	37.81
50	30.60	2.42	3.74^{-3}	28.12	50	40.96	0.75	0	38.28
100	27.76	3.42	1.15^{-2}	25.15	100	38.91	0.94	1.70^{-5}	36.33
150	22.86	6.39	6.71^{-2}	20.03	150	35.55	1.40	1.15^{-4}	32.88
200	—	—	—	—	200	28.00	3.66	5.70^{-2}	25.18
250	—	—	—	—	250	20.70	8.53	1.57^{-1}	17.83

— represents immeasurable BER (values below 10^{-5} threshold).

The early results indicated that some error rates were very high, and the main limiting factors were the system's hardware components, which are not ideal. However, the modularity of the system will allow for gradually eliminating these limiting factors and achieving superior results. Despite the problems, the system functions adequately and allows the transmission of data through a commercial and affordable LED ceiling light. In this respect, VLC technology offers benefits that can be integrated into the concept of SH or smart cities in the future. However, further experiments in this area are necessary, as the testing platform still has number of bugs that require fixing or adjustments. The system is also unoptimized and thus places high demands on the computing power of the connected PC. This concept will be further expanded with the fourth version of the VLC system, which will be much more flexible, thus providing a better way for integration into KNX system.

7.3 Industry

VLC has a huge potential in modern industrial plants. With the ongoing fourth industrial revolution, a lot of machinery is being connected to centralized servers or computational nodes. Due to the characteristics of this very specific environment a lot of interference from multiple sources is present, including mainly the electromagnetic interference (EMI). VLC is in its design resistant to EMI, but has other disadvantages mentioned before. Nevertheless,

there are scenarios, where VLC can be used as a reliable way to authenticate, authorize or localize workers/machines and connect them to local network.

This concept was presented by Danys et al. in 2022 [LD2]. This study on tracking solutions for Industry 4.0 and Operator 4.0 concept presented a novel integration of VLC technology into industrial plants and its comparison to conventional RF technologies. Advantages of both RF based technologies as well as VLC solutions were presented with possible gaps included as well. Various Visible Light Positioning (VLP) techniques were presented, including both active and passive solutions.

7.3.1 Integration of VLC into Industry 4.0 and Operator 4.0

This topic was explored in publication called "Visible Light Communication and localization: A study on tracking solutions for Industry 4.0 and the Operator 4.0" [LD2].

Value-driven manufacturing brings the design and implementation of *human-centric smart manufacturing systems (HCSM)*, like new-generation intelligent manufacturing [89]. Wireless technologies are very important for HCSM because operators are not restricted to working in one place - they therefore have freedom of movement and their localization is simpler to implement. Wide-spread wireless technologies have some restrictions like range, bandwidth, electromagnetic interference, or battery life. Some of these restrictions can be reduced or removed with *Light Communication (VLC)* and *Visible Light Positioning (VLP)*, which help to provide a *resilient manufacturing through human* [90].

As the whole industry is shifting towards the Industry 4.0 paradigm, different topics arise as well. The massive digitalization of industrial complexes is directly connected to the deployment of smart manufacturing solutions. These machines are directly interfacing with the workforce, significantly influencing the workflows of manufacturing plants in an Industrial Internet of Things, Services, and People (IIoTSP). As dangerous, difficult, or repetitive tasks can be maintained by robots, the human workers can focus on other, more complex, tasks. While the human workers will focus on more complex tasks, they will still use their unique abilities to innovate and adapt to completely new working environments. Workers are slowly starting to rely on modern smart and collaborative technologies, often donning virtual assistants, wearable sensors, smartwatches, augmented reality headsets, powered exoskeletons, and much more. While the people will be still an essential part of smart manufacturing processes, their appearance will also change. This new generation of technologically augmented human workers is called: *"Operators 4.0"* [91, 92]. These complex tasks and unique abilities open options for *human-robot collaborative assembly and human-automation symbiosis* in new working environments.

While modern technologies are often designed with collaboration in mind, they rely on a vast array of supplementary solutions, which are necessary for the reliable functionality of

these complex smart manufacturing ecosystems. The reliable localization of (mobile) robots and the (human) workforce on the shop floor is essential for smart factories. While the current machinery often employs lasers and other solutions for precise localization and tracking on a smaller scale, a different solution for larger-scale monitoring is necessary as well. New working environments will directly influence the nature of work, with new interactions not only between humans and machines but also the software and hardware side of things. Automation and advanced manufacturing are a driving power of further human augmentation, enhancing workers physical, cognitive, and sensorial capabilities. The complete *human-machine symbiosis* requires a complex and robust telecommunication system with precise localization, high transmit speeds and low latency.

VLC is currently considered as one of the major development areas of modern telecommunication systems. With the widespread deployment of the Industry 4.0 paradigm and its technological solutions, there is major pressure on the development of low-energy technologies for precise localization and communication. VLC is slowly rising as a suitable competition or supplementary technology to modern radio frequency solutions. While the 5G and its Narrowband-IoT certainly offers a robust and modern standardization, there can be scenarios, where the deployment of these technologies is unsuitable. Communication in certain industrial complexes is among these specific scenarios. Integration of VLC functionalities into Industry 4.0 concept can be seen in Figure 7.36.

Industrial complexes are nowadays often covered by cellular networks or other wireless technologies. Modern 5G or older 4G networks are offering their own IoT sub-technologies that can be used to transmit data or localize connected workers and equipment. However, cellular networks can be considered as a source of Electromagnetic Interference (EMI), which can influence some sensitive equipment that is often used in manufacturing processes. On the other side, some deployed machinery can also be considered as a source of EMI and therefore influence the proper operation of cellular networks of radio frequency technologies. VLC itself is not constrained by EMI and can work despite it, offering a solution for potentially uncoverable locations.

Wireless Industrial Internet of Things (IIoT) networks have unique operational characteristics and differ significantly from traditional computer networks: *communication* is often event-based, and they can also show significant irregularity and business. In addition, devices that rely on wireless communication in industrial environments are usually limited by the power and capacity of their battery, which, together with the non-optimized characteristics of the environment, creates notable barriers to the mutual exchange of information.

IIoT does not have a single standardized protocol package, as is the case with conventional computer networks, but the full range of network protocols used is available. These protocols differ from each other in features such as communication range, bandwidth, battery life, etc.

With the increasing amount of *human-automation symbiosis systems,* there is also an

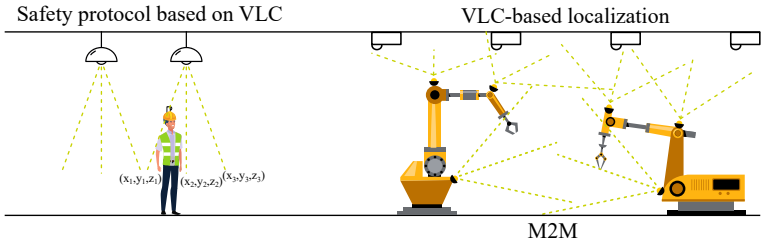

(a) Localization, Safety and M2M Protocols based on VLC.

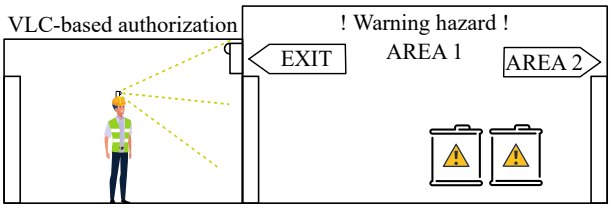

(b) VLC based Authorization in Dangerous Environments.

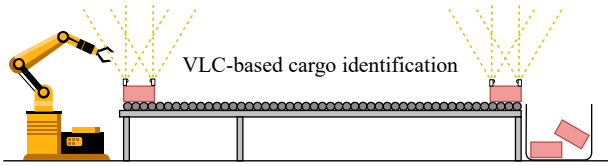

(c) VLC based Cargo Identification and Localization.

Figure 7.36: Integration of VLC Technologies into an Industry 4.0 Environment.

increasing number of applications that use location determination and object identification. It is needed to locate and identify objects and humans to ensure safety and provide cognitive support for modern operators (a.k.a. Operators 4.0).

The integration of VLC into modern well-known technologies is an achievable task. We propose a system that is fully integrated into modern 3GPP standardization (see Figure 7.37). The VLC development is focused on modern modulation formats that fully leverage the allocated frequency band while also maintaining a certain degree of reliability or robustness. While the VLC can be reliant on its own infrastructure (for further info, refer to LiFi), which connect a User Equipment (UE) directly via visible or infrared light, the proposed system employs the backbone network infrastructure of different technology. In this specific scenario, the VLC standalone block (VLC SA) is directly connected to transmitting elements of four different blocks – LTE, 5G not-standalone (5G NSA), 5G standalone (5G SA) and LTE Femtocell. The vast majority of mobile networks are still running on LTE infrastructure, which is slowly shifting towards 5G NSA integration. The 5G is in its first deployment phase directly dependent on the LTE core network (EPC). The transmission to the second phase, which is basically a fully functional standalone 5G model with virtualized networks elements, that can be adjusted on the go is still planned. There is even a possibility, that the SA mode will be

bypassed altogether in favor of currently developed 6G networks. The industrial complexes themselves are often connected via smaller femtocell solutions with limited coverage. The local gateway is therefore managing only a limited number of devices/people and can be considered more reliable. The presented VLC SA system is proposed mainly as a physical medium for mobile network cores. The main part of the system is a media converting center (MCC) which is converting the received Ethernet-based packet stream for the VLC/IR transmitter itself. As was mentioned before, the VLC light sources are transmitting data only to those devices that are in their field of view or near reflective areas. There might be specific scenarios when the visible light is unwanted. That is why the presented system also offers a different solution - infrared communication. The individual nodes can be then deployed based on the requirements either in standalone VLC/IR modes or in hybrid solutions. The system can operate either in simplex or duplex modes. The manufacturing robots are often fitted with light sources, which can be used as transmitters. They can be also adjusted and retrofitted with IR diodes, which are not visible so that the communication/localization system does not interfere with workers FoV. The localization and data transmissions can be therefore rerouted to these light sources and the whole system can maintain a duplex VLC-VLC, IR-IR, or VLC-IR link.

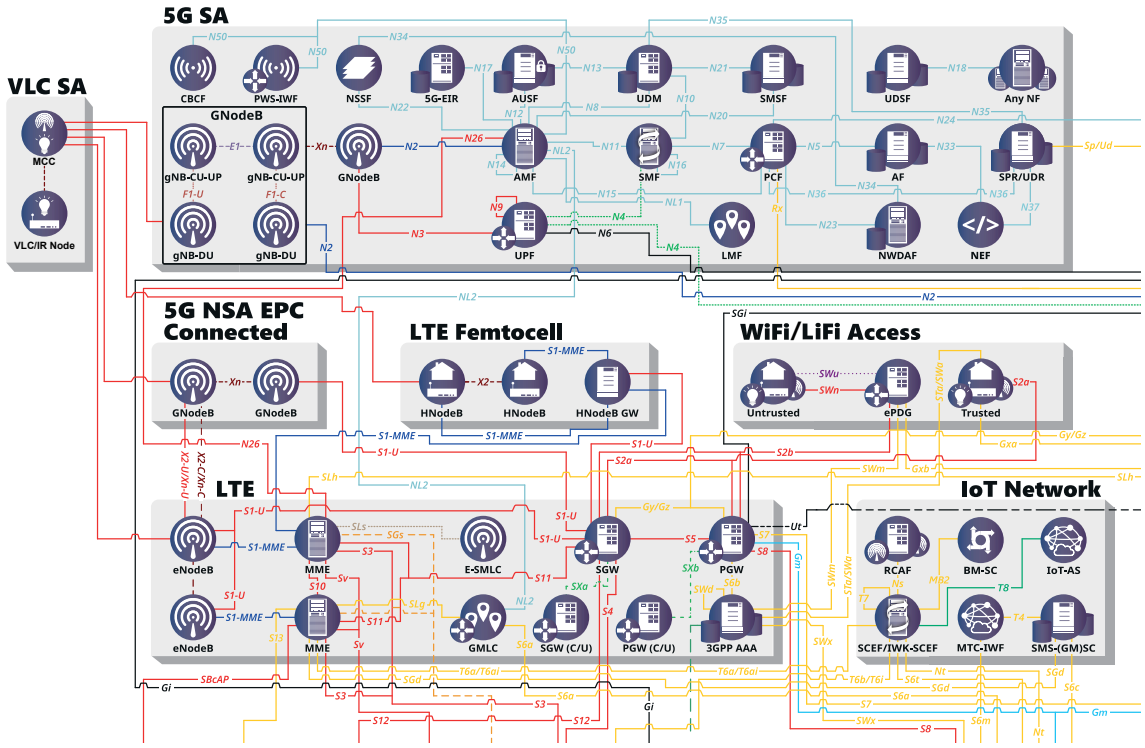

Figure 7.37: Integration of VLC into 3GPP Release 15 Standard (relevant part outsourced from [93]).

The presented concept of 4G/5G media conversion for VLC/IR communication and localization can be also utilized in the Operator 4.0 concept. These heavily augmented workers are highly reliant on a robust communication system. Precise localization and fast downlink/uplink transmissions with low latency are key elements of the whole system. Many of these points are already covered by 5G networks. The addition of VLC can in certain scenarios fill in the gaps – mainly in highly explosive areas or areas with sensitive equipment that can be influenced by EMI. These areas are nowadays highly reliant on either Ethernet or optical fibers - VLC could offer an alternative wireless connection, since it can leverage LED-based lighting infrastructure that is most of the time already present. Local administrator or automated system can therefore decide between 4G/5G standalone mode, VLC standalone mode or hybrid solution based on the environmental risks or needs.

7.4 Other Areas of Interest and Experiments

A novel VLC use case scenario is currently explored by the author and his colleagues. A consortium of universities, including VSB–TUO, developed an autonomous train for storage of nuclear waste. Each individual car was developed by different university and had different purpose. These trains are connected via mechanical joins and have to travel together. The team wanted to introduce a way, how to wirelessly transfer data through individual train cars. Since the train carries nuclear waste in cramped underground environments, RF based technologies could not be reliably used. VLC therefore offered an alternative, since each car has LED-based front and tail lights. As described before, the experimental VLC platform is capable of maintaining link up to 45 m, which should be more than enough for the train. This again proves the multidisciplinary aspect of the platform. Real tests will be conducted in the future, but since the VLC is often used in underground mines, it is expected to work in nuclear waste repositories. Future tests are planned with adjusted third version of the VLC platform and also with currently developed fourth version. This article currently has a work in progress title: "Integration of VLC into Autonomous Rail Vehicle for Nuclear Waste Disposal"

Author was also part of the publication team behind "Measurement of the Effect of Luminescent Layer Parameters on Light and Communication Properties" [LD6], which further progressed into Ph.D. Thesis by Mgr. et Mgr. Jan Jargus, Ph.D. In this article a modified first version of the VLC platform was used, since it focused on long-term measurements of a specific issue – various parameters of luminescent layer of LEDs. As mentioned before, the cheapest white led LEDs have a luminiscent layer, which basically "changes" the color of emitted light. However it also negatively influences the VLC capabilities of the light source. Experimental measurements have clearly shown that even a slightest change in the thickness of the luminescent layer has a non-negligible effect on both luminous and communication

parameters. Based on the results, samples containing only yellow phosphor have the best communication parameters, but the worst colorimetric parameters. To reach a suitable trade-off between both set of measured parameters a combination of yellow and red phosphor was chosen. Further research in this area is needed, but in the end, it could lead into fabrication of small-area luminescent layers that are optimised for VLC use cases.

Chapter 8

Conclusion

This dissertation thesis focused on deployment of software defined radios in SMART applications and other areas. Multiple versions of VLC platform that was improved over the years were described, along with individual experiments that were carried out in different application areas. The current version of the system is running in LabVIEW Communications and employ USRP 2954R as a dedicated SDR transmitter and receiver and OFDM modulation scheme with QAM modulation for individual subcarriers. While still having multiple bugs and problems, the system was integrated and tested in commercial vehicles. This latest version is able to maintain a successful communication to up to 50 meters. New and improved fourth version was also described, along with first insight into design of the next generation of the whole communication chain. The work itself is divided into multiple chapters.

The first chapter focused general description of modern software defined radios. It presents insights into general architecture of SDRs, which incorporates both digital and analog parts and their limitations. The chapter further continues with SDR hardware variants, software development tools and a description of SDR as a tool for SMART Technologies.

Second chapter mainly incorporates information about visible light communication technology including basic description of LEDs, advantages and disadvantages of VLC in comparison to RF, short insight into VLC IEEE standardization and mainly modulation formats, that are nowadays used for VLC deployment. VLP techniques are also mentioned, as VLC also support multiple positioning techniques.

Third chapter describes individual dissertation thesis objectives, which are based on previous two chapters. Each objective is presented and further explained, giving reader overview of the presented dissertation.

Fourth chapter focused on the description of the ongoing research, mentioning and explaining individual versions of the VLC platform and how it evolved over time. Advantages and limitations of every version is presented, including their schematics. In addition, a future

fourth version is presented, which will be a subject of further research. Finally, a table that compares all versions is included.

Fifth chapter presents a brief overview of the current version of the VLC platform, describing individual parts and controlling software. Modifications of hardware elements are included, explaining their role in the communication chain.

Sixth and final chapter presents a compilation of experimental results, that were published in high quality peer reviewed journals. Each subchapter presents results in individual application area, which offers an important insight into adaptability of the whole system to different environments.

By studying the current state of the art in the area of SDR and VLC technologies, 4 main objectives were identified, see Chapter 4. All of the established objectives of the doctoral dissertation have been accomplished. The following sections outline all the objectives and the process of achieving them.

1. *State of the art research of SDR platforms, VLC systems, modulations or technologies and SDR-based VLC solutions* – This objective was fulfilled in Chapter 2 and Chapter 3, which focus on the background of the whole platform. These chapters present the idea behind the direction of the whole system, why the author used software-defined radio for development and why the VLC technology was chosen.
2. *Creation of the function description of the next generation of modular VLC platform, pinpointing important design choices and hardware/software limitations* – This objective was fulfilled in the first part of Chapter 5, which focus on description of ongoing VLC platform development. By describing each individual version of the VLC system a road to the new version can be further explained, as multiple limitations were encountered along the way. Problems with the development of fully fledged OFDM platform are also presented, while multiple software and hardware limitations are discussed.
3. *Development of new iteration of VLC system, that offers high degree of modularity while maintaining its key multidisciplinary concept* – This objective was fulfilled in the second part of Chapter 5, where the description of third version, along with its modifications was presented. In addition, a short insight into the future of the whole system is presented, with a description of the future fourth version. The description of the modified version, that is used nowadays was presented in the Chapter 6, which in-depth focus on individual hardware parts and the core of the OFDM LabVIEW application.
4. *Experimental verification of the developed VLC system, along with optimization of the whole platform and evaluation of the obtained results* – This objective was fulfilled in the Chapter 7, which incorporates a compilation of multiple peer reviewed articles with experimental results from individual VLC system versions. Each publication is included in one of the relevant fields of interest. In addition, a new article from the field of nuclear waste disposal, that is work in progress is mentioned. Each experiment also

provided valuable info for further optimization of the platform, which will be reflected in the future fourth version.

The results of experiments clearly showed that the developed SDR based VLC platform reached a certain degree of modularity and is capable of adapting to multiple use cases. Each consecutive version improved the effective communication distance and transmit speeds as both software and hardware side were changed and improved. Nevertheless, the system is still plagued by problematic and unsupported hardware parts (daughterboards) and older OFDM LabVIEW code that requires further optimization.

The first major breakthrough was the introduction of the beta OFDM system, which revealed many of the future problems. The first testing OFDM system almost tripled the effective transmit distance from 5.5 m to 15 m, while matching the transmission speed and performance. The introduction of new SDR and adjustment of the application lead to further enhancements. Third version achieved communication distance up to 50 m, while running in low-speed scenario suitable for critical data only. The third version was therefore the first major iteration that was suitable for integration into vehicles, as the three second gap between two vehicles traveling in urban area was achievable. MXIe interface helped to maintain reliable connection between the controlling PC and the SDR.

However these new major advantages brought along some major issues. The most concerning one is the all-in-one design of the transmitter/receiver. Since the current version of OFDM requires a strict bus-based synchronization and since the inventory of the university is limited, the system is running only on one SDR. The receiving element as well as the transmitting element must be directly connected to the same SDR via coaxial cable. Both sides therefore share the same "node" they have to communicate with. Additionally, since the code is still not completely optimized, the application suffers from slow downs even when ran on high performance PCs.

First draft of the fourth version, which should counter at least one of these concerning factors was introduced as well. It is likely that the fourth version will be designed for the new Ettus NI USRP X410, which is fully compatible with newest LabVIEW and operates in suitable frequency range. If a set of these USRPs could be acquired, the code can be again split into two parts, as was originally intended. The author would like to continue with this further research and improve the system even further.

Overall, VLC definitely has a potential as a standalone or alternative communication technology. The developed platform, in its current state, needs a further refinement and consequent minimization. Experiments will continue along with modified third version while the fourth is still in development. It is expected that the next scenarios will focus on smart water metering, underwater VLC deployment, further integration into vehicles, including powering of the equipment from the in-built vehicular grid or deployment in specific environments, such as hospitals, manufacturing plants and underground nuclear waste disposing sites or mines.

Bibliography

1. MITOLA, J. Software Radios: Survey, Critical Evaluation and Future Directions. *IEEE Aerospace and Electronic Systems Magazine*. 1993-04, vol. 8, no. 4, pp. 25–36. ISSN 0885-8985. Available from DOI: 10.1109/62.210638.

2. COOK, P.G.; BONSER, W. Architectural Overview of the SPEAKeasy System. *IEEE Journal on Selected Areas in Communications*. 1999-04, vol. 17, no. 4, pp. 650–661. ISSN 07338716. Available from DOI: 10.1109/49.761042.

3. EDN; SHANDLE, Jack. *DSP Meets FPGA: Is Massive Parallelism Enough?* 2003-11.

4. KAZAZ, Tarik; VAN PRAET, Christophe; KULIN, Merima; WILLEMEN, Pieter; MOERMAN, Ingrid. Hardware Accelerated SDR Platform for Adaptive Air Interfaces. 2017. Available from DOI: 10.48550/ARXIV.1705.00115.

5. KHIEM V. CAI; KENT, S.D. SDR Approach to 3G Cellular/PCS and Position Location Services. In: *IEEE 60th Vehicular Technology Conference, 2004. VTC2004-Fall. 2004.* Los Angeles, CA, USA: IEEE, 2004, vol. 6, pp. 4103–4107. ISBN 978-0-7803-8521-4. Available from DOI: 10.1109/VETECF.2004.1404851.

6. ANTTILA, Lauri; LAMPU, Vesa; HASSANI, Seyed Ali; CAMPO, Pablo Pascual; KORPI, Dani; TURUNEN, Matias; POLLIN, Sofie; VALKAMA, Mikko. Full-Duplexing With SDR Devices: Algorithms, FPGA Implementation, and Real-Time Results. *IEEE Transactions on Wireless Communications*. 2021-04, vol. 20, no. 4, pp. 2205–2220. ISSN 1536-1276, ISSN 1558-2248. Available from DOI: 10.1109/TWC.2020.3040226.

7. MOLLA, Dereje M.; BADIS, Hakim; GEORGE, Laurent; BERBINEAU, Marion. Software Defined Radio Platforms for Wireless Technologies. *IEEE access : practical innovations, open solutions*. 2022, vol. 10, pp. 26203–26229. ISSN 2169-3536. Available from DOI: 10.1109/ACCESS.2022.3154364.

8. SEUNGHEON HYEON; KIM, J.; SEUNGWON CHOI. Evolution and Standardization of the Smart Antenna System for Software Defined Radio. *IEEE Communica-*

tions Magazine. 2008-09, vol. 46, no. 9, pp. 68–74. ISSN 0163-6804. Available from DOI: 10.1109/MCOM.2008.4623709.

9. KAFETZIS, Dimitrios; VASSILARAS, Spyridon; VARDOULIAS, Georgios; KOUTSOPOULOS, Iordanis. Software-Defined Networking Meets Software-Defined Radio in Mobile Ad Hoc Networks: State of the Art and Future Directions. *IEEE access : practical innovations, open solutions*. 2022, vol. 10, pp. 9989–10014. ISSN 2169-3536. Available from DOI: 10.1109/ACCESS.2022.3144072.

10. Transceiver Architectures. In: *Wireless Transceiver Design*. Chichester, UK: John Wiley & Sons, Ltd, 2016-09, pp. 27–62. ISBN 978-1-119-31565-0 978-1-118-93740-2. Available from DOI: 10.1002/9781119315650.ch2.

11. MACHADO, Raquel G.; WYGLINSKI, Alexander M. Software-Defined Radio: Bridging the Analog–Digital Divide. *Proceedings of the IEEE*. 2015-03, vol. 103, no. 3, pp. 409–423. ISSN 0018-9219, ISSN 1558-2256. Available from DOI: 10.1109/JPROC.2015.2399173.

12. MINDEN, G. J.; EVANS, J. B.; SEARL, L.; DEPARDO, D.; PETTY, V. R.; RAJBANSHI, R.; NEWMAN, T.; CHEN, Q.; WEIDLING, F.; GUFFEY, J.; DATLA, D.; BARKER, B.; PECK, M.; CORDILL, B.; WYGLINSKI, A. M.; AGAH, A. KUAR: A Flexible Software-Defined Radio Development Platform. In: *2007 2nd IEEE International Symposium on New Frontiers in Dynamic Spectrum Access Networks*. Dublin, Ireland: IEEE, 2007-04, pp. 428–439. ISBN 978-1-4244-0663-0. Available from DOI: 10.1109/DYSPAN.2007.62.

13. *How Does NI USRP Hardware Work?* 2022.

14. BANSAL, Manu; SCHULMAN, Aaron; KATTI, Sachin. Atomix: A Framework for Deploying Signal Processing Applications on Wireless Infrastructure. In: *12th USENIX Symposium on Networked Systems Design and Implementation (NSDI 15)*. 2015, pp. 173–188.

15. AKEELA, Rami; DEZFOULI, Behnam. Software-Defined Radios: Architecture, State-of-the-Art, and Challenges. *Computer Communications*. 2018-09, vol. 128, pp. 106–125. ISSN 01403664. Available from DOI: 10.1016/j.comcom.2018.07.012.

16. *Zynq UltraScale+ RFSoC* [https://www.xilinx.com/products/silicon-devices/soc/rfsoc.html]. 2022.

17. *Ettus USRP X410 Specifications - NI* [https://www.ni.com/docs/en-US/bundle/ettus-usrp-x410-specs/page/specs.html]. 2022.

18. *MathWorks - Makers of MATLAB and Simulink* [https://www.mathworks.com/]. 2022.

19. *What Is Software-Defined Radio / SDR Software* [https://www.mathworks.com/discovery/sdr.html]. 2022.

20. *GNU Radio - The Free & Open Source Radio Ecosystem · GNU Radio* [https://www.gnuradio.org/]. 2022.

21. *What Is LabVIEW? Graphical Programming for Test & Measurement - NI* [https://www.ni.com/cs-cz/shop/labview.html]. 2022.

22. BONAVOLONTA, Francesco; TEDESCO, Annarita; MORIELLO, Rosario Schiano Lo; TUFANO, Antonio. Enabling Wireless Technologies for Industry 4.0: State of the Art. In: *2017 IEEE International Workshop on Measurement and Networking (M&N)*. Naples, Italy: IEEE, 2017-09, pp. 1–5. ISBN 978-1-5090-5679-8. Available from DOI: 10.1109/IWMN.2017.8078381.

23. MOGENSEN, Rasmus Suhr; BARBERA, Simone; RODRIGUEZ, Ignacio; BERARDINELLI, Gilberto; FINK, Andreas; MARCKER, Rene; MARKUSSEN, Soren; RAUNHOLT, Taus; KOLDING, Troels; POCOVI, Guillermo. Implementation and Trial Evaluation of a Wireless Manufacturing Execution System for Industry 4.0. In: *2019 IEEE 90th Vehicular Technology Conference (VTC2019-Fall)*. Honolulu, HI, USA: IEEE, 2019-09, pp. 1–7. ISBN 978-1-72811-220-6. Available from DOI: 10.1109/VTCFall.2019.8891231.

24. HERNANDEZ, D. M.; PERALTA, G.; MANERO, L.; GOMEZ, R.; BILBAO, J.; ZUBIA, C. Energy and Coverage Study of LPWAN Schemes for Industry 4.0. In: *2017 IEEE International Workshop of Electronics, Control, Measurement, Signals and Their Application to Mechatronics (ECMSM)*. Donostia, San Sebastian, Spain: IEEE, 2017-05, pp. 1–6. ISBN 978-1-5090-5582-1. Available from DOI: 10.1109/ECMSM.2017.7945893.

25. NOOR-A-RAHIM, Md.; JOHN, Jobish; FIRYAGUNA, Fadhil; ZORBAS, Dimitrios; SHERAZI, Hafiz Husnain Raza; KUSHCH, Sergii; CONNELL, Eoin O; PESCH, Dirk; FLYNN, Brendan O; HAYES, Martin; ARMSTRONG, Eddie. Wireless Communications for Smart Manufacturing and Industrial IoT: Existing Technologies, 5G, and Beyond. 2022. Available from DOI: 10.48550/ARXIV.2208.06697.

26. AIJAZ, Adnan. Private 5G: The Future of Industrial Wireless. *IEEE Industrial Electronics Magazine*. 2020-12, vol. 14, no. 4, pp. 136–145. ISSN 1932-4529, ISSN 1941-0115. Available from DOI: 10.1109/MIE.2020.3004975.

27. MATHEUS, Luiz Eduardo Mendes; VIEIRA, Alex Borges; VIEIRA, Luiz F. M.; VIEIRA, Marcos A. M.; GNAWALI, Omprakash. Visible Light Communication: Concepts, Applications and Challenges. *IEEE Communications Surveys & Tutorials*.

2019, vol. 21, no. 4, pp. 3204–3237. ISSN 1553-877X, ISSN 2373-745X. Available from DOI: 10.1109/COMST.2019.2913348.

28. GFELLER, Fritz R.; BAPST, Urs. Wireless In-House Data Communication via Diffuse Infrared Radiation. *Proceedings of the IEEE*. 1979, vol. 67, no. 11, pp. 1474–1486.

29. KARBALAYGHAREH, Mehdi; MIRAMIRKHANI, Farshad; ELDEEB, Hossien B.; KIZILIRMAK, Refik Caglar; SAIT, Sadiq M.; UYSAL, Murat. Channel Modelling and Performance Limits of Vehicular Visible Light Communication Systems. *IEEE Transactions on Vehicular Technology*. 2020-07, vol. 69, no. 7, pp. 6891–6901. ISSN 0018-9545, ISSN 1939-9359. Available from DOI: 10.1109/TVT.2020.2993294.

30. ELDEEB, Hossien B.; ELAMASSIE, Mohammed; SAIT, Sadiq M.; UYSAL, Murat. Infrastructure-to-Vehicle Visible Light Communications: Channel Modelling and Performance Analysis. *IEEE Transactions on Vehicular Technology*. 2022-03, vol. 71, no. 3, pp. 2240–2250. ISSN 0018-9545, ISSN 1939-9359. Available from DOI: 10.1109/TVT.2022.3142991.

31. RAHAIM, M.; MIRAVAKILI, A.; BOROGOVAC, T.; LITTLE, T.; JOYNER, V. Demonstration of a Software Defined Visible Light Communication System. In: *Proc. 17th Annu. Int. Conf. Mobicom*. 2011, pp. 1–4.

32. HUSSAIN, Waqas; UGURDAG, H. Fatih; UYSAL, Murat. Software Defined VLC System: Implementation and Performance Evaluation. In: *2015 4th International Workshop on Optical Wireless Communications (IWOW)*. IEEE, 2015, pp. 117–121.

33. NAIR, Akhilesh Kumar; ARUNRAJ; KUMAR, Naveen; RAMYA, J.C; KIRUBAKARAN, V. Performance Analysis of LED and Florescent Lamps a Case Study of Street Lightning System. In: *2016 International Conference on Energy Efficient Technologies for Sustainability (ICEETS)*. Nagercoil, India: IEEE, 2016-04, pp. 850–855. ISBN 978-1-5090-1534-4 978-1-4673-9925-8. Available from DOI: 10.1109/ICEETS.2016.7583865.

34. DUPUIS, Russell D.; KRAMES, Michael R. History, Development, and Applications of High-Brightness Visible Light-Emitting Diodes. *Journal of Lightwave Technology*. 2008-05, vol. 26, no. 9, pp. 1154–1171. ISSN 0733-8724. Available from DOI: 10.1109/JLT.2008.923628.

35. TEIXEIRA, Lucas; LOOSE, Felipe; BRUM, Joao Paulo; BARRIQUELLO, Carlos Henrique; REGUERA, Vitalio Alfonso; COSTA, Marco Antonio Dalla. On the LED Illumination and Communication Design Space for Visible Light Communication. *IEEE Transactions on Industry Applications*. 2019-05, vol. 55, no. 3, pp. 3264–3273. ISSN 0093-9994, ISSN 1939-9367. Available from DOI: 10.1109/TIA.2019.2900209.

36. MURATA, Naoya; KOZAWA, Yusuke; UMEDA, Yohtaro. Digital Color Shift Keying With Multicolor LED Array. *IEEE Photonics Journal*. 2016-08, vol. 8, no. 4, pp. 1–13. ISSN 1943-0655. Available from DOI: 10.1109/JPHOT.2016.2582645.

37. TEIXEIRA, Lucas; LOOSE, Felipe; BARRIQUELLO, Carlos Henrique; REGUERA, Vitalio Alfonso; COSTA, Marco Antonio Dalla; ALONSO, J. Marcos. On Energy Efficiency of Visible Light Communication Systems. *IEEE Journal of Emerging and Selected Topics in Power Electronics*. 2021-10, vol. 9, no. 5, pp. 6396–6407. ISSN 2168-6777, ISSN 2168-6785. Available from DOI: 10.1109/JESTPE.2021.3073245.

38. ANDJAMBA, Taleni Shirley; ZODI, Guy-Alain Lusilao; JAT, Dharm Singh. Interference Analysis of IEEE 802.11 Wireless Networks: A Case Study of Namibia University of Science and Technology. In: *2016 International Conference on ICT in Business Industry & Government (ICTBIG)*. Indore, India: IEEE, 2016, pp. 1–5. ISBN 978-1-5090-5515-9. Available from DOI: 10.1109/ICTBIG.2016.7892726.

39. BERGER, Stephen. Spectrum Congestion - Is It a Technical Problem? In: *2014 United States National Committee of URSI National Radio Science Meeting (USNC-URSI NRSM)*. Boulder, CO, USA: IEEE, 2014-01, pp. 1–1. ISBN 978-1-4799-3120-0 978-1-4799-3119-4. Available from DOI: 10.1109/USNC-URSI-NRSM.2014.6928004.

40. LIU, Xiangyu; WEI, Xuetao; GUO, Lei; LIU, Yejun. SecLight: A New and Practical VLC Eavesdropping-Resilient Framework for IoT Devices. *IEEE Access*. 2019, vol. 7, pp. 19109–19124. ISSN 2169-3536. Available from DOI: 10.1109/ACCESS.2019.2897565.

41. AL-MOLIKI, Yahya Mohammed; ALRESHEEDI, Mohammed Thamer; AL-HARTHI, Yahya. Secret Key Generation Protocol for Optical OFDM Systems in Indoor VLC Networks. *IEEE Photonics Journal*. 2017-04, vol. 9, no. 2, pp. 1–15. ISSN 1943-0655. Available from DOI: 10.1109/JPHOT.2017.2667400.

42. OBEED, Mohanad; SALHAB, Anas M.; ALOUINI, Mohamed-Slim; ZUMMO, Salam A. On Optimizing VLC Networks for Downlink Multi-User Transmission: A Survey. *IEEE Communications Surveys & Tutorials*. 2019, vol. 21, no. 3, pp. 2947–2976. ISSN 1553-877X, ISSN 2373-745X. Available from DOI: 10.1109/COMST.2019.2906225.

43. CHEEMA, Ahmad; ALSMADI, Malek; IKKI, Salama. Distance Estimation in Visible Light Communications: The Case of Imperfect Synchronization and Signal-Dependent Noise. *IEEE Transactions on Vehicular Technology*. 2021-10, vol. 70, no. 10, pp. 11044–11049. ISSN 0018-9545, ISSN 1939-9359. Available from DOI: 10.1109/TVT.2021.3107808.

44. CHEEMA, Ahmad; ALSMADI, Malek; IKKI, Salama. Effect of Signal-Dependent Shot Noise on Visible Light Positioning. *IEEE Photonics Journal*. 2022-06, vol. 14, no. 3, pp. 1–7. ISSN 1943-0655, ISSN 1943-0647. Available from DOI: 10.1109/JPHOT.2022.3170693.

45. BASTIAENS, Sander; GERWEN, Jono Vanhie-Van; MACOIR, Nicola; DEPREZ, Kenneth; DE COCK, Cedric; JOSEPH, Wout; DE POORTER, Eli; PLETS, David. Experimental Benchmarking of Next-Gen Indoor Positioning Technologies (Unmodulated) Visible Light Positioning and Ultra-Wideband. *IEEE Internet of Things Journal*. 2022-09, vol. 9, no. 18, pp. 17858–17870. ISSN 2327-4662, ISSN 2372-2541. Available from DOI: 10.1109/JIOT.2022.3161791.

46. *IEEE SA - IEEE 802.15.7-2018* [https://standards.ieee.org/ieee/802.15.7/6820/]. 2016.

47. *IEEE SA - P802.15.7a* [https://standards.ieee.org/ieee/802.15.7a/10367/]. 2020.

48. MICHAILOW, Nicola; MATTHE, Maximilian; GASPAR, Ivan Simoes; CALDEVILLA, Ainoa Navarro; MENDES, Luciano Leonel; FESTAG, Andreas; FETTWEIS, Gerhard. Generalized Frequency Division Multiplexing for 5th Generation Cellular Networks. *IEEE Transactions on Communications*. 2014-09, vol. 62, no. 9, pp. 3045–3061. ISSN 0090-6778. Available from DOI: 10.1109/TCOMM.2014.2345566.

49. CHO, Yong Soo; KIM, Jaekwon; YANG, Won Young; KANG, Chung G. *MIMO-OFDM Wireless Communications with MATLAB®: Cho/MIMO-OFDM Wireless Communications with MATLAB®*. Chichester, UK: John Wiley & Sons, Ltd, 2010-08. ISBN 978-0-470-82563-1 978-0-470-82561-7. Available from DOI: 10.1002/9780470825631.

50. WANG, Yiru; GUAN, Weipeng; HUSSAIN, Babar; YUE, C. Patrick. High Precision Indoor Robot Localization Using VLC Enabled Smart Lighting. In: *Optical Fiber Communication Conference*. Optical Society of America, 2021, M1B–8.

51. IGBOANUSI, Ikechi Saviour; NWAKANMA, Cosmas Ifeanyi; LEE, Jae Min; KIM, Dong-Seong. VLC-UWB Hybrid (VUH) Network for Indoor Industrial Robots at Military Warehouses / Distribution Centers. In: *2019 International Conference on Information and Communication Technology Convergence (ICTC)*. Jeju Island, Korea (South): IEEE, 2019-10, pp. 762–766. ISBN 978-1-72810-893-3. Available from DOI: 10.1109/ICTC46691.2019.8939766.

52. HUSSAIN, Babar; WANG, Yiru; CHEN, Runzhou; CHENG, Hoi Chuen; YUE, C. Patrick. LiDR: Visible Light Communication-Assisted Dead Reckoning for Accurate Indoor Localization. *IEEE Internet of Things Journal*. 2022, pp. 1–1. ISSN 2327-4662, ISSN 2372-2541. Available from DOI: 10.1109/JIOT.2022.3151664.

53. DO, Trong-Hop; YOO, Myungsik. An in-Depth Survey of Visible Light Communication Based Positioning Systems. *Sensors* [online]. 2016-05, vol. 16, no. 5, p. 678 [visited on 2021-05-20]. ISSN 1424-8220. Available from DOI: 10.3390/s16050678.

54. KROMMENACKER, Nicolas; VASQUEZ, Oscar C.; ALFARO, Miguel D.; SOTO, Ismael. A self-adaptive cell-ID positioning system based on visible light communications in underground mines. In: *2016 IEEE International Conference on Automatica (ICA-ACCA)* [online]. Curicó, Chile: IEEE, 2016-10, pp. 1–7 [visited on 2021-05-20]. ISBN 978-1-5090-1147-6. Available from DOI: 10.1109/ICA-ACCA.2016.7778427.

55. MAJEED, Khaqan; HRANILOVIC, Steve. Passive Indoor Visible Light Positioning System using Deep Learning. *IEEE Internet of Things Journal* [online]. 2021, pp. 1–1 [visited on 2021-05-31]. ISSN 2327-4662, ISSN 2372-2541. Available from DOI: 10.1109/JIOT.2021.3072201.

56. SATO, Takuto; SHIMADA, Shota; MURAKAMI, Hiroaki; WATANABE, Hiroki; HASHIZUME, Hiromichi; SUGIMOTO, Masanori. ALiSA: a Visible-Light Positioning System using the Ambient Light Sensor Assembly in a Smartphone. *IEEE Sensors Journal* [online]. 2021, pp. 1–1 [visited on 2021-05-20]. ISSN 1530-437X, ISSN 1558-1748, ISSN 2379-9153. Available from DOI: 10.1109/JSEN.2021.3074580.

57. LI, Zhengpeng; QIU, Guodong; ZHAO, Lei; JIANG, Ming. Dual-Mode LED Aided Visible Light Positioning System Under Multi-Path Propagation: Design and Demonstration. *IEEE Transactions on Wireless Communications* [online]. 2021, pp. 1–1 [visited on 2021-05-20]. ISSN 1536-1276, ISSN 1558-2248. Available from DOI: 10.1109/TWC.2021.3071469.

58. SONER, Burak; COLERI, Sinem. Visible Light Communication Based Vehicle Localization for Collision Avoidance and Platooning. *IEEE Transactions on Vehicular Technology* [online]. 2021-03, vol. 70, no. 3, pp. 2167–2180 [visited on 2021-05-31]. ISSN 0018-9545, ISSN 1939-9359. Available from DOI: 10.1109/TVT.2021.3061512.

59. MASINI, Barbara; BAZZI, Alessandro; ZANELLA, Alberto. A Survey on the Roadmap to Mandate on Board Connectivity and Enable V2V-Based Vehicular Sensor Networks. *Sensors* [online]. 2018-07, vol. 18, no. 7, p. 2207 [visited on 2023-04-04]. ISSN 1424-8220. Available from DOI: 10.3390/s18072207.

60. GOTO, Yuki; TAKAI, Isamu; YAMAZATO, Takaya; OKADA, Hiraku; FUJII, Toshiaki; KAWAHITO, Shoji; ARAI, Shintaro; YENDO, Tomohiro; KAMAKURA, Koji. A New Automotive VLC System Using Optical Communication Image Sensor. *IEEE Photonics Journal* [online]. 2016-06, vol. 8, no. 3, pp. 1–17 [visited on 2023-04-04]. ISSN 1943-0655. Available from DOI: 10.1109/JPHOT.2016.2555582.

61. RAZA, Naeem; JABBAR, Sohail; HAN, Jihun; HAN, Kijun. Social Vehicle-to-Everything (V2X) Communication Model for Intelligent Transportation Systems Based on 5G Scenario. In: *Proceedings of the 2nd International Conference on Future Networks and Distributed Systems* [online]. Amman Jordan: ACM, 2018-06, pp. 1–8 [visited on 2023-04-04]. ISBN 978-1-4503-6428-7. Available from DOI: 10.1145/3231053.3231120.

62. KINOSHITA, Masayuki; YAMAZATO, Takaya; OKADA, Hiraku; FUJII, Toshiaki; ARAI, Shintaro; YENDO, Tomohiro; KAMAKURA, Koji. Motion Modeling of Mobile Transmitter for Image Sensor Based I2V-VLC, V2I-VLC, and V2V-VLC. In: *2014 IEEE Globecom Workshops (GC Wkshps)* [online]. Austin, TX, USA: IEEE, 2014-12, pp. 450–455 [visited on 2023-04-04]. ISBN 978-1-4799-7470-2. Available from DOI: 10.1109/GLOCOMW.2014.7063473.

63. KIM, Byung Wook; JUNG, Sung-Yoon. Vehicle Positioning Scheme Using V2V and V2I Visible Light Communications. In: *2016 IEEE 83rd Vehicular Technology Conference (VTC Spring)* [online]. Nanjing, China: IEEE, 2016-05, pp. 1–5 [visited on 2023-04-04]. ISBN 978-1-5090-1698-3. Available from DOI: 10.1109/VTCSpring.2016.7504526.

64. VAEZI, Mojtaba; DING, Zhiguo; POOR, H. Vincent. *Multiple Access Techniques for 5G Wireless Networks and Beyond*. Vol. 159. Springer, 2019.

65. BOBAN, Mate; KOUSARIDAS, Apostolos; MANOLAKIS, Konstantinos; EICHINGER, Josef; XU, Wen. Connected Roads of the Future: Use Cases, Requirements, and Design Considerations for Vehicle-to-Everything Communications. *IEEE Vehicular Technology Magazine* [online]. 2018-09, vol. 13, no. 3, pp. 110–123 [visited on 2023-04-04]. ISSN 1556-6072, ISSN 1556-6080. Available from DOI: 10.1109/MVT.2017.2777259.

66. KIM, Yong-Hyeon; CAHYADI, Willy Anugrah; CHUNG, Yeon Ho. Experimental Demonstration of LED-based Vehicle to Vehicle Communication under Atmospheric Turbulence. In: *2015 International Conference on Information and Communication Technology Convergence (ICTC)* [online]. Jeju Island, South Korea: IEEE, 2015-10, pp. 1143–1145 [visited on 2023-04-04]. ISBN 978-1-4673-7116-2. Available from DOI: 10.1109/ICTC.2015.7354759.

67. CAILEAN, Alin-Mihai; CAGNEAU, Barthelemy; CHASSAGNE, Luc; POPA, Valentin; DIMIAN, Mihai. A Survey on the Usage of DSRC and VLC in Communication-Based Vehicle Safety Applications. In: *2014 IEEE 21st Symposium on Communications and Vehicular Technology in the Benelux (SCVT)* [online]. Delft, Netherlands: IEEE, 2014-11, pp. 69–74 [visited on 2023-04-04]. ISBN 978-1-4799-8030-7. Available from DOI: 10.1109/SCVT.2014.7046710.

68. CAMPOLO, Claudia; MOLINARO, Antonella; SCOPIGNO, Riccardo. From Today's VANETs to Tomorrow's Planning and the Bets for the Day After. *Vehicular Communications* [online]. 2015-07, vol. 2, no. 3, pp. 158–171 [visited on 2023-04-04]. ISSN 22142096. Available from DOI: 10.1016/j.vehcom.2015.06.002.

69. YAMAZATO, Takaya. Overview of Visible Light Communications with Emphasis on Image Sensor Communications. In: *2017 23rd Asia-Pacific Conference on Communications (APCC)* [online]. Perth, WA: IEEE, 2017-12, pp. 1–6 [visited on 2023-04-04]. ISBN 978-1-74052-390-5. Available from DOI: 10.23919/APCC.2017.8304093.

70. YAMAZATO, Takaya. Image Sensor Communications for Future ITS. In: *Advanced Photonics 2018 (BGPP, IPR, NP, NOMA, Sensors, Networks, SPPCom, SOF)* [online]. Zurich: OSA, 2018, SpW2G.6 [visited on 2023-04-04]. ISBN 978-1-943580-43-9. Available from DOI: 10.1364/SPPCOM.2018.SpW2G.6.

71. TSADO, Yakubu; LUND, David; GAMAGE, Kelum A.A. Resilient Communication for Smart Grid Ubiquitous Sensor Network: State of the Art and Prospects for next Generation. *Computer Communications* [online]. 2015-11, vol. 71, pp. 34–49 [visited on 2023-04-04]. ISSN 01403664. Available from DOI: 10.1016/j.comcom.2015.05.015.

72. TAREEN, Wajahat Ullah Khan; MEKHILEF, Saad; NAKAOKA, Mutsuo. A Transformerless Reduced Switch Counts Three-Phase APF-assisted Smart EV Charger. In: *2017 IEEE Applied Power Electronics Conference and Exposition (APEC)* [online]. Tampa, FL, USA: IEEE, 2017-03, pp. 3307–3312 [visited on 2023-04-04]. ISBN 978-1-5090-5366-7. Available from DOI: 10.1109/APEC.2017.7931171.

73. ROCHE, Robin; BERTHOLD, Florence; GAO, Fei; WANG, Fei; RAVEY, Alexandre; WILLIAMSON, Sheldon. A Model and Strategy to Improve Smart Home Energy Resilience during Outages Using Vehicle-to-Home. In: *2014 IEEE International Electric Vehicle Conference (IEVC)* [online]. Florence: IEEE, 2014-12, pp. 1–6 [visited on 2023-04-04]. ISBN 978-1-4799-6075-0. Available from DOI: 10.1109/IEVC.2014.7056106.

74. TURKER, Harun; BACHA, Seddik. Optimal Minimization of Plug-In Electric Vehicle Charging Cost With Vehicle-to-Home and Vehicle-to-Grid Concepts. *IEEE Transactions on Vehicular Technology* [online]. 2018-11, vol. 67, no. 11, pp. 10281–10292 [visited on 2023-04-04]. ISSN 0018-9545, ISSN 1939-9359. Available from DOI: 10.1109/TVT.2018.2867428.

75. YAMAZATO, Takaya. V2X Communications with an Image Sensor. *Journal of Communications and Information Networks* [online]. 2017-12, vol. 2, no. 4, pp. 65–74 [visited on 2023-04-04]. ISSN 2096-1081, ISSN 2509-3312. Available from DOI: 10.1007/s41650-017-0044-4.

76. MARE, Renata Maria; LUIZ MARTE, Claudio; CUGNASCA, Carlos Eduardo. Visible Light Communication Applied to Intelligent Transport Systems: An Overview. *IEEE Latin America Transactions* [online]. 2016-07, vol. 14, no. 7, pp. 3199–3207 [visited on 2023-04-04]. ISSN 1548-0992. Available from DOI: 10.1109/TLA.2016.7587621.

77. KINOSHITA, Masayuki; YAMAZATO, Takaya; OKADA, Hiraku; FUJII, Toshiaki; ARAI, Shintaro; YENDO, Tomohiro; KAMAKURA, Koji. Channel Fluctuation Measurement for Image Sensor Based I2V-VLC, V2I-VLC, and V2V-VLC. In: *2014 IEEE Asia Pacific Conference on Circuits and Systems (APCCAS)* [online]. Ishigaki, Japan: IEEE, 2014-11, pp. 332–335 [visited on 2023-04-04]. ISBN 978-1-4799-5230-4. Available from DOI: 10.1109/APCCAS.2014.7032787.

78. KIM, Yong Hyeon; CAHYADI, Willy Anugrah; CHUNG, Yeon Ho. Experimental Demonstration of VLC-Based Vehicle-to-Vehicle Communications Under Fog Conditions. *IEEE Photonics Journal* [online]. 2015-12, vol. 7, no. 6, pp. 1–9 [visited on 2023-04-04]. ISSN 1943-0655. Available from DOI: 10.1109/JPHOT.2015.2499542.

79. ARENA, Fabio; PAU, Giovanni. An Overview of Vehicular Communications. *Future Internet* [online]. 2019-01, vol. 11, no. 2, p. 27 [visited on 2023-04-04]. ISSN 1999-5903. Available from DOI: 10.3390/fi11020027.

80. VIRIYASITAVAT, Wantanee; BOBAN, Mate; HSIN-MU TSAI; VASILAKOS, Athanasios. Vehicular Communications: Survey and Challenges of Channel and Propagation Models. *IEEE Vehicular Technology Magazine* [online]. 2015-06, vol. 10, no. 2, pp. 55–66 [visited on 2023-04-04]. ISSN 1556-6072. Available from DOI: 10.1109/MVT.2015.2410341.

81. WANG, Yubo; SHEIKH, Omar; HU, Boyang; CHU, Chi-Cheng; GADH, Rajit. Integration of V2H/V2G Hybrid System for Demand Response in Distribution Network. In: *2014 IEEE International Conference on Smart Grid Communications (SmartGridComm)* [online]. Venice, Italy: IEEE, 2014-11, pp. 812–817 [visited on 2023-04-04]. ISBN 978-1-4799-4934-2. Available from DOI: 10.1109/SmartGridComm.2014.7007748.

82. ZHAO, Long; ARAVINTHAN, Visvakumar. Strategies of Residential Peak Shaving with Integration of Demand Response and V2H. In: *2013 IEEE PES Asia-Pacific Power and Energy Engineering Conference (APPEEC)* [online]. Kowloon, Hong Kong: IEEE, 2013-12, pp. 1–5 [visited on 2023-04-04]. ISBN 978-1-4799-2522-3. Available from DOI: 10.1109/APPEEC.2013.6837260.

83. GUILLE, Christophe; GROSS, George. A Conceptual Framework for the Vehicle-to-Grid (V2G) Implementation. *Energy Policy* [online]. 2009-11, vol. 37, no. 11, pp. 4379–4390 [visited on 2023-04-04]. ISSN 03014215. Available from DOI: 10.1016/j.enpol.2009.05.053.

84. OTA, Yutaka; TANIGUCHI, Haruhito; NAKAJIMA, Tatsuhito; LIYANAGE, Kithsiri M.; BABA, Jumpei; YOKOYAMA, Akihiko. Autonomous Distributed V2G (Vehicle-to-Grid) Satisfying Scheduled Charging. *IEEE Transactions on Smart Grid* [online]. 2012-03, vol. 3, no. 1, pp. 559–564 [visited on 2023-04-04]. ISSN 1949-3053, ISSN 1949-3061. Available from DOI: 10.1109/TSG.2011.2167993.

85. ALAM, Mahbubul. Vehicle-to-Everything (V2X) Technology Will Be a Literal Life Saver—But What Is It. *Eng. Guide Automot. Connect. Car, Jun.* 2016.

86. *European Commission - Road Safety* [online]. [N.d.]. [visited on 2022-07-26]. Available from: https://ec.europa.eu/transport/road_safety/going_abroad/czech_republic/speed_limits_en.htm.

87. *Traffic Rules - Ministry of the interior of the Czech Republic* [online]. [N.d.]. [visited on 2022-07-26]. Available from: https://www.mvcr.cz/mvcren/article/traffic-rules.aspx.

88. HUANG, Chuanxi; ZHANG, Xun; ZHOU, Fen; WANG, Zhan; SHI, Lina. NLOS-Aware VLC-based Indoor Localization: Algorithm Design and Experimental Validation. In: *2020 IEEE Wireless Communications and Networking Conference (WCNC)* [online]. Seoul, Korea (South): IEEE, 2020-05, pp. 1–7 [visited on 2023-04-04]. ISBN 978-1-72813-106-1. Available from DOI: 10.1109/WCNC45663.2020.9120725.

89. ZHOU, Ji; ZHOU, Yanhong; WANG, Baicun; ZANG, Jiyuan. Human–Cyber–Physical Systems (HCPSs) in the Context of New-Generation Intelligent Manufacturing. *Engineering*. 2019, vol. 5, no. 4, pp. 624–636. ISSN 2095-8099. Available from DOI: https://doi.org/10.1016/j.eng.2019.07.015.

90. PENG, Tao; HE, Qiqi; ZHANG, Zheng; WANG, Baicun; XU, Xun. Industrial internet-enabled resilient manufacturing strategy in the wake of COVID-19 pandemic: a conceptual framework and implementations in China. *Chinese Journal of Mechanical Engineering*. 2021, vol. 34, no. 1, pp. 1–6.

91. ROMERO, David; STAHRE, Johan; WUEST, Thorsten; NORAN, Ovidiu; BERNUS, Peter; FAST-BERGLUND, Asa; GORECKY, Dominic. TOWARDS AN OPERATOR 4.0 TYPOLOGY: A HUMAN-CENTRIC PERSPECTIVE ON THE FOURTH INDUSTRIAL REVOLUTION TECHNOLOGIES. 2016, p. 12.

92. ROMERO, David; BERNUS, Peter; NORAN, Ovidiu; STAHRE, Johan; FAST-BERGLUND, Asa. The Operator 4.0: Human Cyber-Physical Systems & Adaptive Automation Towards Human-Automation Symbiosis Work Systems. In: NÄÄS, Irenilza; VENDRAMETTO, Oduvaldo; MENDES REIS, João; GONÇALVES, Rodrigo Franco; SILVA, Márcia Terra; CIEMINSKI, Gregor von; KIRITSIS, Dimitris (eds.). *Advances in Production Management Systems. Initiatives for a Sustainable World*. Cham: Springer International Publishing, 2016, pp. 677–686. IFIP Advances in Information and Communication Technology. ISBN 978-3-319-51133-7. Available from DOI: 10.1007/978-3-319-51133-7_80.

93. *Who is Terence?* [online]. [N.d.]. [visited on 2021-05-28]. Available from: http://whoisterence.com/Portfolio.html.

List of Own Publication Activities and Other Outcomes

Publications and Outcomes Related to Thesis

LD1. MARTINEK, Radek; DANYS, Lukas; JAROS, Rene. Visible Light Communication System Based on Software Defined Radio: Performance Study of Intelligent Transportation and Indoor Applications. *Electronics*. 2019-04, vol. 8, no. 4, p. 433. ISSN 2079-9292. Available from DOI: 10.3390/electronics8040433.

LD2. DANYS, Lukas; ZOLOTOVA, Iveta; ROMERO, David; PAPCUN, Peter; KAJATI, Erik; JAROS, Rene; KOUDELKA, Petr; KOZIOREK, Jiri; MARTINEK, Radek. Visible Light Communication and localization: A study on tracking solutions for Industry 4.0 and the Operator 4.0. *Journal of Manufacturing Systems* [online]. 2022-07, vol. 64, pp. 535–545 [visited on 2022-10-19]. ISSN 02786125. Available from DOI: 10.1016/j.jmsy.2022.07.011.

LD3. DANYS, Lukas; MARTINEK, Radek; JAROS, Rene; BAROS, Jan; SIMONIK, Petr; SNASEL, Vaclav. Enhancements of SDR-Based FPGA System for V2X-VLC Communications. *Computers, Materials & Continua* [online]. 2021, vol. 68, no. 3, pp. 3629–3652 [visited on 2022-10-19]. ISSN 1546-2226. Available from DOI: 10.32604/cmc.2021.017333.

LD4. MARTINEK, Radek; DANYS, Lukas; JAROS, Rene. Adaptive Software Defined Equalization Techniques for Indoor Visible Light Communication. *Sensors* [online]. 2020-03-14, vol. 20, no. 6, p. 1618 [visited on 2022-10-19]. ISSN 1424-8220. Available from DOI: 10.3390/s20061618.

LD5. VANUS, Jan; MARTINEK, R.; DANYS, L.; NEDOMA, J.; BILIK, P. Occupancy Detection in Smart Home Space Using Interoperable Building Automation Technologies. *Human-centric Computing and Information Sciences* [online]. 2022-10, vol. 12, no. 0, pp. 616–632 [visited on 2023-05-04]. Available from DOI: 10.22967/HCIS.2022.12.047.

Publications and Outcomes Not Related to Thesis

LD6. JARGUS, Jan; TOMIS, Martin; BAROS, Jan; DANYS, Lukas; JAROS, Rene; MARTINEK, Radek; VASINEK, Vladimir; NEDOMA, Jan. Measurement of the Effect of Luminescent Layer Parameters on Light and Communication Properties. *IEEE Transactions on Instrumentation and Measurement* [online]. 2022, pp. 1–1 [visited on 2023-05-04]. ISSN 0018-9456, ISSN 1557-9662. Available from DOI: 10.1109/TIM.2022.3224530.

LD7. JAROS, Rene; MARTINEK, Radek; DANYS, Lukas. Comparison of Different Electrocardiography with Vectorcardiography Transformations. *Sensors* [online]. 2019-07-11, vol. 19, no. 14, p. 3072 [visited on 2022-10-19]. ISSN 1424-8220. Available from DOI: 10.3390/s19143072.

LD8. MARTINEK, Radek; BILIK, Petr; BAROS, Jan; BRABLIK, Jindrich; KAHANKOVA, Radana; JAROS, Rene; DANYS, Lukas; RZIDKY, Jaroslav; WEN, He. Design of a Measuring System for Electricity Quality Monitoring within the SMART Street Lighting Test Polygon: Pilot Study on Adaptive Current Control Strategy for Three-Phase Shunt Active Power Filters. *Sensors* [online]. 2020-03-19, vol. 20, no. 6, p. 1718 [visited on 2022-10-19]. ISSN 1424-8220. Available from DOI: 10.3390/s20061718.

LD9. SIDIKOVA, Michaela; MARTINEK, Radek; KAWALA-STERNIUK, Aleksandra; LADROVA, Martina; JAROS, Rene; DANYS, Lukas; SIMONIK, Petr. Vital Sign Monitoring in Car Seats Based on Electrocardiography, Ballistocardiography and Seismocardiography: A Review. *Sensors* [online]. 2020-10-06, vol. 20, no. 19, p. 5699 [visited on 2022-10-19]. ISSN 1424-8220. Available from DOI: 10.3390/s20195699.

LD10. SLANY, Vlastimil; KOUDELKA, Petr; KRCALOVA, Eva; JOBBAGY, Jan; DANYS, Lukas; JAROS, Rene; SLANINA, Zdenek; PRAUZEK, Michal; MARTINEK, Radek. New Hybrid IoT LoRaWAN/IRC Sensors: SMART Water Metering System. *Computers, Materials & Continua* [online]. 2022, vol. 71, no. 3, pp. 5201–5217 [visited on 2022-10-19]. ISSN 1546-2226. Available from DOI: 10.32604/cmc.2022.021349.

LD11. MARTINEK, Radek; BAROS, Jan; JAROS, Rene; DANYS, Lukas; NEDOMA, Jan. Hybrid In-Vehicle Background Noise Reduction for Robust Speech Recognition: The Possibilities of Next Generation 5G Data Networks. *Computers, Materials & Continua* [online]. 2022, vol. 71, no. 3, pp. 4659–4676 [visited on 2022-10-19]. ISSN 1546-2226. Available from DOI: 10.32604/cmc.2022.019904.

LD12. FAJKUS, Marcel; NEDOMA, Jan; MARTINEK, Radek; DANYS, Lukas; FRIDRICH, Michael; MEC, Pavel; ZABKA, Stanislav. Fiber-Optic Bragg System for the Dynamic Weighing of Municipal Waste: A Pilot Study. *IEEE Access* [online]. 2021,

vol. 9, pp. 99050–99059 [visited on 2022-10-19]. ISSN 2169-3536. Available from DOI: 10.1109/ACCESS.2021.3095219.

LD13. BAROS, Jan; SOTOLA, Vojtech; BILIK, Petr; MARTINEK, Radek; JAROS, Rene; DANYS, Lukas; SIMONIK, Petr. Review of Fundamental Active Current Extraction Techniques for SAPF. *Sensors* [online]. 2022-01, vol. 22, no. 20, p. 7985 [visited on 2022-10-19]. ISSN 1424-8220. Available from DOI: 10.3390/s22207985. Number: 20 Publisher: Multidisciplinary Digital Publishing Institute.

LD14. HAJOVSKY, Radovan; PIES, Martin; VELICKA, Jan; SLANY, Vlastimil; ROUS, Robert; DANYS, Lukas; MARTINEK, Radek. Design of an IoT-Based Monitoring System as a Part of Prevention of Thermal Events in Mining and Landfill Waste Disposal Sites: A Pilot Case Study. *IEEE Transactions on Instrumentation and Measurement* [online]. 2023, vol. 72, pp. 1–14 [visited on 2023-05-04]. ISSN 0018-9456, ISSN 1557-9662. Available from DOI: 10.1109/TIM.2022.3225046.

LD15. JAROS, Rene; BYRTUS, Radek; DOHNAL, Jakub; DANYS, Lukas; BAROS, Jan; KOZIOREK, Jiri; ZMIJ, Petr; MARTINEK, Radek. Advanced Signal Processing Methods for Condition Monitoring. *Archives of Computational Methods in Engineering* [online]. 2023-04, vol. 30, no. 3, pp. 1553–1577 [visited on 2023-05-04]. ISSN 1134-3060, ISSN 1886-1784. Available from DOI: 10.1007/s11831-022-09834-4.

LD16. KRYL, Martin; DANYS, Lukas; JAROS, Rene; MARTINEK, Radek; KODYTEK, Pavel; BILIK, Petr. Wood Recognition and Quality Imaging Inspection Systems. *Journal of Sensors* [online]. 2020-09, vol. 2020, pp. 1–19 [visited on 2023-05-04]. ISSN 1687-725X, ISSN 1687-7268. Available from DOI: 10.1155/2020/3217126.

Lukáš Danys

PhD Student · Technical Cybernetics

VSB - Technical University of Ostrava, 17. listopadu 2172/15, Ostrava-Poruba 708 00

lukas.danys@vsb.cz

Education

VSB - Technical University of Ostrava
17. listopadu 2172/15, Ostrava-Poruba 708 00

PhD in Technical Cybernetics
2018 - present

- Advisor: prof. Ing. Radek Martinek, Ph.D.
- Dissertation Thesis: Software-defined Radio in SMART Technology and Industry 4.0

VSB - Technical University of Ostrava
17. listopadu 2172/15, Ostrava-Poruba 708 00

Master's Degree in Mobile Technologies
2016 - 2018

- Diploma Thesis: Outdoor Visible Light Communications (Public Lighting Systems, Vehicle to Vehicle - V2V, etc.)

VSB - Technical University of Ostrava
17. listopadu 2172/15, Ostrava-Poruba 708 00

Bachelor's Degree in Mobile Technologies
2013 - 2016

- Bachelor Thesis in company.

Professional Experience

2018-present	**Research Fellow**, VSB - Technical University of Ostrava
2015-2019	**Microwave Specialist**, ha-vel internet s.r.o.

Publications

Related Publications

Martinek, R., **Danys, L.**, & Jaros, R. (2019). Visible light communication system based on software defined radio: Performance study of intelligent transportation and indoor applications. Electronics, 8(4), 433. **IF=3.271**

Danys, L., Zolotova, I., Romero, D., Papcun, P., Kajati, E., Jaros, R., ... & Martinek, R. (2022). Visible Light Communication and localization: A study on tracking solutions for Industry 4.0 and the Operator 4.0. Journal of Manufacturing Systems, 64, 535-545. **IF=10.218**

Martinek, R., **Danys, L.**, & Jaros, R. (2020). Adaptive software defined equalization techniques for indoor visible light communication. Sensors, 20(6), 1618. **IF=4.352**

Danys, L., Martinek, R., Jaros, R., Baros, J., Simonik, P., & Snasel, V. (2021). Enhancements of SDR-based FPGA system for V2X-VLC communications. CMC-COMPUTERS MATERIALS & CONTINUA, 68(3), 3629-3652. **IF=4.152**

Vanus, J., Martinek, R., **Danys, L.**, Nedoma, J., & Bilik, P. (2022). Occupancy Detection in Smart Home Space Using Interoperable Building Automation Technologies. HUMAN-CENTRIC COMPUTING AND INFORMATION SCIENCES, 12. **IF=6.558**

Non-Related Publications

Jargus, J., Tomis, M., Baros, J., **Danys, L.**, Jaros, R., Martinek, R., ... & Nedoma, J. (2022). Measurement of the Effect of Luminescent Layer Parameters on Light and Communication Properties. IEEE Transactions on Instrumentation and Measurement.

Hajovsky, R., Pies, M., Velicka, J., Slany, V., Rous, R., **Danys, L.**, & Martinek, R. (2022). Design of a IoT-based Monitoring System as a Part of Prevention of Thermal Events in Mining and Landfill Waste Disposal Sites: A Pilot Case Study. IEEE Transactions on Instrumentation and Measurement.

Jaros, R., Martinek, R., & **Danys, L.** (2019). Comparison of different electrocardiography with vectorcardiography transformations. Sensors, 19(14), 3072.

Sidikova, M., Martinek, R., Kawala-Sterniuk, A., Ladrova, M., Jaros, R., **Danys, L.**, & Simonik, P. (2020). Vital sign monitoring in car seats based on electrocardiography, ballistocardiography and seismocardiography: A review. Sensors, 20(19), 5699.

Slany, V., Koudelka, P., Krcalova, E., Jobbagy, J., **Danys, L.**, Jaros, R., ... & Martinek, R. (2022). New Hybrid IoT LoRaWAN/IRC Sensors: SMART Water Metering System. CMC-COMPUTERS MATERIALS & CONTINUA, 71(3), 5201-5217.

Martinek, R., Baros, J., Jaros, R., **Danys, L.**, & Nedoma, J. (2022). Hybrid in-vehicle background noise reduction for robust speech recognition: The possibilities of next generation 5G data networks.

Fajkus, M., Nedoma, J., Martinek, R., **Danys, L.**, Fridrich, M., Mec, P., & Zabka, S. (2021). Fiber-optic Bragg system for the dynamic weighing of municipal waste: A pilot study. IEEE Access, 9, 99050-99059.

Martinek, R., Bilik, P., Baros, J., Brablik, J., Kahankova, R., Jaros, R., **Danys, L.**, ... & Wen, H. (2020). Design of a measuring system for electricity quality monitoring within the smart street lighting test polygon: Pilot study on adaptive current control strategy for three-phase shunt active power filters. Sensors, 20(6), 1718.

Baros, J., Sotola, V., Bilik, P., Martinek, R., Jaros, R., **Danys, L.**, & Simonik, P. (2022). Review of Fundamental Active Current Extraction Techniques for SAPF. Sensors, 22(20), 7985.

Jaros, R., Byrtus, R., Dohnal, J., **Danys, L.**, Baros, J., Koziorek, J., ... & Martinek, R. (2023). Advanced signal processing methods for condition monitoring. Archives of Computational Methods in Engineering, 30(3), 1553-1577.

Kryl, M., **Danys, L.**, Jaros, R., Martinek, R., Kodytek, P., & Bilik, P. (2020). Wood recognition and quality imaging inspection systems. Journal of Sensors, 2020, 1-19.

Hirsch Index

Web of Science: 6.

Scopus: 7.

Projects

Virtual Instrumentation for Measurement and Testing V.
SP2018/170 *2018*

Research Centre of Advanced Mechatronic Systems
CZ.02.1.01/0.0/0.0/16_019/0000867 *2018–2022*

A Research Platform focused on Industry 4.0 and Robotics in Ostrava Agglomeration
CZ.02.1.01/0.0/0.0/17_049/0008425 *2018–2022*

Advanced Signal Processing
SP2019/85 *2019*

Advanced Signal Processing II
SP2020/156 *2020*

Advanced Signal Processing III
SP2021/32 *2021*

The Comprehensive System for the Development of Non-Invasive Fetal ECG Monitoring
FW03010392 *2021–present*

Advanced Signal Processing IV: Bioinspired Algorithms
SP2022/34 *2022*

Advanced Signal Processing V: Application of Hybrid Signal Processing and Machine Learning Methods for Sensor Systems
SP2023/002 *2023*

Research and development of innovative technology for the pin hole detection in the metal strip
CZ.01.1.02/0.0/0.0/20_321/0024287 *2023–present*

MR Relaxometry of Basal Ganglia Damage in Newborns With Hypoxic-Ischemic Encephalopathy
FW06010498 *2023–present*

Teaching Experience

Since 2018 **Measurement in Information and Communication Technologies**, Teaching Assistant
Since 2018 **Measurement in Telecommunication Systems**, Teaching Assistant